

# On the Control of Soil Heterogeneity, Peclet number and Spatially Variable Diffusion over Unsaturated Transport

Christopher Vincent Henri<sup>1</sup> and Efstathios Diamantopoulos<sup>2</sup>

<sup>1</sup>Geological Survey of Denmark and Greenland

<sup>2</sup>University of Copenhagen

January 3, 2023

## Abstract

Physical properties of soils are ubiquitously heterogeneous. This spatial variability has a profound, yet still partially understood, impact on conservative transport. Moreover, molecular diffusion is often a disregarded process that can have an important counter-intuitive effect on transport: diffusion can prevent non-Fickian tailing by mobilizing mass otherwise trapped in low velocity zones.

Here, we focus on macroscopically homogeneous soils presenting small scale heterogeneity, as described by the Miller-Miller method. We then analyze the dynamic control of soil heterogeneity, advection and diffusion on conservative transport. We focus especially on the importance of diffusion and of its tortuosity-dependent spatial variability on the overall transport.

Our results indicate that high Peclet number systems are highly sensitive to the degree of heterogeneity, which promotes non-Fickian transport. Also, diffusion appears to have a profound impact on transport, depending on both the degree of heterogeneity and the Peclet number. For a high Peclet number and a very heterogeneous system, diffusion leads to the counter-intuitive decrease of non-Fickian macrodispersion described previously. This is not observed for a low Peclet number due to the non-trivial impact of the spatial variability in the diffusion coefficient, which appears to be a significant controlling factor of transport by promoting or preventing the accumulation of mass in low velocity zones.

Globally, this work (1) highlights the complex, synergistic effect of soil heterogeneity, advective fluxes and diffusion on transport and (2), alerts on potential upscaling challenges when the spatial variability of such key processes cannot be properly described.

1       **On the Control of Soil Heterogeneity, Peclet number**  
2       **and Spatially Variable Diffusion over Unsaturated**  
3       **Transport**

4                   **Christopher V. Henri<sup>1</sup>, Efstathios Diamantopoulos<sup>2</sup>**

5                   <sup>1</sup>Geological Survey of Denmark and Greenland, Copenhagen, Denmark

6                   <sup>2</sup>Chair of Soil Physics, University of Bayreuth, Bayreuth, Germany

7       **Key Points:**

- 8       • Small scale soil heterogeneity has a significant Peclet number dependent impact  
9       on main transport characteristics.
- 10      • Diffusion can have a profound impact on transport, which is dependent on soil het-  
11      erogeneity and the Peclet number.
- 12      • The spatial variability in the diffusion coefficient significantly controls transport,  
13      but remains complex to upscale.

---

Corresponding author: Christopher V. Henri, [cvh@geus.dk](mailto:cvh@geus.dk)

**Abstract**

Physical properties of soils are ubiquitously heterogeneous. This spatial variability has a profound, yet still partially understood, impact on conservative transport. Moreover, molecular diffusion is often a disregarded process that can have an important counter-intuitive effect on transport: diffusion can prevent non-Fickian tailing by mobilizing mass otherwise trapped in low velocity zones. Here, we focus on macroscopically homogeneous soils presenting small scale heterogeneity, as described by the Miller-Miller method. We then analyze the dynamic control of soil heterogeneity, advection and diffusion on conservative transport. We focus especially on the importance of diffusion and of its tortuosity-dependent spatial variability on the overall transport. Our results indicate that high Peclet number systems are highly sensitive to the degree of heterogeneity, which promotes non-Fickian transport. Also, diffusion appears to have a profound impact on transport, depending on both the degree of heterogeneity and the Peclet number. For a high Peclet number and a very heterogeneous system, diffusion leads to the counter-intuitive decrease of non-Fickian macrodispersion described previously. This is not observed for a low Peclet number due to the non-trivial impact of the spatial variability in the diffusion coefficient, which appears to be a significant controlling factor of transport by promoting or preventing the accumulation of mass in low velocity zones. Globally, this work (1) highlights the complex, synergistic effect of soil heterogeneity, advective fluxes and diffusion on transport and (2), alerts on potential upscaling challenges when the spatial variability of such key processes cannot be properly described.

**1 Introduction**

Understanding and predicting the dynamics of chemicals in soils is key to optimize agrochemical application while ensuring the protection of the water resources. However, the fate of chemicals in soils results from a complex interplay of physical, chemical and biological processes which are still not well understood. For a non-reactive, non-sorbing and non-volatile conservative solute, it is well established that the main physical processes controlling transport are advection, diffusion and dispersion (Bear, 1972). Thus, the advection-dispersion-diffusion equation (ADE), which mathematically describes those processes at the continuum scale (Cushman, 1984), represents to this day the most popular theory describing solute transport into porous media. Yet, the parameters in the

45 ADE are effective parameters, integrating small scale spatial variability in the physical  
46 properties of soils, which often challenges its application.

47 Soils are heterogeneous at any spatial scale, from the pore scale (mm) up to the  
48 catchment scale (km). Soil heterogeneity can result from diverse origins such as parent  
49 material, pedogenesis, soil organisms, plant roots and anthropogenic impact like man-  
50 agement operations (Schelle et al., 2013). Soil heterogeneity is intrinsically spatial scale  
51 dependent and it may include spatial variability of different properties. A heterogeneous  
52 soil can for example originate from different soil textures observed at relatively large scales  
53 ( $> \text{dm}$ , e.g., soil horizons), and/or from different arrangements of the same mineral grains  
54 at smaller spatial scales (cm). Some components can also span different spatial scales  
55 like macropores from earthworms, roots, etc (Jarvis et al., 2016; Holbak et al., 2022). In  
56 any ways, the variability in physical properties provokes variability in soil hydraulic prop-  
57 erties (SHPs), subsequently leading to dynamic hydraulic structures (Javaux et al., 2006a)  
58 exposing, e.g., a complex network of high flux channels with interspersed small volumes  
59 of low-flux domains (Roth, 1995).

60 The spatial variability of the physical properties of soils has a substantial effect on  
61 transport of conservative solutes, which has been extensively reported since the 1990's  
62 (e.g., Roth, 1995; Hammel & Roth, 1998; Javaux et al., 2006b; Russo & Fiori, 2009; C. J. M. Cre-  
63 mer & Neuweiler, 2019, among many others). Understanding this effect of heterogene-  
64 ity on transport dynamics is key to accurately estimate and predict solute transport to-  
65 ward the water resources (Russo, 2015) and to develop useful upscaling techniques (e.g.,  
66 dual-permeability approach, Vogel et al., 2000). Unsaturated heterogeneous transport  
67 has been experimentally observed under laboratory (Khan & Jury, 1990), large soil mono-  
68 liths (Javaux et al., 2006b) and field conditions (Forrer et al., 1999; Ursino & Gimmi,  
69 2004). Yet, the vast complexity of unsaturated systems has often led researchers to study  
70 the transport of conservative solutes in saturated/unsaturated porous media through nu-  
71 merical experiments. In most of those studies, soil heterogeneity has been explicitly rep-  
72 resented at the cm scale (Roth & Hammel, 1996), assuming the validity of a similarity  
73 model for the small scale SHPs, as done by, e.g., the Miller-Miller Similar Media The-  
74 ory (MMT) (Miller & Miller, 1956; Sadeghi et al., 2016).

75 Results from such studies show that the impact of heterogeneity on transport ap-  
76 pears to not be a well defined soil dependent feature, but results instead from the syn-

77 ergistic effect of constitutive material spatial variability and of dynamic flow conditions.  
78 For instance, decreasing the degree of saturation will increase the spread of the solute  
79 (Russo, 1993) and the effective recharge rate (i.e. vertical flux) controls more specifically  
80 the transverse dispersion (Roth & Hammel, 1996; Hammel & Roth, 1998; Forrer et al.,  
81 1999; Cirpka & Kitanidis, 2002). Thus, considering more realistic conditions in terms  
82 of contaminant input fluxes (Vanderborght et al., 1998), flow dynamic characterized by  
83 infiltration (downward fluxes)-evaporation (upward fluxes) periods (Russo et al., 2000,  
84 2001; C. J. Cremer et al., 2016; Henri & Diamantopoulos, 2022), or topography (Woods  
85 et al., 2013) results to even more complex transport behavior, which remains to this day  
86 challenging to systematically describe.

87 Despite an improved understanding of heterogeneous transport in soils, to this day,  
88 even models considering some type of heterogeneity generally fail to predict observed plume  
89 behavior, in terms of travel times and spread (Ursino & Gimmi, 2004), scale and flow  
90 rate dependency of transport (Javaux et al., 2006b), and contaminant concentrations (Botros  
91 et al., 2012). While it is a common knowledge that applying the ADE or any of its ex-  
92 tension (e.g., Mobile-Immobile theory (Van Genuchten & Wierenga, 1974)) can success-  
93 fully describe experimental data under different spatial scales, the predicting capabil-  
94 ities of those theories remain indeed limited, which highlight the complexity to fully rep-  
95 resent the variety of processes engaged in the subsurface.

96 In this context, it is worth mentioning that, although molecular diffusion is a pro-  
97 cess that is sometimes accounted for in numerical experiments (C. J. Cremer et al., 2016),  
98 its effect on transport is often disregarded. Nevertheless, some theoretical studies have  
99 highlighted diffusive transport as a potentially important process controlling factor of  
100 solute behavior under both unsaturated and saturated conditions (Weissmann et al., 2002;  
101 Nissan & Berkowitz, 2019; Cirpka & Kitanidis, 2002).

102 The importance of diffusion is in most cases studied relatively to advection. The  
103 Peclet number ( $Pe$ ), comparing advective and diffusive characteristic times, is then the  
104 reference metric to characterize dominance of either process to the overall transport. Im-  
105 portantly, it has been shown that the Peclet number controls the effect of heterogene-  
106 ity on solute transport. This observation has been made at different spatial scales and  
107 in both saturated and unsaturated conditions. For instance, studies by Nissan & Berkowitz  
108 (2019) at the (saturated) pore scale, Cirpka & Kitanidis (2002) at the (unsaturated) site

109 scale and (Weissmann et al., 2002) in a regional aquifer show that high  $Pe$  values (i.e.,  
110 a predominance of advection over diffusion) leads to more anomalous behavior compared  
111 to low  $Pe$  values. Inversely, transport at low  $Pe$  (i.e., diffusion-dominant) is character-  
112 ized by shorter residence times in stagnant zones, which reduces the anomalous behav-  
113 ior of transport. In simple terms, a strong diffusion reduces the “delay” in very low ve-  
114 locity zones of the porous medium by favoring the transfer of solute mass from these quasi-  
115 stagnant areas to more mobile ones. It has been also shown at the pore scale and un-  
116 der saturated conditions that this sensitivity of transport to  $Pe$  is accentuated by increas-  
117 ing the degree of heterogeneity in the porous media (Nissan & Berkowitz, 2019). Such  
118 transport dynamic remains to be confirmed at larger scale and under unsaturated con-  
119 ditions.

120 From the previous, it is obvious that the effect of molecular diffusion on transport  
121 is well documented, but the process is in most cases represented as being uniform (i.e.,  
122 described by a constant diffusion coefficient). Yet, it is also well documented that in any  
123 porous system, the presence of solid-air-liquid interfaces influences the diffusion paths  
124 of solute species (Boudreau, 1996). The effect of water content/porosity on the effective  
125 diffusive process is often represented as a dependence of the diffusion coefficient to tor-  
126 tuosity (Shen & Chen, 2007; Ghanbarian et al., 2013; Van Cappellen & Gaillard, 2018).  
127 In unsaturated soils, spatial and temporal variability in the water content can then make  
128 the diffusion process highly heterogeneous. Yet, rare are the studies that have explic-  
129 itly analyzed the effect of a tortuosity-dependency of the diffusion coefficient, especially  
130 under heterogeneous conditions. For instance, C. J. Cremer et al. (2016) uses the Milling-  
131 ton & Quirk (1961) method to account for tortuosity but the authors do not assess the  
132 relevance or the importance of such approach on diffusive transport.

133 This study aims on the understanding of conservative transport in unsaturated soils,  
134 and more specifically on the complex interplay between spatial heterogeneity of SHPs,  
135 advection and diffusion. As mentioned above, real soils are structured at many differ-  
136 ent scales (horizons, macropores, anisotropy, etc) and these components are expected to  
137 add additional complexity to water flow. In this study, we focused solely on the effect  
138 of small scale heterogeneity and its impact on transport, similar to the studies of Roth  
139 & Hammel (1996) and Hammel & Roth (1998). After analyzing the complex synergis-  
140 tic control of soil heterogeneity and infiltration flux, we will focus more specifically on

141 the superposed impact of diffusion and of its spatial variability on heterogeneous trans-  
 142 port.

## 143 2 Method

144 In the following, we briefly present the theory for i) simulating water flow and con-  
 145 servative transport in unsaturated soils, ii) representing heterogeneity with MMT, and  
 146 finally, iii) we provide an overview of all the tested numerical experiments.

### 147 2.1 Flow and transport

148 *Flow.* For a rigid, non-swelling, isotropic porous medium, water flow under vari-  
 149 able saturated conditions is described by the Richards-Richardson equation (Richards,  
 150 1931; Richardson, 1922):

$$\frac{\partial \theta}{\partial t} = -\nabla \cdot \theta \mathbf{u} = \nabla \cdot [K \nabla h] + \frac{\partial K}{\partial z} \quad (1)$$

151 where  $z$  is the vertical coordinate [L],  $h$  is the pressure head [L],  $\theta$  is the volumetric wa-  
 152 ter content [ $L^3 L^{-3}$ ],  $\mathbf{u}$  is the pore water velocity [ $L T^{-1}$ ] and  $K$  [ $L T^{-1}$ ] is the saturated/unsaturated  
 153 conductivity as a function of  $\theta$  or  $h$ . A prerequisite of Equation 1 is that the air pres-  
 154 sure in the soil at any system state is equal to the atmospheric pressure (single flow).

155 Eq. 1 assumes that, at the continuum scale (Cushman, 1984), a local equilibrium  
 156 between water content and pressure head is always valid (Diamantopoulos & Durner, 2012).  
 157 This relationship is described by the water retention curve:

$$h(S_e) = \frac{1}{\alpha} [S_e^{-n/(n-1)} - 1]^{(1/n)}, \quad (2)$$

158 where  $S_e$  [-] is the effective saturation given by:

$$S_e(\theta) = \frac{\theta - \theta_r}{\theta_s - \theta_r}, \quad (3)$$

and  $\alpha$  [ $L^{-1}$ ] and  $n$  [-] are shape parameters.  $\theta_s$  [ $L^3 L^{-3}$ ] and  $\theta_r$  [ $L^3 L^{-3}$ ] are saturated  
 and residual water contents. Finally, the conductivity as a function of effective satura-  
 tion is given by:

$$K(S_e) = K_s S_e^\tau [1 - (1 - S_e^{n/(n-1)})^{1-1/n}]^2 \quad (4)$$

159 For all the simulations presented in this work, we assumed a simulation domain of  
 160 80 cm in the horizontal direction ( $L_x$ ) and 240 cm in the vertical direction ( $L_z$ ). The  
 161 domain was discretized in cells of size  $d_x = 1$  cm and  $d_z = 2$  cm, respectively, resulting  
 162 in  $n_x = 80$  numerical nodes in the x-direction and  $n_z = 120$  in the z-direction. The length  
 163 of the domain was chosen to ensure 10 correlation lengths in each direction in order to  
 164 capture the full (i.e., ergodic) effect of heterogeneity (presented below in paragraph 2.2).  
 165 At the top nodes ( $z=0$  cm), a constant flux boundary condition was chosen, whereas at  
 166 the bottom ( $z=240$  cm) a unit-hydraulic head gradient was assumed. For the numer-  
 167 ical solution of Eq. 1, the finite-volume method as implemented in the Daisy model (Hansen  
 168 et al., 2012; Holbak et al., 2021) has been used.

*Transport.* Transport in the unsaturated zone for a conservative solute is described  
 by the advection-dispersion equation:

$$\frac{\partial(\theta c)}{\partial t} = -\nabla \cdot (\theta \mathbf{u} c) + \nabla \cdot (\theta \mathbf{D} \cdot \nabla c), \quad (5)$$

169 where  $c$  [ $\text{M L}^{-3}$ ] is the solute concentration,  $\theta$  [ $\text{L}^3 \text{L}^{-3}$ ] is the water content and  $\mathbf{D}^w$  [ $\text{L}^2$   
 170  $\text{T}^{-1}$ ] is the hydrodynamic dispersion tensor in the water phase given by (Bear, 1972):

$$\mathbf{D} = (\alpha_T |\mathbf{u}| + D_m) \delta + (\alpha_L - \alpha_T) \frac{\mathbf{u} \mathbf{u}^T}{|\mathbf{u}|}, \quad (6)$$

171 where  $\alpha_L$  [L] and  $\alpha_T$  [L] is the longitudinal and transverse dispersivities, respectively,  
 172  $D_m$  [ $\text{L}^2 \text{T}^{-1}$ ] is the molecular diffusion and  $\delta$  is the Kronecker delta function.

The ADE was solved using the Random Walk Particle Tracking (RWPT) method,  
 expressed as:

$$\mathbf{x}_p(t + \Delta t) = \mathbf{x}_p(t) + \mathbf{A}(\mathbf{x}_p, t) \Delta t + \mathbf{B}(\mathbf{x}_p, t) \cdot \xi(t) \sqrt{\Delta t}, \quad (7)$$

173 where  $\mathbf{x}_p$  is the particle location,  $\Delta t$  is the time step of the particles jump and  $\xi$  is a vec-  
 174 tor of independent, normally distributed random variables with zero mean and unit vari-  
 175 ance.

$$\mathbf{A} = \mathbf{u}(\mathbf{x}_p) + \nabla \cdot \mathbf{D}(\mathbf{x}_p) + \frac{1}{\theta(\mathbf{x}_p)} \mathbf{D}(\mathbf{x}_p) \cdot \nabla \theta(\mathbf{x}_p). \quad (8)$$

The displacement matrix relates to the dispersion tensor as:

$$2\mathbf{D} = \mathbf{B} \cdot \mathbf{B}^T. \quad (9)$$

176 The RWPT approach, implemented in the code RW3D (Fernández-García et al.,  
 177 2005; Henri & Fernández-García, 2014, 2015), is further described for application in un-  
 178 saturated conditions by Henri & Diamantopoulos (2022), who also shows how the La-  
 179 grangian method avoids numerical issues typically produced by Eulerian schemes.

*Diffusion.* The effective diffusion coefficient ( $D_m$ ) was considered to be dependent on the local water content value (Shen & Chen, 2007):

$$D_m(\theta) = D_w \times \tau_w(\theta), \quad (10)$$

where  $D_w$  [ $L^2 T^{-1}$ ] is the diffusion coefficient in free water, and  $\tau_w(\theta)$  is the water content dependent tortuosity.  $\tau_w(\theta)$  is typically described empirically. Different models are frequently used, and in this study the relationship described by Millington & Quirk (1961) was used:

$$\tau_w(\theta) = \frac{\theta^{7/3}}{\theta_s^2}. \quad (11)$$

For comparison, we also consider the relationship proposed by Møldrup et al. (1997):

$$\tau_w(\theta) = 0.66 \times \left( \frac{\theta}{\theta_s} \right)^{8/3}. \quad (12)$$

180 The Millington & Quirk (1961) tortuosity model is expected to perform better for  
 181 sands, since it was derived assuming randomly distributed particles of equal size. On the  
 182 other hand, the tortuosity model proposed by Møldrup et al. (1997) is expected to per-  
 183 form better across soil types (Šimunek et al., 2013).

184 For each simulation,  $10^5$  particles were injected randomly over a transect of 40 cm  
 185 located at the center of the top of the domain. To avoid potential subsampling due to  
 186 particles leaving the sides of the domain, a semi-infinite width was considered by trans-  
 187 ferring particles leaving the domain at  $x=0$  and  $x=L_x$  to the other side of the domain,  
 188 at  $x=L_x$  and  $x=0$ , respectively. The impact of such approximation, previously used by,  
 189 e.g., Cirpka & Kitanidis (2002), appears to be minor on both apparent velocity and dis-  
 190 persion, and does not therefore affect our conclusions (see Supplementary Information,  
 191 Figure S1).

The time step between particle jumps was defined to preserve the advective displacement, which was done using a grid Courant number ( $gCu$ ) as:

$$\Delta t = gCu \times \Delta s / \min\{u_x, u_y, u_z\}, \quad (13)$$

**Table 1.** Hydraulic properties of the reference material used for all simulations: saturated ( $\theta_s$ ) and residual ( $\theta_r$ ) water contents, shape parameters ( $\alpha$ ,  $n$ ), saturated hydraulic conductivity ( $K_s$ ).

Material	$\theta_r$ [ $\text{cm}^3 \text{cm}^{-3}$ ]	$\theta_s$ [ $\text{cm}^3 \text{cm}^{-3}$ ]	$\alpha$ [ $\text{cm}^{-1}$ ]	$n$ [-]	$K_s$ [ $\text{cm h}^{-1}$ ]
Loam	0.00	0.49	0.0066	1.68	1.8

192 where  $\Delta s$  is the characteristic size of the grid cell.

## 193 2.2 Representation of soil heterogeneity

194 Small scale soil heterogeneity was modeled using the MMT method (Miller & Miller,  
195 1956; Sadeghi et al., 2016). Briefly, the theory assumes that similarities at the pore scale  
196 geometry yields characteristic length or scaling factors ( $\zeta$ ), which scale the physical prop-  
197 erties of porous media, in this case the water retention and hydraulic conductivity curve  
198 (Roth & Hammel, 1996; Schelle et al., 2013; Sadeghi et al., 2016). For each location  $\mathbf{x}$ ,  
199 we can then calculate location-dependent soil hydraulic properties by:

$$h(\mathbf{x}, \theta) = h^*(\theta) \frac{1}{\zeta(\mathbf{x})}, \quad (14)$$

$$K(\mathbf{x}, \theta) = K^*(\theta) \zeta(\mathbf{x})^2, \quad (15)$$

200 where  $h^*(\theta)$  and  $K^*(\theta)$  are reference material properties, described in Eq. 2 and  
201 Eq. 4. Detailed theoretical considerations for MMT along with an overview of theory  
202 applications is provided in Sadeghi et al. (2016). For all simulations, we assumed a sin-  
203 gular loam material and the parameters of Eq. 2-4 are provided in Table 1. The spatial  
204 distribution of the log-scaling factor  $\chi \equiv \log_{10}(\zeta)$  (presented above) was geostatistically  
205 described as a multi-Gaussian model characterized by an isotropic Gaussian covariance  
206 function with zero mean and a standard deviation  $\sigma_\chi$ . Different  $\sigma_\chi$  values have been tested  
207 in this study. Finally, the correlation length in  $x$  ( $\lambda_x$ ) and  $z$  ( $\lambda_z$ ) was fixed to 8 cm and  
208 24 cm, respectively, following the work of Schlüter et al. (2012).

209 The Miller-Miller theory assumes that porosity, and thus water content at satu-  
210 ration ( $\theta_s$ ), is constant (through out this work equal to  $0.49 \text{ cm}^3 \text{cm}^{-3}$ , Table 1). To test

211 the implications of spatial distributed  $\theta_s$ , we also ran a set of simulations scaling  $\theta_s$  lin-  
 212 early as a function of the local  $K_s$  value, with a minimum and maximum value of 0.3 and  
 213 0.6, respectively. In that way, the test simulations assumed that high values of  $\theta_s$  coin-  
 214 cide with high values of  $K_s$ . This was only done for a high heterogeneity and a low mean  
 215 velocity ( $\sigma_\chi = 0.5$  and  $q = 0.01$  mm/h, diffusion dominated process), which represent  
 216 the scenario most likely to be affected by an assumed constant  $\theta_s$ .

### 217 **2.3 Tested scenarios**

218 Water flow was simulated for a series of steady-state simulations, assuming three  
 219 different degrees of heterogeneity ( $\sigma_\chi = 0.1, 0.3, 0.5$ ) and two different imposed verti-  
 220 cal water fluxes ( $q_{z,in} = 0.01, 1$  mm/h), and thus, different hydraulic structures (Ta-  
 221 ble 2). The low flux represents a scenario strongly dominated by diffusion (low mean ve-  
 222 locity), whereas the high flux represents a scenario with a stronger advective component,  
 223 as observed during an infiltration period. For each combination of  $\sigma_\chi$  and  $q_{z,in}$ , 20 re-  
 224 alizations have been created. While this limited number of realization is not likely to be  
 225 sufficient for a stochastic analysis, observing results from a series of equiprobable flow  
 226 fields will allow to determine if our observation are realization specific or systematic.

227 For all the water flow simulations, solute transport was also simulated. The non-  
 228 represented effect of heterogeneity within a grid cell was accounted for by setting a grid-  
 229 scale dispersivity values of 0.1 cm in the longitudinal direction (i.e.,  $z$ ), and 0.01 cm in  
 230 in the transverse direction (i.e.,  $x$ ). Moreover,  $D_w$  was fixed to  $1.6 \text{ cm}^2/\text{d}$  ( order of mag-  
 231 nitude similar to, e.g., C. J. Cremer et al. (2016)). To better understand the implica-  
 232 tions of a spatially variable diffusion process, we tested 2 different methods on simulat-  
 233 ing the diffusion coefficient (Table 2):

- 234 • A spatially variable, tortuosity (i.e., water content) dependent diffusion coefficient  
 235 ( $D_m(\mathbf{x})$ ), with a tortuosity model described by (Millington & Quirk, 1961), as de-  
 236 scribed in Eq. 11;
- 237 • A spatially averaged diffusion coefficient ( $\bar{D}_m$ ).

238 The diffusion coefficient was considered to be the same values in the  $x$  and  $z$  direction.

239 Finally, we evaluated the effect of transient conditions on solute transport in a highly  
 240 heterogeneous soil ( $\sigma_\chi = 0.5$ , Table 2). Transient conditions are caused by an infiltra-

**Table 2.** Tested scenarios.

Description	Heterogeneity	Water flow	Diffusion
Steady state simulations (20 realizations)	$\sigma_\chi = 0.1$	$q_{z,in} = 0.01$ mm/h	Constant, averaged ( $\bar{D}_m$ )
	$\sigma_\chi = 0.3$	$q_{z,in} = 1$ mm/h	Tortuosity dependent ( $D_m(x)$ )
	$\sigma_\chi = 0.5$		
Transient simulations (1 realization)	$\sigma_\chi = 0.5$	1 day of strong infiltration	Constant, averaged ( $\bar{D}_m$ )
		15 days of strong infiltration	Tortuosity dependent ( $D_m(x)$ )

241 tion period followed by a long redistribution period. Two different infiltration periods  
 242 ( $t_{inf}$ ) are considered: 1 and 15 days. The two models of diffusion tested for the steady  
 243 state simulations are here also considered.

### 244 3 Results

#### 245 3.1 Small scale soil heterogeneity and advective flux

246 In this section, we analyze simulation results of a single realization. Nevertheless,  
 247 we also present outputs from the ensemble of 20 realizations in term of arrival time statis-  
 248 tics to ensure that observations made on a single realization are consistent across real-  
 249 ization.

250 *Flow fields.* Throughout our analysis, the intensity of the advective flux is char-  
 251 acterized by the Peclet number ( $Pe$ ), which is estimated as:

$$Pe = \frac{\bar{u}_z \lambda_z}{D_m}. \quad (16)$$

252 where  $\bar{u}_z$  [ $L T^{-1}$ ] is the average pore water velocity in the  $z$  direction.

253 The resulting Peclet numbers, for each degree of heterogeneity, was equal to  $3.3 \times 10^{-1}$ ,  
 254  $3.3 \times 10^{-1}$ ,  $3.4 \times 10^{-1}$ , respectively, for the high flux; and equal to  $4.0 \times 10^{-2}$ ,  $2.9 \times 10^{-2}$ ,  
 255  $1.9 \times 10^{-2}$ , respectively, for the low flux. According to the calculated Peclet numbers, all  
 256 scenarios are diffusion dominated ( $Pe < 1$ ). However, the low  $q_{z,in}$  simulations can be  
 257 characterised as strongly dominated by diffusion, due to the one order of magnitude lower  
 258 Peclet number.

259 The spatial variability of SHPs appears to significantly control both saturation and  
 260 local water fluxes. Clear patterns of quasi-dry ( $\theta < 0.1$ ) and near-saturated ( $\theta \approx \theta_s$ )  
 261 zones emerges when the degree of heterogeneity is increased (Figure 1, left frames; re-  
 262 sults from the lower degree of heterogeneity are shown in Supplementary Information,  
 263 Figure S2 and Figure S3).

264 The spatial variability in saturation is also highly sensitive to the intensity of the  
 265 infiltration flux (Figure 1, compare upper and lower left frames). Globally, saturation  
 266 is logically increased in case of higher  $Pe$ . Moreover, the degree of heterogeneity in com-  
 267 puted  $\theta$  in case of high  $\sigma_\chi$  appears to decrease when infiltration is stronger. We indeed  
 268 observe an increased predominance of fully saturated areas ( $\theta \approx \theta_s$ ), which is a direct  
 269 effect of MMT and the inherent assumption of equal saturated water content.

270 Similar observation can be made while analyzing the combined effect of soil het-  
 271 erogeneity and input flux on the spatial variability of computed water (Darcian) fluxes  
 272 (Figure 1, middle frame) and pore velocities (Figure 1, right frame): (1) Increasing  $\sigma_\chi$   
 273 generates clear zones of low velocity and fast paths, and (2) increasing the infiltration  
 274 flux globally increases fluxes and increase the portion of the soil column occupied by high  
 275 velocity zones. These results are globally consistent with past work such that of Roth  
 276 (1995), who also observed the clear formation of islands of low and high fluxes due to  
 277 a similar Miller-Miller heterogeneous media and the sensitivity of this hydraulic struc-  
 278 ture to the input flux.

279 *Spatial moments.* The effect of heterogeneity and infiltration flux on the dynamic  
 280 hydraulic structure is reflected on the transport behavior of the applied particles. We  
 281 first analyze the lower spatial moments of the plume: the first moment,  $z_g$ , represents  
 282 the location of the center of mass, and the second spatial moment,  $S_{zz}$ , quantifies the  
 283 spread around the centroid of the plume.

284 Spatial moments are evaluated until particles start to leave the downstream edge  
 285 of the domain to reflect the dynamics of the entire plume. Only results from simulations  
 286 using the ‘‘Millington and Quirk’’ model of tortuosity is shown throughout our analy-  
 287 sis. The analysis using the ‘‘Moldrup et al.’’ model leads to similar results as shown in  
 288 Supplementary Information, Figure S4.

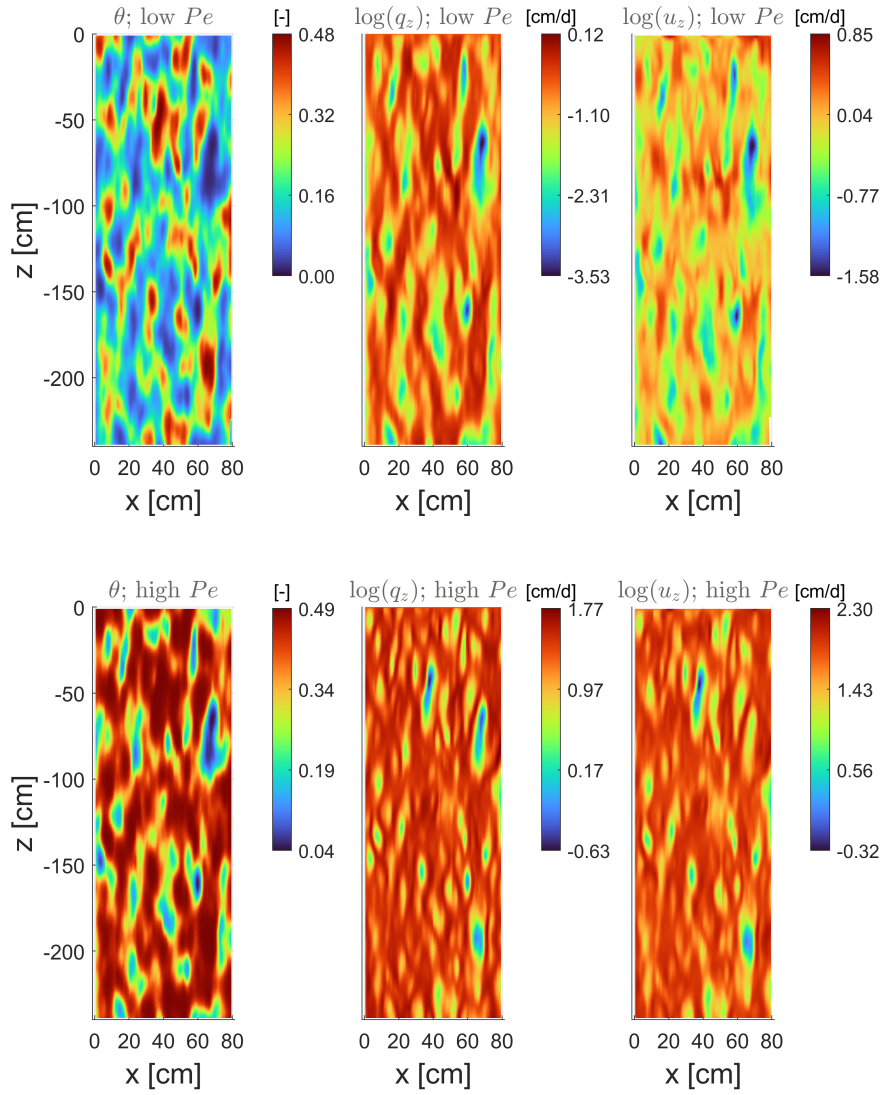


**Figure 1.** Resulting spatial distribution of the water content ( $\theta$ ) for the highest degree of soil heterogeneity ( $\sigma_\chi = 0.5$ ) and for a high recharge flux (i.e., high Peclet number; bottom frames) and a low recharge flux (i.e., low Peclet number; top frames).

289 The center of mass of the plume is highly sensitive to the degree of heterogeneity  
 290 in SHPs for the case of low  $Pe$  number (Figure 2). For the same infiltration flux, the plume  
 291 moves downward faster in case of low  $\sigma_\chi$  (Figure 2, top left frame). The effective veloc-  
 292 ities in the downward direction associated to each  $\sigma_\chi$  values,  $v_z^*$ , can be quantified as the  
 293 slope of the linear regression of  $z_g(t)$ , giving: 0.12, 0.08 and 0.05 cm/d for the low in-  
 294 put flux scenario, respectively, and 6.1, 6.0, 5.2 cm/d for the high input flux scenario.  
 295 Characteristic advection times can then be estimated as:  $t_{adv} = L_z/v_z^*$ .

296 Interestingly, the temporal evolution of the first spatial moment observed for the  
 297 low  $Pe$  case presents a non-linearity that increases with  $\sigma_\chi$ . This results to periods of  
 298 acceleration and of slowing down of the center of mass of the plume and not to a con-  
 299 stant effective velocity as observed in case of  $\sigma_\chi=0.1$ . The sensitivity of the effective ve-  
 300 locity to the degree of heterogeneity is lower in case of high  $Pe$  (Figure 2, top right frame).  
 301 This non-linearity appears to be more or less pronounced depending on the realizations  
 302 (Supplementary Information, Figure S5).

303 The spread of the plume appears to be less sensitive to  $\sigma_\chi$  in case of a low  $Pe$  than  
 304 in case of a high  $Pe$  (Figure 2, compare bottom frames). For a high  $Pe$ , the spread is  
 305 significantly increased for the highest degree of heterogeneity. For the low  $Pe$ , a low in-  
 306 put flux applied on a highly heterogeneous media leads to different regimes of spread of  
 307 the plume, with an intensification of the spread at early and intermediate times (Fig-  
 308 ure 2, bottom left frame). These fluctuations are observed for most realizations (Sup-  
 309 plementary Information, Figure S6). Yet, the average magnitude of the spread remains  
 310 globally similar for all  $\sigma_\chi$ , unlike for a high  $Pe$ .

311 *Breakthrough curves.* Such observations have clear implications in term of mass  
 312 transfer from the soil to deeper layers and into the aquifer. When heterogeneity is in-  
 313 creased in a low velocity system, the breakthrough curve recorded at the bottom of the  
 314 simulated domain presents a later mass arrival and an increased spread, i.e., lower peak  
 315 of mass and mass arrival for a longer period (Figure 3, top left frame). Distinctively, early  
 316 mass arrival appears insensitive to the degree of heterogeneity in case of high input flux,  
 317 unlike macrodispersion, which sensitively increases with  $\sigma_\chi$  (Figure 3, bottom left frame).

318 Globally, those results are consistent with the direct observation of non-Fickian trans-  
 319 port in macroscopically homogeneous unsaturated media with similar high velocity (Bromly  
 320 & Hinz, 2004).

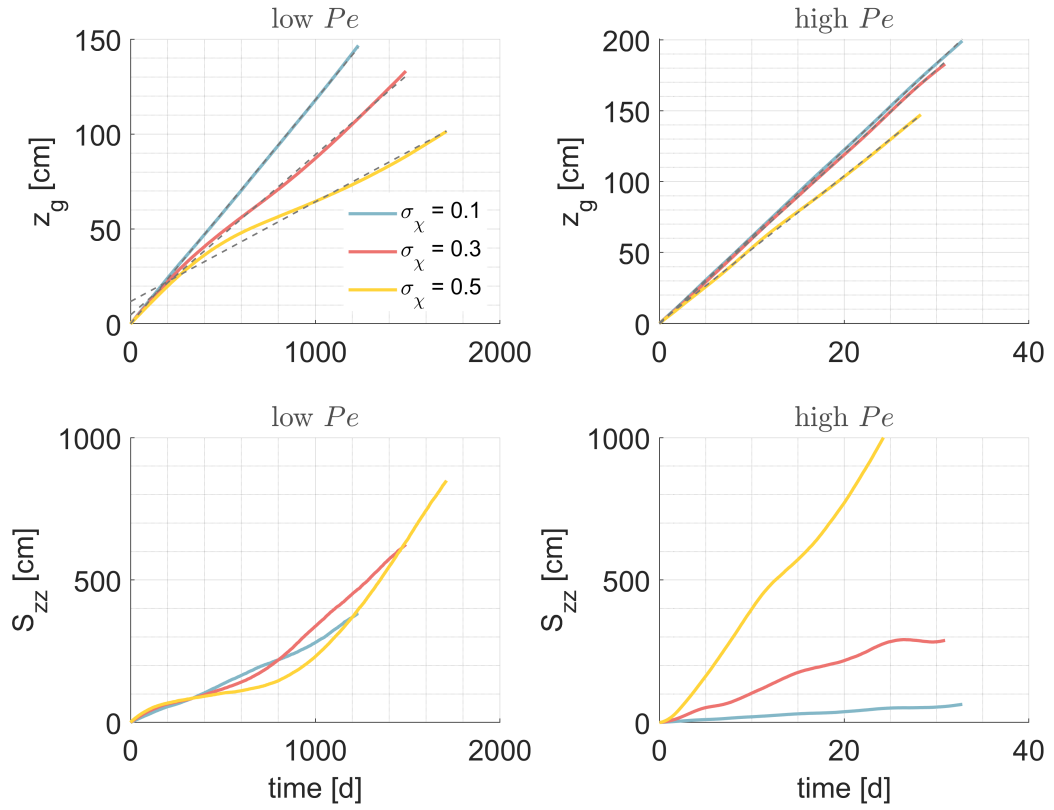


**Figure 2.** First (center of mass location,  $z_g$ ; top frames) and second (spread about the centroid,  $S_{zz}$ ; bottom frames) normalized spatial moments for each degree of heterogeneity of the soil structure and for the 2 input fluxes. The dashed grey lines on the top frames are linear regressions for the temporal evolution of  $z_g$ . The slopes of the regression represent effective velocities.

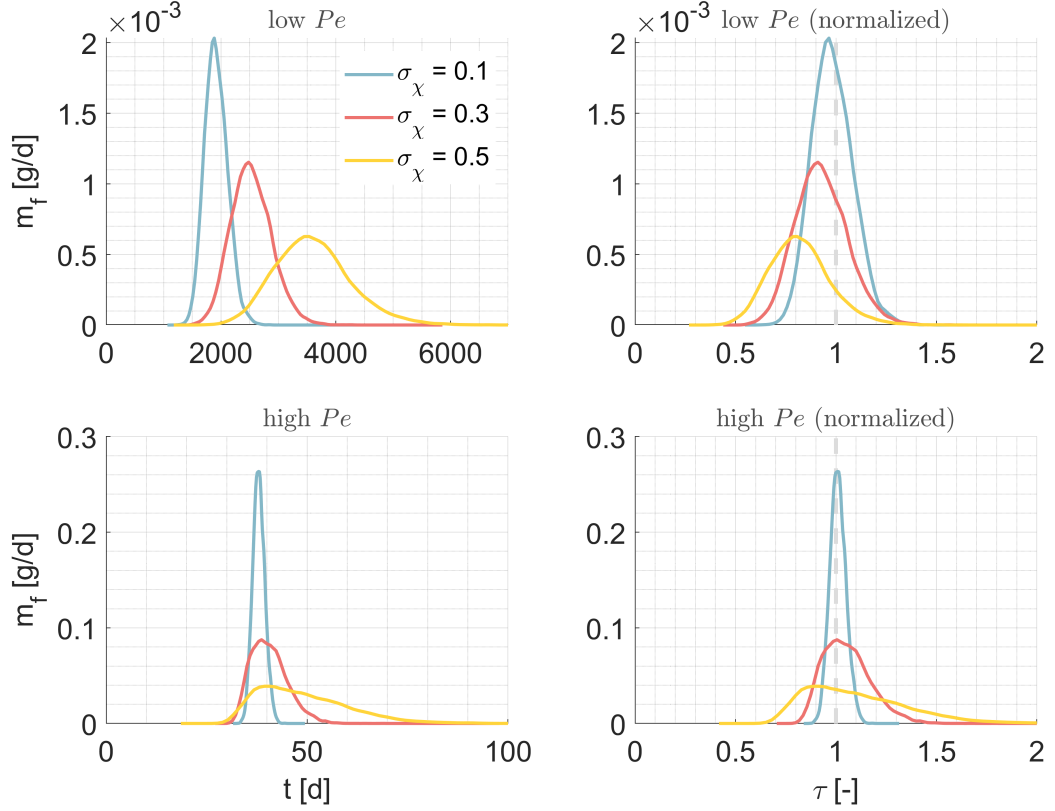


**Figure 3.** Breakthrough curves (BTCs) resulting from simulations in soil of different degree of heterogeneity, for a high recharge flux (i.e., high Peclet number; bottom frames) and a low recharge flux (i.e., low Peclet number; top frames). Right frames show the BTCs considering a time normalized by the advective time. The diffusion coefficient is considered spatially variable (tortuosity dependent).

321 Observing the plume behavior in a series of 20 realization of the heterogeneity in  
 322 the SHPs is consistent with the analysis made on single BTCs. For the high  $Pe$  system,  
 323 early arrival times ( $t_5$ ) are less sensitive to  $\sigma_\chi$  than late arrival times ( $t_{95}$ ; Supplemen-  
 324 tary Information, Figure S7, left frames), while all arrival times are increased with het-  
 325 erogeneity when  $Pe$  is lower (Figure S7, right frames). Also, travel times *pdfs* allow to  
 326 observe that the variability among realizations in late arrival times is significantly in-  
 327 creased with the degree of heterogeneity.

328 The first spatial moment is often used to subsequently estimate the effective ve-  
 329 locity ( $v_z^*$ ) and the time of arrival of the center of mass of the plume at *any* distance from  
 330 the source. Applying this approach is valid in case of high input flux (Figure 3, bottom

331 right frame). The BTCs are centered around a unit values of time normalized by  $t_{adv}$ ,  
 332 regardless of the degree of heterogeneity. However, we observe that  $v_z^*$  does not prop-  
 333 erly predict the motion of the plume in case of low flux and high  $\sigma_\chi$  (Figure 3, top right  
 334 frame). Normalizing the BTCs' time by the characteristic advective time ( $t_{adv}$ ) leads to  
 335 faster first arrival of mass for low  $Pe$  and high  $\sigma_\chi$  systems, reflecting an overall overes-  
 336 timation of the effective velocity.

337 This results from the non-linear behavior of the first spatial moment observed in  
 338 soils characterized by a low  $Pe$  and a high  $\sigma_\chi$  (Figure 2). Indeed, the predictive capac-  
 339 ities of the first spatial moment implies a linear evolution of the center of mass location,  
 340 reflecting a constant effective velocity, which is often observed in saturated conditions.  
 341  $t = t_{adv}$  would then be associated to the arrival of the center of the plume at the char-  
 342 acteristic distance used to estimated  $t_{adv}$  ( $L_z$  in our case). Yet, in case of low flux, the  
 343 center of mass of the plume is affected by critical moments of fast and slow motion, which  
 344 render more complex the estimation of an effective behavior.

### 345 **3.2 Importance of diffusion**

346 In this section, our analysis focuses on the effect of diffusion on transport. We first  
 347 analyze the relevance of considering a realistically heterogeneous diffusion coefficient ( $D_m(x)$ ,  
 348 blue curves in Figures 4 and 5) by comparing corresponding BTCs from simulations dis-  
 349 regarding the diffusive process (yellow lines). The implications of considering a spatially  
 350 homogeneous diffusion coefficient ( $\bar{D}_m$ ) will be analyzed in the following section.

351 *High Peclet number.* For a high  $Pe$ , considering diffusion has a moderate effect  
 352 on macrodispersion. In case of low heterogeneity, disregarding diffusion all together de-  
 353 creases macrodispersion (Figure 4), which is the expected expression of the process. In-  
 354 creasing  $\sigma_\chi$  renders more complex the impact of diffusion on transport: Early arrival times  
 355 are mostly unchanged but macrodispersion is decreased by adding diffusion, decreasing  
 356 the very pronounced tailing (i.e., elongated late arrivals) generated by the heterogene-  
 357 ity in the advective flux. This phenomena has been previously observed by few studies  
 358 under various conditions (Nissan & Berkowitz, 2019; Cirpka & Kitanidis, 2002; Weiss-  
 359 mann et al., 2002) and is explained by the capacity of diffusive motion to move mass away  
 360 from quasi-stagnant zones, reducing this way the potential for very late arrivals (i.e., tail-

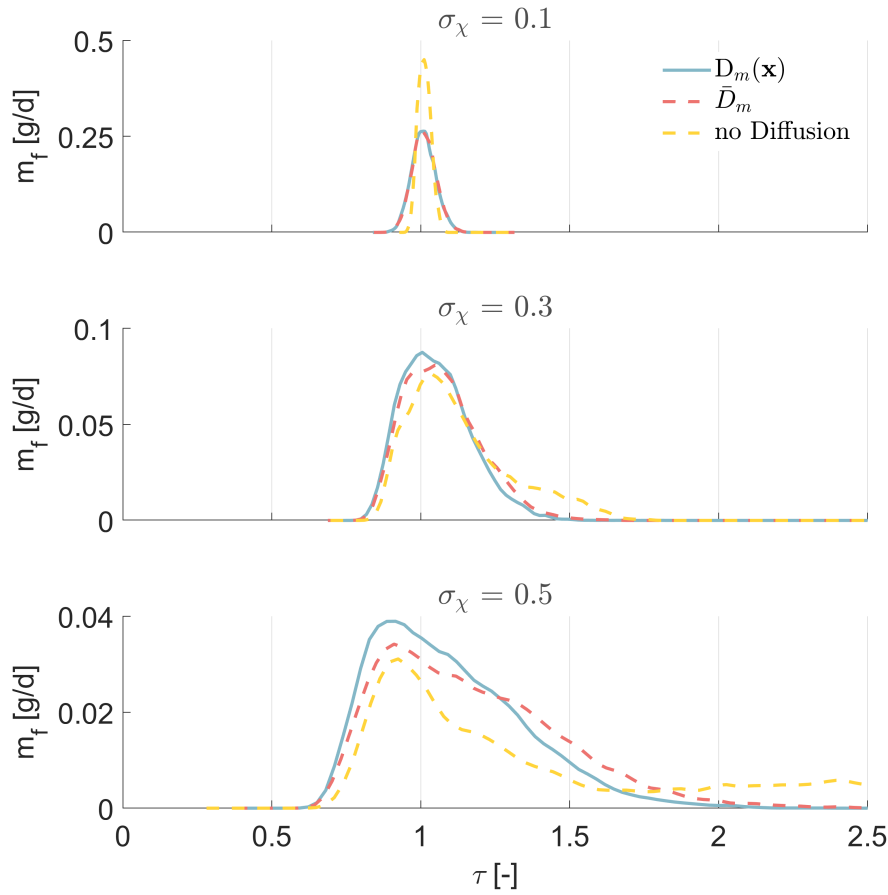


**Figure 4.** Breakthrough curves (BTCs) resulting from simulations using a spatially variable, tortuosity-dependent diffusion coefficient ( $D_m(x)$ ) and a spatially averaged diffusion coefficient ( $\bar{D}_m$ ) and no diffusion, for soils of different degree of heterogeneity. Results are shown for the higher Peclet number. Times are normalized by the characteristic advective time of the  $D_m(x)$  scenario.

361 ing). Here again, these observations are valid across realizations (Supplementary Infor-  
 362 mation, Figure S8).

363 *Low Peclet number.* The effect of diffusion on the overall transport dynamics for  
 364 the low  $Pe$  case is significant, both in term of arrival time and plume spread. For low  
 365 degree of heterogeneity ( $\sigma_\chi=0.1$ ), macrodispersion is increased by including diffusion in  
 366 the simulations (Figure 5, top frame), which is expected and similar to the effect observed  
 367 in case of a high  $Pe$ . However, when  $\sigma_\chi$  increases, not including diffusion does not sig-  
 368 nificantly change the early arrivals but prevents late arrival of mass, leading to a non-

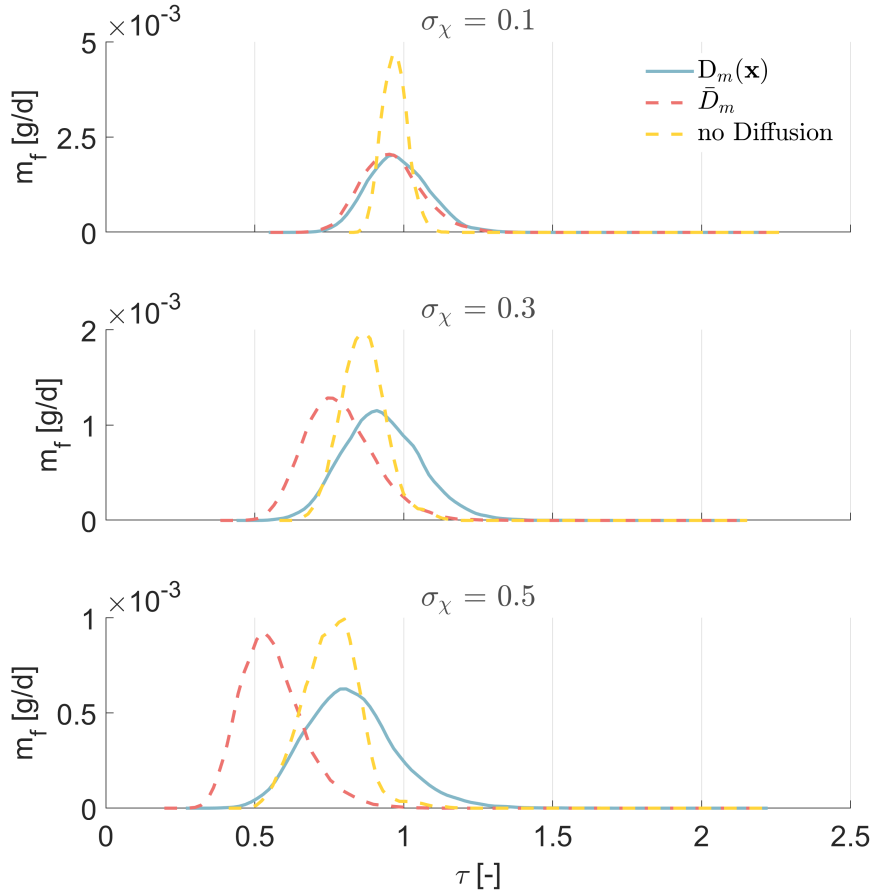


**Figure 5.** Breakthrough curves (BTCs) resulting from simulations using a spatially variable, tortuosity-dependent diffusion coefficient ( $D_m(x)$ ), a spatially averaged diffusion coefficient ( $\bar{D}_m$ ) and no diffusion, for soils of different degree of heterogeneity. Results are shown for the lower Peclet number. Times are normalized by the characteristic advective time of the  $D_m(x)$  scenario.

369 Gaussian, negatively skewed BTC (Figure 5, lower frame). BTCs appears then to be more  
 370 sensitive to  $Pe$  as the degree of heterogeneity increases.

371 At the same time, BTCs sensitivity to  $\sigma_\chi$  is specific to the  $Pe$  number. When  $\sigma_\chi$   
 372 increases, the counter-intuitive macrodispersion-reducing effect of diffusion observed for  
 373 high  $Pe$  is not observed for a lower  $Pe$ , which disagrees with the previous works of Nis-  
 374 san & Berkowitz (2019); Cirpka & Kitanidis (2002); Weissmann et al. (2002). This re-  
 375 lates with our consideration of spatial variable diffusion process. In case of high  $q_{z,in}$ ,  
 376 low velocity zones are characterized by high diffusion coefficients ( $> 10^0$  cm<sup>2</sup>/d; Fig-  
 377 ure 6 lower frame). This is because these zones are characterized by close to saturation

378 water content but low hydraulic conductivity. This favors the mobilizing of mass that  
 379 would be otherwise trapped in a system without diffusion, due to the low local veloc-  
 380 ities. Late arrivals are then prevented. Due to the tortuosity model, the opposite is ob-  
 381 served in case of low flux: diffusion values in quasi-stagnant zones are the lowest ( $< 10^{-3}$   
 382  $\text{cm}^2/\text{d}$ ; Figure 6 upper frame), due to the low local water content. Residence times in  
 383 low velocity zones can then remain relatively high, which allows late arrivals. Interest-  
 384 ingly, in a low velocity system without diffusion, mass reaching a fast channel is likely  
 385 to remain in high velocity zones for the remaining of its transport toward the bottom  
 386 of the domain. Transport occurs then predominantly in fast channels, reducing the im-  
 387 portance of late arrivals. Adding diffusion would favor the transfer of mass from these  
 388 high velocity zones to more stagnant ones, increasing this way the contribution of late  
 389 arrivals. Such behavior is consistent across realizations (Supplementary Information, Fig-  
 390 ure S9). Moreover, accounting for a spatially variable saturated water content leads to  
 391 similar conclusions (Supplementary Information, Figure S10).

### 392 **3.3 Effect of Spatially Variable Diffusion**

393 To further understand the implications of spatial variability in the diffusion coef-  
 394 ficient, we compare BTCs resulting from simulations with a water content dependent dif-  
 395 fusion ( $D_m(x)$ ) coefficient (assuming tortuosity model of Millington and Quirk) and with  
 396 a homogeneous, averaged diffusion ( $\bar{D}_m$ ).

397 In our modeling setting, the range of diffusion coefficient for a single realization is  
 398 highly dependent on the degree of heterogeneity of the SHPs and on the infiltration rate.  
 399 In case of lower  $q_{z,in}$ , we obtain exponentially decreasing histograms of  $D_m$  values in case  
 400 of a high degree of heterogeneity, with a range of diffusion coefficient from 0 to  $1.2 \text{ cm}^2/\text{d}$   
 401 (Figure 7, top frame). The histogram turns more and more Gaussian-like when  $\sigma_\chi$  de-  
 402 creases, with a narrowing range of values (from 0 to 0.3 for  $\sigma_\chi = 0.1$ ).

403 In case of a larger infiltration rate, ranges of  $D_m(x)$  values are globally more spread  
 404 (Figure 7, bottom frame). Histograms are slightly increasing in case of high degree of  
 405 heterogeneity, and still Gaussian-like for  $\sigma_\chi = 0.1$ .

406 *Advection dominated scenario* For the high  $Pe$  scenario, the spatial variability  
 407 in the diffusion coefficient appears to have no real impact on transport in a mildly het-  
 408 erogeneous soil (Figure 4, top frame, compare blue and red lines). When the spatial vari-

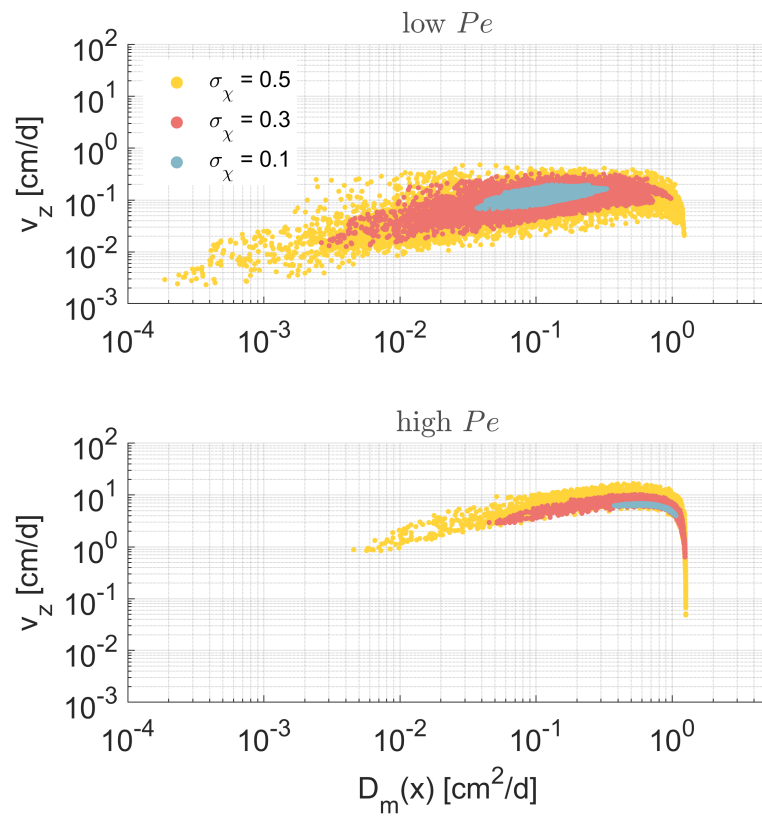


**Figure 6.** Relationship between the vertical velocity and the water content dependent diffusion coefficient for each degree of the heterogeneity in the soil structure and for the 2 Peclet numbers.

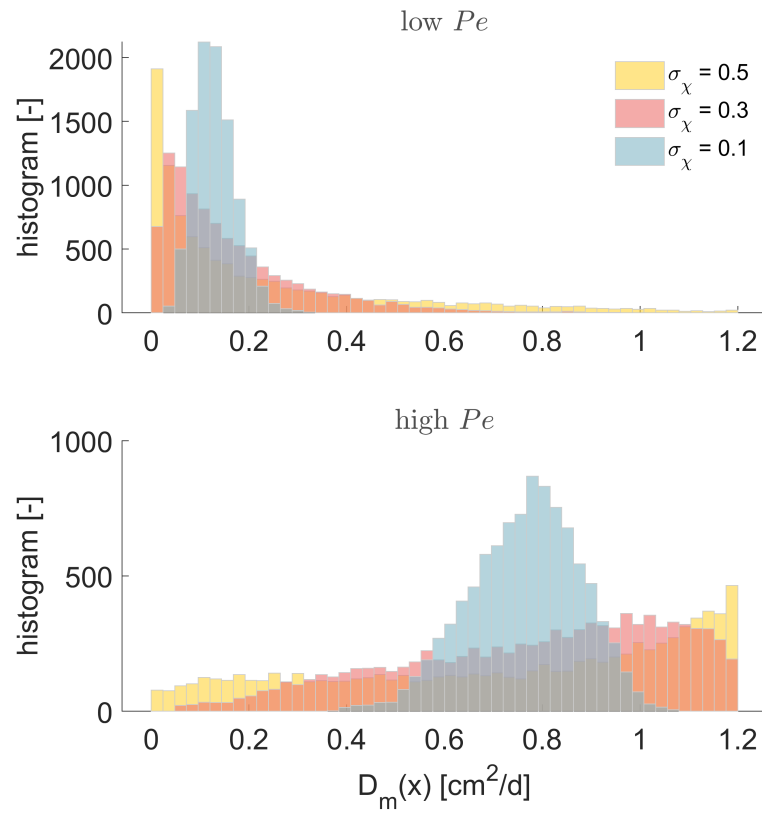


**Figure 7.** Histograms of the spatially variable, tortuosity-dependent diffusion coefficient for each degree of soil heterogeneity and for a high recharge flux (i.e., high Peclet number; bottom frame) and a low recharge flux (i.e., low Peclet number; top frame).

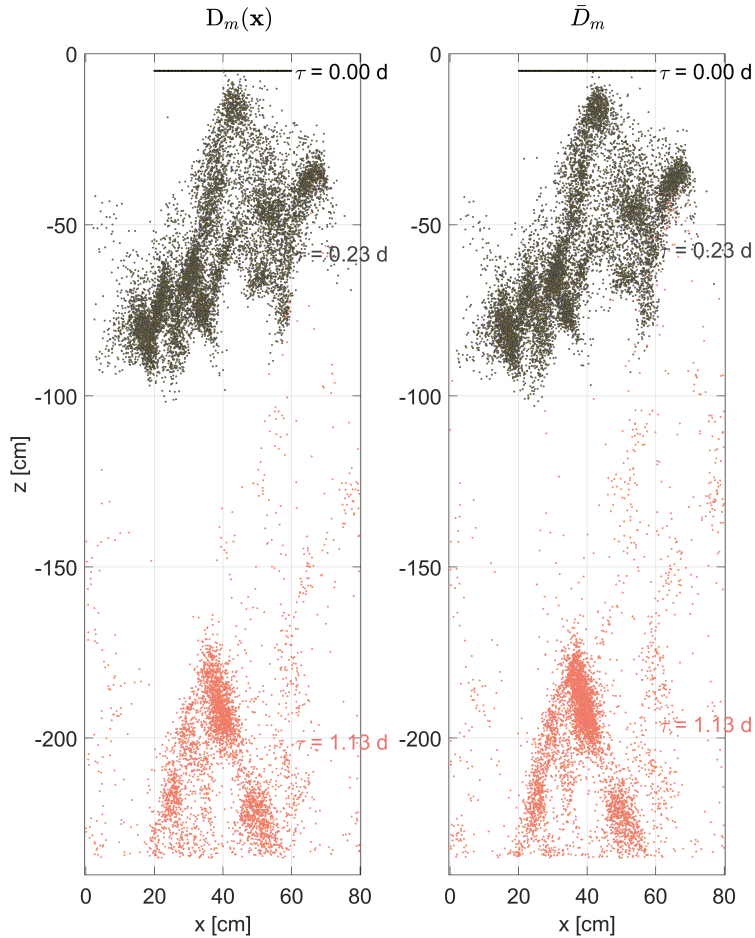


**Figure 8.** Plume snapshots from simulations using a spatially variable, tortuosity-dependent diffusion coefficient ( $D(x)$ ) and a spatially averaged diffusion coefficient ( $\bar{D}_m$ ), for soils of a high degree of heterogeneity ( $\sigma_\chi = 0.5$ ). Results are shown for the higher Peclet number.

409 ability in SHPs is more pronounced, correlating the local diffusion coefficient to the tor-  
 410 tuosity (and therefore the water content) slightly decreases the macrodispersion and the  
 411 tailing of the BTC (Figure 4, bottom frame).

412 Observing the plume of particles in a highly heterogeneous soil allows to identify  
 413 zones of accumulation of mass, which is slightly accentuated in case of spatially averaged  
 414 diffusion coefficient (Figure 8). Globally, the implications in considering the spatial vari-  
 415 ability in diffusion coefficient for a strongly advective system are moderate. Diffusion co-  
 416 efficients in low velocity zones are higher than the mean values, which, following the pre-  
 417 viously discussed phenomena, leads to a reduction of late arrivals.

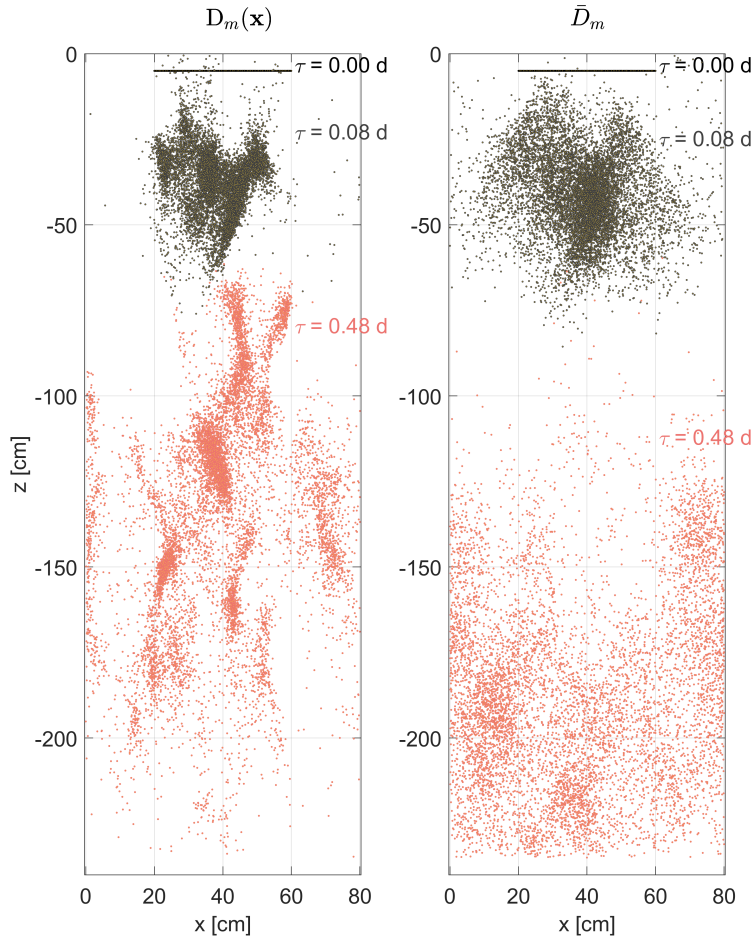


**Figure 9.** Plume snapshots from simulations using a spatially variable, tortuosity-dependent diffusion coefficient ( $D(x)$ ) and a spatially averaged diffusion coefficient ( $\bar{D}_m$ ), for soils of a high degree of heterogeneity ( $\sigma_\chi = 0.5$ ). Results are shown for the low Peclet number.

418 *Diffusion dominated scenario.* When diffusive process is more dominant, account-  
 419 ing for the spatial variability of the diffusion coefficient has a much greater impact on  
 420 plume behavior. For a high  $\sigma_\chi$ , applying a spatially averaged diffusion coefficient leads  
 421 to significantly earlier arrival of mass and to a lesser spread of the plume (Figure 5, lower  
 422 frames).

423 Snapshots of the particle plume in a highly heterogeneous soil display a significantly  
 424 pronounced accumulation of mass in specific zones of the soil if diffusion is considered  
 425 tortuosity-dependent (Figure 9).

426 Low diffusion coefficient values in low velocity zones result in an increased residence  
 427 time in those areas, forming pockets of mass, which can only leave the domain at rel-  
 428 atively late time. On the other hand, applying an average (but still larger) diffusion co-  
 429 efficient in those low velocity zones allows an earlier mobilization of mass, generating an-  
 430 ticipated arrivals. Note that this remains true even compared to a purely advective sys-  
 431 tem, which, despite maintaining mass in fast channels, can still be affected by the rel-  
 432 atively long presence of mass in low velocity areas at early times (partly due to the in-  
 433 jection of mass in low velocity zones).

### 434 3.4 Transient conditions.

435 Natural systems are characterized by periods of infiltration (i.e., strongly advec-  
 436 tive flux) and others of mostly slow mass redistribution (i.e., mostly diffusive transport).  
 437 Figure 10 shows BTCs resulting from simulations with homogeneous and heterogeneous  
 438 diffusion coefficients, for different distances of the control plane ( $x_{cp}$ ) and for 2 differ-  
 439 ent durations of the infiltration period ( $t_{inf}=1$  day and 15 days). The temporal discretiza-  
 440 tion of fluxes, water contents and diffusion coefficients was set to 1 hour, which produces  
 441 similar results than for a finer time step (Supplementary Information, Figure S11). The  
 442 effect of transience in the diffusion process is displayed by comparing BTCs resulting from  
 443 temporally variable diffusion coefficients (plain lines) and from temporally averaged co-  
 444 efficients (dashed lines). For these 2 cases, the water flux and the water content are still  
 445 considered transient.

446 For any infiltration period, results display an insensitivity of the BTCs to the spa-  
 447 tial variability in diffusion at the control plane near the source ( $x_{cp} = 2 \times \lambda_z$ ; Figure  
 448 10, top frames).

449 For BTCs recorded near the center of the domain ( $x_{cp} = 4 \times \lambda_z$ ), the spatial vari-  
 450 ability in the diffusion coefficient generates slightly more diffuse mass arrival, with a later  
 451 peak and later late arrivals, only if the infiltration period is short (1 day; Figure 10, mid-  
 452 dle frames). In case of a longer infiltration period (characterized by a strongly advec-  
 453 tive transport), BTCs at mid-distance are mostly identical for a homogeneous or a het-  
 454 erogeneous diffusion coefficient.

455 Further downstream ( $x_{cp} = 9\lambda_z$ ), applying a tortuosity-dependent diffusion co-  
 456 efficient produces significantly more diffuse BTCs, with similar early mass arrival than

457 with a homogeneous  $D_m$ , but with a lower peak of mass and later late arrivals (Figure  
 458 10, bottom frames). This mass dynamic is observed for both a short (1 day) and a long  
 459 (15 days) initial period of strongly advective transport. For all tested BTCs, we observed  
 460 no significant effect of transience in the diffusion coefficient itself.

461 The two very distinct regimes of diffusive transport associated to a high and a low  
 462 advective flux explains the main dynamic of the simulated transient transport. At short  
 463 travel distance, the insensitivity of the solution to the diffusion model can be explained  
 464 by both the limited sampling of soil heterogeneity occurring over only 2 correlation lengths  
 465 and by the low impact of spatial variability in diffusion on strongly advective systems.  
 466 For longer infiltration period, the limited impact of heterogeneity in the diffusion is ob-  
 467 served further downstream ( $x_{cp} = 2\lambda_z$ ). Yet, with increased travel distances, the ef-  
 468 fect of spatially variable diffusion coefficient on strongly diffusive systems takes over, re-  
 469 gardless of the infiltration duration.

### 470 **3.5 Homogenization of diffusion**

471 To evaluate the relevancy in determining effective, homogenized diffusion coefficient  
 472 other than a spatially averaged values, we tested the performance of the minimum and  
 473 the maximum values of  $D(x)$ .

474 Homogenizing the diffusion coefficient leads to poor performances in case of low  
 475  $Pe$  systems, regardless of the diffusion coefficient values used (Figure 11, upper frame).  
 476 Applying the maximum values of diffusion overestimates macrodispersion and leads to  
 477 early travel times, while the minimum values underestimates the plume spread, despite  
 478 reproducing relatively well the time of first arrivals.

479 Thus, no effective, homogenized values of diffusion can be determined in a low  $Pe$   
 480 system. When velocity is relatively low, zones of low and of high diffusion coefficient have  
 481 a complex combined effect on transport that evolves as the plume moves through the het-  
 482 erogeneous domain. Therefore, even when the spatial variability in the SPHs, control-  
 483 ling advective fluxes is explicitly described, not accounting for the spatial variability of  
 484 the diffusion would require to artificially adjust effective advection. Such curve-fitting  
 485 approach would compromise the physical understanding of the system, which may have  
 486 detrimental consequences on the applicability of the model.

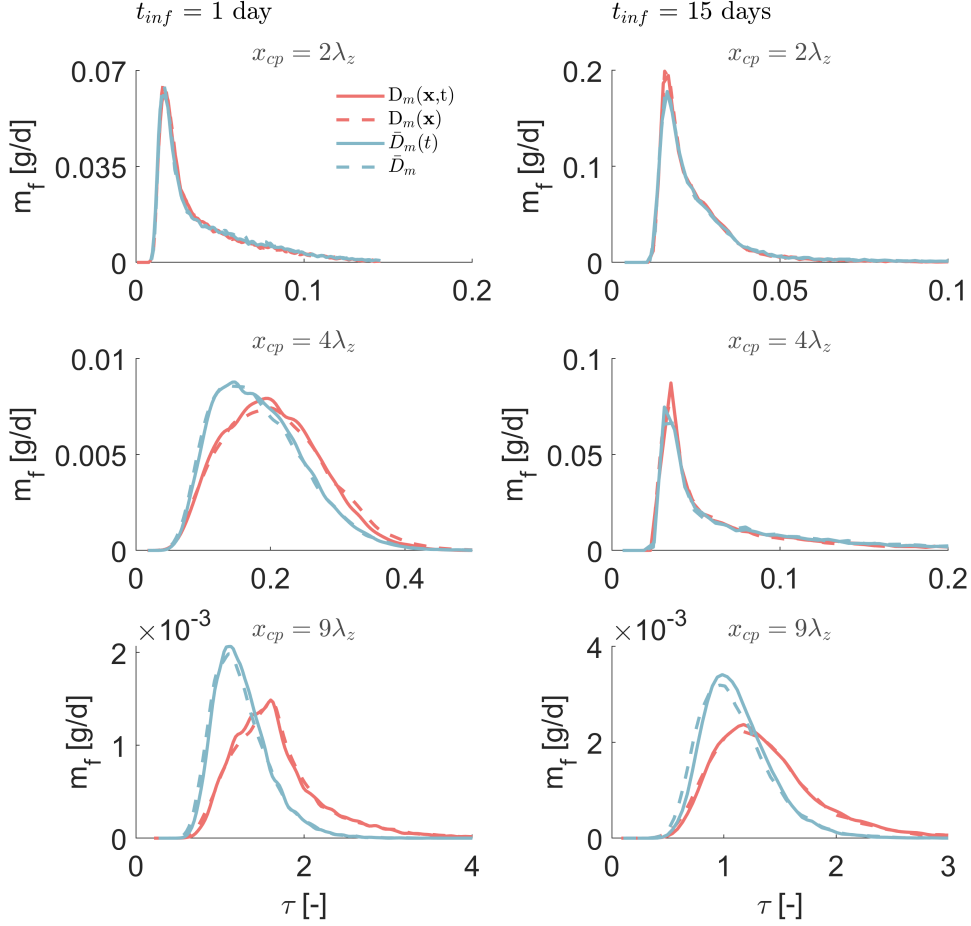


**Figure 10.** Breakthrough curves (BTCs) at three control planes (CP) resulting from simulations using a spatially variable, tortuosity-dependent diffusion coefficient ( $D_m(x)$ ) and a spatially averaged diffusion coefficient ( $\bar{D}_m$ ) for 1 day of infiltration (left hand) and 15 days of infiltration (right hand). Diffusion coefficients are considered transient ( $D_m(x,t)$  and  $\bar{D}_m(t)$ ) or steady state (temporally averaged). For all simulations, a high degree of heterogeneity in the SHPs ( $\sigma_\chi = 0.5$ ) is considered. Times are normalized by the characteristic advective time estimated for each duration of the infiltration period ( $t_{inf}$ ).

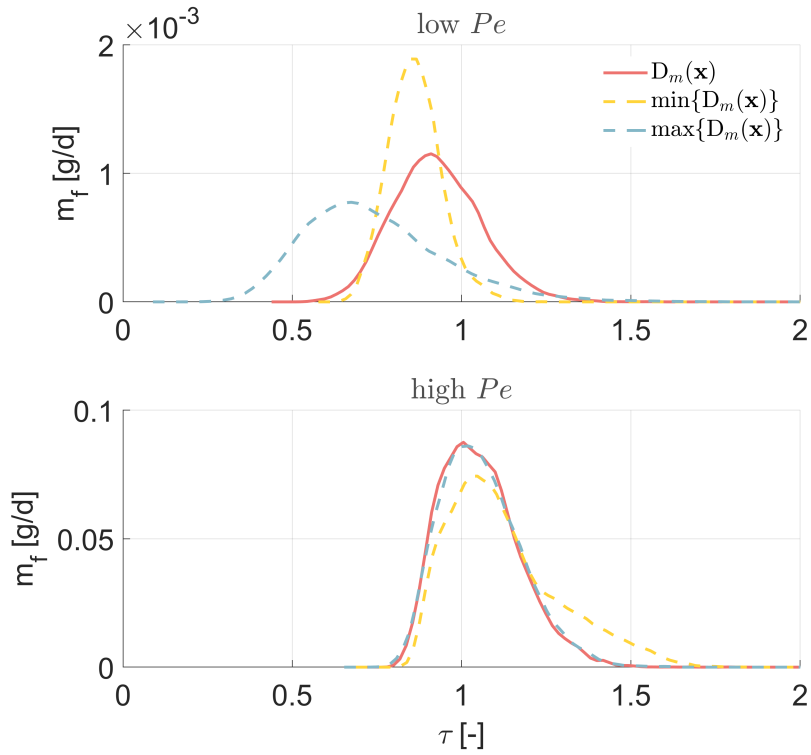


**Figure 11.** Breakthrough curves (BTCs) resulting from simulations using a spatially variable diffusion coefficient (red plain lines), the minimum (yellow dashed lines) and the maximum (blue dashed lines) values of  $D(x)$ , for a high recharge flux (bottom frames) and a low recharge flux (top frames). The degree of heterogeneity is described by  $\sigma_\chi=0.3$ . Times are normalized by the characteristic advective time of the  $D_m(x)$  scenario.

487 In case of high  $Pe$  number, a maximum values of  $D(x)$  produces satisfactory re-  
488 sults, while a minimum values tends to overestimate BTC tailing ((Figure 11, lower frame)).  
489 As advection remains the main controlling process, only the zones of high values of dif-  
490 fusion coefficients impact the transport. Maximizing the homogenized diffusion coeffi-  
491 cient reproduces then properly the release of mass from low velocity zones that prevent  
492 tailing to occur.

#### 493 **4 Concluding remarks**

494 Through a series of numerical simulations, this study analyzed the complex, syn-  
495 ergistic effect of (small scale) soil heterogeneity, advection and diffusion on conservative  
496 transport in unsaturated soils. Key findings are:

- 497 • The control of heterogeneity on transport is Peclet number dependent. For a low  
498 Peclet number, the mean advective time increases with the degree of soil hetero-  
499 geneity, while macrodispersion remains globally unchanged. The opposite is ob-  
500 served for the high Peclet case, which is characterized by a significant increase of  
501 (non-Fickian) macrodispersion and no real change in the mean advective flux when  
502 soil heterogeneity increases. The sensitivity of high Peclet systems to the degree  
503 of soil heterogeneity observed at the pore scale under saturated conditions by Nis-  
504 san & Berkowitz (2019) remains then valid at larger scale and for unsaturated con-  
505 ditions.
- 506 • Diffusion appears to be a key process controlling residence time of solutes in soils  
507 since it distributes contaminant mass in or out of low velocity zones. Thus, the  
508 impact of diffusion on transport is also highly dependent to the Peclet number,  
509 but only for a relatively high degree of heterogeneity. In this case, for a high Peclet  
510 number, diffusion decreases macrodispersion by allowing the remobilization of mass  
511 trapped in quasi-stagnant zones. This phenomena have been previously described  
512 by e.g., Weissmann et al. (2002) for a saturated aquifer and are now also observed  
513 for unsaturated conditions. Yet, in a low Peclet system, diffusion increases late  
514 arrival of mass. This appears to be linked to the tortuosity dependence of the dif-  
515 fusion coefficient assumed in this study. Unlike for high Peclet systems, our sim-  
516 ulated low Peclet soils are characterized by low values of the diffusion coefficient

517 in low velocity zones (due to the low water saturation value), which prevents the  
518 counter-intuitive reduction of macrodispersion when diffusion is considered.

- 519 • Thus, the spatial variability in the diffusion process is also a potential significant  
520 factor to understand transport behavior of solutes in soils. The impact of tortuosity-  
521 dependent diffusion process was found highly dependent on both the degree of het-  
522 erogeneity and the Peclet number due to (1) the importance that the diffusive pro-  
523 cess has in regard to the advective flux, and (2) the saturation dependence of the  
524 distribution of diffusion coefficients over the soil profile. Homogenizing the diffu-  
525 sion coefficient will disregard the dynamic feedback between mass accumulation  
526 in zones of low advective flux and the potential release of this mass, which is func-  
527 tion of the magnitude of the local diffusive process. The empirical relationship be-  
528 tween local tortuosity and the diffusion coefficient has then important implications  
529 in the dynamic of transport.

530 The practical implications of our theoretical study are potentially important. In-  
531 deed, different parametrization of the heterogeneity, velocity and diffusion can lead to  
532 significantly different first arrival of mass to the groundwater, more or less long term late  
533 arrivals and different peak concentrations reaching soil-connected water bodies. More-  
534 over, natural and cultivated soils are ubiquitously transient systems characterized by im-  
535 portant temporal variation in the advection flux. Periods of low and high Peclet num-  
536 bers due to infiltration or irrigation will result in periods of Fickian and non-Fickian trans-  
537 port characterized with significantly different mean advective velocity and effective dis-  
538 persion. The flow condition at the moment of field or laboratory observations is there-  
539 fore a key element to be considered to understand in depth the dynamic of the solute  
540 plume. This possible complex control of soil heterogeneity, Peclet number and diffusion  
541 on transport is expected to critically affect reaction and reactive transport, which remains  
542 to be investigated.

543 Globally, our outputs clearly highlight that small scale heterogeneity in soils and  
544 its overall impact on the spatial variability in diffusion must be considered to properly  
545 predict transport. Yet, a detailed characterization of this spatial variability is in most  
546 cases technically and economically infeasible. Upscaling approaches reproducing this com-  
547 plex impact of heterogeneity on advection, diffusion and therefore hydraulic structure  
548 are then required. Upscaling the effect of heterogeneity on *advective* fluxes has been the

549 focus on an important effort, mostly in saturated aquifers. Techniques such as the Multi-  
550 Rate Mass Transfer model (Haggerty & Gorelick, 1995), Continuous Time Random Walk  
551 (Berkowitz et al., 2006), and the fractional Advection-Dispersion Equation (Benson et  
552 al., 2000) have indeed been developed to reproduce late arrival times, which is typically  
553 the main BTC feature characterizing non-Fickian transport in saturated media. Yet, our  
554 work shows that both the heterogeneous advective flux and diffusive flux should be si-  
555 multaneously upscaled in soils. Indeed, as our results display, (1) a simple homogeniza-  
556 tion of the diffusion coefficient is not sufficient due to the complex and dynamic mass  
557 transfer from and into zones of low velocities, and (2) temporal variations in fluxes con-  
558 ditions the effective impact of diffusion on transport. Guo et al. (2019) exposed the dif-  
559 ficulties of upscaling techniques to perform well under transient conditions, which the  
560 authors attempted to solve later on by explicitly accounting for the advective flux de-  
561 pendence of mass transfer coefficients (Guo et al., 2020). In a future study, one could  
562 attempt to develop a similar approach for unsaturated soils, accounting for both tran-  
563 sient advective fluxes and transient diffusive fluxes.

564 To finish, it is important to emphasize on the theoretical and incomplete nature  
565 of this work. For instance, real soils are in more cases more heterogeneous than what has  
566 been assumed in this study (biopores, cracks, hydrophobicity, etc). Moreover, our con-  
567 clusions rely on the application of a series of (well established) equations but also on an  
568 empirical relationship between diffusion and tortuosity. While this relation is based on  
569 observations, its impact on transport under heterogeneous conditions remains to also be  
570 validated by in-situ or laboratory observations.

## 571 **Open Research Section**

572 This study is theoretical by nature and does not utilize any known database. In-  
573 stead, model parameters are listed throughout the manuscript. Flow simulations can be  
574 reproduced using the Daisy model (Hansen et al., 2012; Holbak et al., 2022) available  
575 at: <https://daisy.ku.dk/download/>. Transport simulations can be reproduced using  
576 the code RW3D (Henri & Diamantopoulos, 2022). Its source files and an executable are  
577 available at: <https://doi.org/10.5281/zenodo.6607599>.

578 **Acknowledgments**

579 The authors gratefully acknowledge the financial support through the Research Exec-  
 580 utive Agency of the European Commission, Grant Agreement number: 896470.

581 **References**

- 582 Bear, J. (1972). *Dynamics of Fluids in Porous Media*. New York: American Elsevier  
 583 Publishing Company. (764 p.)
- 584 Benson, D. A., Wheatcraft, S. W., & Meerschaert, M. M. (2000). The fractional-  
 585 order governing equation of lévy motion. *Water Resources Research*, *36*(6), 1413-  
 586 1423. Retrieved from [https://agupubs.onlinelibrary.wiley.com/doi/abs/10](https://agupubs.onlinelibrary.wiley.com/doi/abs/10.1029/2000WR900032)  
 587 [.1029/2000WR900032](https://doi.org/10.1029/2000WR900032) doi: <https://doi.org/10.1029/2000WR900032>
- 588 Berkowitz, B., Cortis, A., Dentz, M., & Scher, H. (2006). Modeling non-fickian  
 589 transport in geological formations as a continuous time random walk. *Re-*  
 590 *views of Geophysics*, *44*(2). Retrieved from [https://agupubs.onlinelibrary](https://agupubs.onlinelibrary.wiley.com/doi/abs/10.1029/2005RG000178)  
 591 [.wiley.com/doi/abs/10.1029/2005RG000178](https://doi.org/10.1029/2005RG000178) doi: [https://doi.org/10.1029/](https://doi.org/10.1029/2005RG000178)  
 592 [2005RG000178](https://doi.org/10.1029/2005RG000178)
- 593 Botros, F. E., Onsoy, Y. S., Ginn, T. R., & Harter, T. (2012, nov). Richards  
 594 Equation-Based Modeling to Estimate Flow and Nitrate Transport in a Deep  
 595 Alluvial Vadose Zone. *Vadose Zone Journal*, *11*(4), vzj2011.0145. Retrieved from  
 596 <http://doi.wiley.com/10.2136/vzj2011.0145> doi: [10.2136/vzj2011.0145](https://doi.org/10.2136/vzj2011.0145)
- 597 Boudreau, B. P. (1996). The diffusive tortuosity of fine-grained unlithified sedi-  
 598 ments. *Geochimica et Cosmochimica Acta*, *60*(16), 3139-3142. Retrieved from  
 599 <https://www.sciencedirect.com/science/article/pii/0016703796001585>  
 600 doi: [https://doi.org/10.1016/0016-7037\(96\)00158-5](https://doi.org/10.1016/0016-7037(96)00158-5)
- 601 Bromly, M., & Hinz, C. (2004). Non-fickian transport in homogeneous unsat-  
 602 urated repacked sand. *Water Resources Research*, *40*(7). Retrieved from  
 603 <https://agupubs.onlinelibrary.wiley.com/doi/abs/10.1029/2003WR002579>  
 604 doi: <https://doi.org/10.1029/2003WR002579>
- 605 Cirpka, O. A., & Kitanidis, P. K. (2002). Numerical evaluation of solute disper-  
 606 sion and dilution in unsaturated heterogeneous media. *Water Resources Research*,  
 607 *38*(11), 2-1-2-15. doi: [10.1029/2001wr001262](https://doi.org/10.1029/2001wr001262)
- 608 Cremer, C. J., Neuweiler, I., Bechtold, M., & Vanderborght, J. (2016, jun). So-  
 609 lute Transport in Heterogeneous Soil with Time-Dependent Boundary Condi-

- 610 tions. *Vadose Zone Journal*, 15(6), vzj2015.11.0144. Retrieved from <http://doi.wiley.com/10.2136/vzj2015.11.0144> doi: 10.2136/vzj2015.11.0144
- 611
- 612 Cremer, C. J. M., & Neuweiler, I. (2019, dec). How Dynamic Boundary Conditions  
613 Induce Solute Trapping and Quasi-stagnant Zones in Laboratory Experiments  
614 Comprising Unsaturated Heterogeneous Porous Media. *Water Resources Research*,  
615 55(12), 10765–10780. Retrieved from <https://onlinelibrary.wiley.com/doi/10.1029/2018WR024470> doi: 10.1029/2018WR024470
- 616
- 617 Cushman, J. H. (1984). On unifying the concepts of scale, instrumentation, and  
618 stochastics in the development of multiphase transport theory. *Water Resources  
619 Research*, 20(11), 1668-1676. Retrieved from [https://agupubs.onlinelibrary  
620 .wiley.com/doi/abs/10.1029/WR020i011p01668](https://agupubs.onlinelibrary.wiley.com/doi/abs/10.1029/WR020i011p01668) doi: [https://doi.org/10.1029/  
621 WR020i011p01668](https://doi.org/10.1029/WR020i011p01668)
- 622 Diamantopoulos, E., & Durner, W. (2012). Dynamic nonequilibrium of water flow in  
623 porous media: A review. *Vadose Zone J.*, 11(0).
- 624 Fernández-García, D., Illangasekare, T. H., & Rajaram, H. (2005). Differences in the  
625 scale-dependence of dispersivity estimated from temporal and spatial moments in  
626 chemically and physically heterogeneous porous media. *Adv. Water Res.*, 28(7),  
627 745-759.
- 628 Forrer, I., Kasteel, R., Flury, M., & Flühler, H. (1999, oct). Longitudinal and lateral  
629 dispersion in an unsaturated field soil. *Water Resources Research*, 35(10), 3049–  
630 3060. Retrieved from <http://doi.wiley.com/10.1029/1999WR900185> doi: 10  
631 .1029/1999WR900185
- 632 Ghanbarian, B., Hunt, A. G., Ewing, R. P., & Sahimi, M. (2013). Tortuosity in  
633 Porous Media: A Critical Review. *Soil Science Society of America Journal*, 77(5),  
634 1461–1477. doi: 10.2136/sssaj2012.0435
- 635 Guo, Z., Fogg, G. E., Brusseau, M. L., LaBolle, E. M., & Lopez, J. (2019). Mod-  
636 eling groundwater contaminant transport in the presence of large heterogeneity:  
637 a case study comparing mt3d and rwhet. *Hydrogeology Journal*, 27(4), 1363–  
638 1371. Retrieved from <https://doi.org/10.1007/s10040-019-01938-9> doi:  
639 10.1007/s10040-019-01938-9
- 640 Guo, Z., Henri, C. V., Fogg, G. E., Zhang, Y., & Zheng, C. (2020). Adaptive mul-  
641 tivariate mass transfer (ammt) model: A new approach to upscale regional-scale  
642 transport under transient flow conditions. *Water Resources Research*, 56(2),

- 643 e2019WR026000. Retrieved from <https://agupubs.onlinelibrary.wiley.com/doi/abs/10.1029/2019WR026000> doi: <https://doi.org/10.1029/2019WR026000>
- 644
- 645 Haggerty, R., & Gorelick, S. M. (1995). Multiple-rate mass transfer for modeling diffusion and surface reactions in media with pore-scale heterogeneity. *Water Resources Research*, *31*(10), 2383–2400. Retrieved from <https://agupubs.onlinelibrary.wiley.com/doi/abs/10.1029/95WR10583> doi: <https://doi.org/10.1029/95WR10583>
- 646
- 647
- 648
- 649
- 650 Hammel, K., & Roth, K. (1998, apr). Approximation of asymptotic dispersivity of conservative solute in unsaturated heterogeneous media with steady state flow. *Water Resources Research*, *34*(4), 709–715. Retrieved from <http://doi.wiley.com/10.1029/98WR00004> doi: 10.1029/98WR00004
- 651
- 652
- 653
- 654 Hansen, B., Dalgaard, T., Thorling, L., Sørensen, B., & Erlandsen, M. (2012). Regional analysis of groundwater nitrate concentrations and trends in denmark in regard to agricultural influence. *Biogeosciences*, *9*, 3277–3286.
- 655
- 656
- 657 Henri, C. V., & Diamantopoulos, E. (2022). Unsaturated transport modeling: Random-walk particle-tracking as a numerical-dispersion free and efficient alternative to eulerian methods. *Journal of Advances in Modeling Earth Systems*, *14*(9), e2021MS002812. Retrieved from <https://agupubs.onlinelibrary.wiley.com/doi/abs/10.1029/2021MS002812> (e2021MS002812 2021MS002812) doi: <https://doi.org/10.1029/2021MS002812>
- 658
- 659
- 660
- 661
- 662
- 663 Henri, C. V., & Fernández-García, D. (2014). Toward efficiency in heterogeneous multispecies reactive transport modeling: A particle-tracking solution for first-order network reactions. *Water Resour. Res.*, *50*(9), 7206–7230.
- 664
- 665
- 666 Henri, C. V., & Fernández-García, D. (2015). A random walk solution for modeling solute transport with network reactions and multi-rate mass transfer in heterogeneous systems: Impact of biofilms. *Adv.in Water Resour.*, *86*, 119.
- 667
- 668
- 669 Holbak, M., Abrahamsen, P., & Diamantopoulos, E. (2022). Modeling preferential water flow and pesticide leaching to drainpipes: The effect of drain-connecting and matrix-terminating biopores. *Water Resources Research*, *58*(7), e2021WR031608.
- 670
- 671
- 672 Holbak, M., Abrahamsen, P., Hansen, S., & Diamantopoulos, E. (2021). A physically based model for preferential water flow and solute transport in drained agricultural fields. *Water Resources Research*, *57*(3), e2020WR027954.
- 673
- 674
- 675 Jarvis, N., Koestel, J., & Larsbo, M. (2016). Understanding preferential flow in the

- 676 vadose zone: Recent advances and future prospects. *Vadose Zone Journal*, 15(12),  
677 1–11.
- 678 Javaux, M., Vanderborght, J., Kasteel, R., & Vanclooster, M. (2006a). Three-  
679 dimensional modeling of the scale-and flow rate-dependency of dispersion in a  
680 heterogeneous unsaturated sandy monolith. *Vadose Zone Journal*, 5(2), 515–528.
- 681 Javaux, M., Vanderborght, J., Kasteel, R., & Vanclooster, M. (2006b, may). Three-  
682 Dimensional Modeling of the Scale- and Flow Rate-Dependency of Dispersion  
683 in a Heterogeneous Unsaturated Sandy Monolith. *Vadose Zone Journal*, 5(2),  
684 515–528. Retrieved from <http://doi.wiley.com/10.2136/vzj2005.0056> doi:  
685 10.2136/vzj2005.0056
- 686 Khan, A. U.-H., & Jury, W. A. (1990). A laboratory study of the dispersion scale  
687 effect in column outflow experiments. *Journal of Contaminant Hydrology*, 5(2),  
688 119–131.
- 689 Miller, E., & Miller, R. (1956). Physical theory for capillary flow phenomena. *Jour-  
690 nal of Applied Physics*, 27(4), 324–332.
- 691 Millington, R. J., & Quirk, J. P. (1961). Permeability of porous solids. *Transactions  
692 of the Faraday Society*, 57, 1200. Retrieved from [http://xlink.rsc.org/?DOI=  
693 tf9615701200](http://xlink.rsc.org/?DOI=tf9615701200) doi: 10.1039/tf9615701200
- 694 Møldrup, P., Olesen, T., Rolston, D., & Yamaguchi, T. (1997). Modeling diffusion  
695 and reaction in soils: Vii. predicting gas and ion diffusivity in undisturbed and  
696 sieved soils. *Soil Science*, 162(9), 632–640.
- 697 Nissan, A., & Berkowitz, B. (2019, mar). Anomalous transport dependence on  
698 Péclet number, porous medium heterogeneity, and a temporally varying velocity  
699 field. *Physical Review E*, 99(3), 033108. Retrieved from [https://link.aps.org/  
700 doi/10.1103/PhysRevE.99.033108](https://link.aps.org/doi/10.1103/PhysRevE.99.033108) doi: 10.1103/PhysRevE.99.033108
- 701 Richards, L. A. (1931). Capillary conduction of liquids through porous mediums.  
702 *Journal of Applied Physics*, 1(5), 318–333.
- 703 Richardson, L. F. (1922). *Weather prediction by numerical process*. New York: Cam-  
704 bridge University Press. (Cambridge: Cambridge mathematical library)
- 705 Roth, K. (1995, sep). Steady State Flow in an Unsaturated, Two-Dimensional,  
706 Macroscopically Homogeneous, Miller-Similar Medium. *Water Resources Research*,  
707 31(9), 2127–2140. Retrieved from <http://doi.wiley.com/10.1029/95WR00946>  
708 doi: 10.1029/95WR00946

- 709 Roth, K., & Hammel, K. (1996, jun). Transport of conservative chemical through an  
710 unsaturated two-dimensional Miller-similar medium with steady state flow. *Water*  
711 *Resources Research*, *32*(6), 1653–1663. Retrieved from [http://doi.wiley.com/10](http://doi.wiley.com/10.1029/96WR00756)  
712 [.1029/96WR00756](http://doi.wiley.com/10.1029/96WR00756) doi: 10.1029/96WR00756
- 713 Russo, D. (1993). Stochastic modeling of macrodispersion for solute transport in  
714 a heterogeneous unsaturated porous formation. *Water Resources Research*, *29*(2),  
715 383–397. Retrieved from [https://agupubs.onlinelibrary.wiley.com/doi/abs/](https://agupubs.onlinelibrary.wiley.com/doi/abs/10.1029/92WR01957)  
716 [10.1029/92WR01957](https://doi.org/10.1029/92WR01957) doi: <https://doi.org/10.1029/92WR01957>
- 717 Russo, D. (2015, may). On the effect of connectivity on solute transport in spatially  
718 heterogeneous combined unsaturated-saturated flow systems. *Water Resources*  
719 *Research*, *51*(5), 3525–3542. Retrieved from [http://doi.wiley.com/10.1002/](http://doi.wiley.com/10.1002/2014WR016434)  
720 [2014WR016434](http://doi.wiley.com/10.1002/2014WR016434) doi: 10.1002/2014WR016434
- 721 Russo, D., & Fiori, A. (2009, mar). Stochastic analysis of transport in a combined  
722 heterogeneous vadose zone-groundwater flow system. *Water Resources Research*,  
723 *45*(3), 1–16. Retrieved from <http://doi.wiley.com/10.1029/2008WR007157>  
724 doi: 10.1029/2008WR007157
- 725 Russo, D., Zaidel, J., & Laufer, A. (2000). Numerical analysis of flow and transport  
726 in a combined heterogeneous vadose zone-groundwater system. *Advances in Water*  
727 *Resources*, *24*(1), 49–62. doi: 10.1016/S0309-1708(00)00026-9
- 728 Russo, D., Zaidel, J., & Laufer, A. (2001, aug). Numerical analysis of flow and  
729 transport in variably saturated bimodal heterogeneous porous media. *Water Re-*  
730 *sources Research*, *37*(8), 2127–2141. Retrieved from [http://doi.wiley.com/10](http://doi.wiley.com/10.1029/2001WR000393)  
731 [.1029/2001WR000393](http://doi.wiley.com/10.1029/2001WR000393) doi: 10.1029/2001WR000393
- 732 Sadeghi, M., Ghahraman, B., Warrick, A. W., Tuller, M., & Jones, S. B. (2016). A  
733 critical evaluation of the miller and miller similar media theory for application to  
734 natural soils. *Water Resources Research*, *52*(5), 3829–3846.
- 735 Schelle, H., Durner, W., Schlüter, S., Vogel, H.-J., & Vanderborght, J. (2013). Vir-  
736 tual soils: Moisture measurements and their interpretation by inverse modeling.  
737 *Vadose Zone Journal*, *12*(3), 1–12.
- 738 Schlüter, S., Vanderborght, J., & Vogel, H. J. (2012). Hydraulic non-equilibrium  
739 during infiltration induced by structural connectivity. *Advances in Water Re-*  
740 *sources*, *44*, 101–112. doi: 10.1016/j.advwatres.2012.05.002
- 741 Shen, L., & Chen, Z. (2007). Critical review of the impact of tortuosity on diffusion.

- 742 *Chemical Engineering Science*, 62(14), 3748-3755. Retrieved from <https://www>  
743 [.sciencedirect.com/science/article/pii/S0009250907003144](https://www.sciencedirect.com/science/article/pii/S0009250907003144) doi: <https://>  
744 [doi.org/10.1016/j.ces.2007.03.041](https://doi.org/10.1016/j.ces.2007.03.041)
- 745 Ursino, N., & Gimmi, T. (2004). Combined effect of heterogeneity, anisotropy  
746 and saturation on steady state flow and transport: Structure recognition  
747 and numerical simulation. *Water Resources Research*, 40(1), 1–12. doi:  
748 10.1029/2003WR002180
- 749 Van Cappellen, P., & Gaillard, J.-F. (2018). Biogeochemical dynamics in aquatic  
750 sediments. In *Reactive transport in porous media* (pp. 335–376). De Gruyter.
- 751 Vanderborght, J., Mallants, D., & Feyen, J. (1998, dec). Solute transport in a  
752 heterogeneous soil for boundary and initial conditions: Evaluation of first-order  
753 approximations. *Water Resources Research*, 34(12), 3255–3270. Retrieved from  
754 <http://doi.wiley.com/10.1029/98WR02685> doi: 10.1029/98WR02685
- 755 Van Genuchten, M., & Wierenga, P. (1974). *Simulation of one-dimensional solute*  
756 *transfer in porous media*. New Mexico State University, Agricultural Experiment  
757 Station. Retrieved from <https://books.google.dk/books?id=kxInAQAAAJ>
- 758 Vogel, T., Gerke, H. H., Zhang, R., & Van Genuchten, M. T. (2000). Model-  
759 ing flow and transport in a two-dimensional dual-permeability system with spa-  
760 tially variable hydraulic properties. *Journal of Hydrology*, 238(1-2), 78–89. doi:  
761 10.1016/S0022-1694(00)00327-9
- 762 Šimunek, J., Šejna, M., Saito, H., Sakai, M., & Van Genuchten, M. (2013). The  
763 hydrus-1d software package for simulating the movement of water, heat, and mul-  
764 tiple solutes in variably saturated media, version 4.17, hydrus software series 3,  
765 department of environmental sciences, university of california riverside, riverside,  
766 california. USA.
- 767 Weissmann, G. S., Zhang, Y., LaBolle, E. M., & Fogg, G. E. (2002). Dispersion of  
768 groundwater age in an alluvial aquifer system. *Water Resour. Res.*, 38(10), 1198.
- 769 Woods, S. A., Dyck, M. F., & Kachanoski, R. G. (2013, may). Spatial and tem-  
770 poral variability of soil horizons and long-term solute transport under semi-  
771 arid conditions. *Canadian Journal of Soil Science*, 93(2), 173–191. Retrieved  
772 from <http://www.nrcresearchpress.com/doi/10.4141/cjss2012-082> doi:  
773 10.4141/cjss2012-082

1       **On the Control of Soil Heterogeneity, Peclet number**  
2       **and Spatially Variable Diffusion over Unsaturated**  
3       **Transport**

4                   **Christopher V. Henri<sup>1</sup>, Efstathios Diamantopoulos<sup>2</sup>**

5                   <sup>1</sup>Geological Survey of Denmark and Greenland, Copenhagen, Denmark

6                   <sup>2</sup>Chair of Soil Physics, University of Bayreuth, Bayreuth, Germany

7       **Key Points:**

- 8       • Small scale soil heterogeneity has a significant Peclet number dependent impact  
9       on main transport characteristics.
- 10      • Diffusion can have a profound impact on transport, which is dependent on soil het-  
11      erogeneity and the Peclet number.
- 12      • The spatial variability in the diffusion coefficient significantly controls transport,  
13      but remains complex to upscale.

---

Corresponding author: Christopher V. Henri, [cvh@geus.dk](mailto:cvh@geus.dk)

**Abstract**

Physical properties of soils are ubiquitously heterogeneous. This spatial variability has a profound, yet still partially understood, impact on conservative transport. Moreover, molecular diffusion is often a disregarded process that can have an important counter-intuitive effect on transport: diffusion can prevent non-Fickian tailing by mobilizing mass otherwise trapped in low velocity zones. Here, we focus on macroscopically homogeneous soils presenting small scale heterogeneity, as described by the Miller-Miller method. We then analyze the dynamic control of soil heterogeneity, advection and diffusion on conservative transport. We focus especially on the importance of diffusion and of its tortuosity-dependent spatial variability on the overall transport. Our results indicate that high Peclet number systems are highly sensitive to the degree of heterogeneity, which promotes non-Fickian transport. Also, diffusion appears to have a profound impact on transport, depending on both the degree of heterogeneity and the Peclet number. For a high Peclet number and a very heterogeneous system, diffusion leads to the counter-intuitive decrease of non-Fickian macrodispersion described previously. This is not observed for a low Peclet number due to the non-trivial impact of the spatial variability in the diffusion coefficient, which appears to be a significant controlling factor of transport by promoting or preventing the accumulation of mass in low velocity zones. Globally, this work (1) highlights the complex, synergistic effect of soil heterogeneity, advective fluxes and diffusion on transport and (2), alerts on potential upscaling challenges when the spatial variability of such key processes cannot be properly described.

**1 Introduction**

Understanding and predicting the dynamics of chemicals in soils is key to optimize agrochemical application while ensuring the protection of the water resources. However, the fate of chemicals in soils results from a complex interplay of physical, chemical and biological processes which are still not well understood. For a non-reactive, non-sorbing and non-volatile conservative solute, it is well established that the main physical processes controlling transport are advection, diffusion and dispersion (Bear, 1972). Thus, the advection-dispersion-diffusion equation (ADE), which mathematically describes those processes at the continuum scale (Cushman, 1984), represents to this day the most popular theory describing solute transport into porous media. Yet, the parameters in the

45 ADE are effective parameters, integrating small scale spatial variability in the physical  
46 properties of soils, which often challenges its application.

47 Soils are heterogeneous at any spatial scale, from the pore scale (mm) up to the  
48 catchment scale (km). Soil heterogeneity can result from diverse origins such as parent  
49 material, pedogenesis, soil organisms, plant roots and anthropogenic impact like man-  
50 agement operations (Schelle et al., 2013). Soil heterogeneity is intrinsically spatial scale  
51 dependent and it may include spatial variability of different properties. A heterogeneous  
52 soil can for example originate from different soil textures observed at relatively large scales  
53 ( $> \text{dm}$ , e.g., soil horizons), and/or from different arrangements of the same mineral grains  
54 at smaller spatial scales (cm). Some components can also span different spatial scales  
55 like macropores from earthworms, roots, etc (Jarvis et al., 2016; Holbak et al., 2022). In  
56 any ways, the variability in physical properties provokes variability in soil hydraulic prop-  
57 erties (SHPs), subsequently leading to dynamic hydraulic structures (Javaux et al., 2006a)  
58 exposing, e.g., a complex network of high flux channels with interspersed small volumes  
59 of low-flux domains (Roth, 1995).

60 The spatial variability of the physical properties of soils has a substantial effect on  
61 transport of conservative solutes, which has been extensively reported since the 1990's  
62 (e.g., Roth, 1995; Hammel & Roth, 1998; Javaux et al., 2006b; Russo & Fiori, 2009; C. J. M. Cre-  
63 mer & Neuweiler, 2019, among many others). Understanding this effect of heterogene-  
64 ity on transport dynamics is key to accurately estimate and predict solute transport to-  
65 ward the water resources (Russo, 2015) and to develop useful upscaling techniques (e.g.,  
66 dual-permeability approach, Vogel et al., 2000). Unsaturated heterogeneous transport  
67 has been experimentally observed under laboratory (Khan & Jury, 1990), large soil mono-  
68 liths (Javaux et al., 2006b) and field conditions (Forrer et al., 1999; Ursino & Gimmi,  
69 2004). Yet, the vast complexity of unsaturated systems has often led researchers to study  
70 the transport of conservative solutes in saturated/unsaturated porous media through nu-  
71 merical experiments. In most of those studies, soil heterogeneity has been explicitly rep-  
72 resented at the cm scale (Roth & Hammel, 1996), assuming the validity of a similarity  
73 model for the small scale SHPs, as done by, e.g., the Miller-Miller Similar Media The-  
74 ory (MMT) (Miller & Miller, 1956; Sadeghi et al., 2016).

75 Results from such studies show that the impact of heterogeneity on transport ap-  
76 pears to not be a well defined soil dependent feature, but results instead from the syn-

77 ergistic effect of constitutive material spatial variability and of dynamic flow conditions.  
78 For instance, decreasing the degree of saturation will increase the spread of the solute  
79 (Russo, 1993) and the effective recharge rate (i.e. vertical flux) controls more specifically  
80 the transverse dispersion (Roth & Hammel, 1996; Hammel & Roth, 1998; Forrer et al.,  
81 1999; Cirpka & Kitanidis, 2002). Thus, considering more realistic conditions in terms  
82 of contaminant input fluxes (Vanderborght et al., 1998), flow dynamic characterized by  
83 infiltration (downward fluxes)-evaporation (upward fluxes) periods (Russo et al., 2000,  
84 2001; C. J. Cremer et al., 2016; Henri & Diamantopoulos, 2022), or topography (Woods  
85 et al., 2013) results to even more complex transport behavior, which remains to this day  
86 challenging to systematically describe.

87 Despite an improved understanding of heterogeneous transport in soils, to this day,  
88 even models considering some type of heterogeneity generally fail to predict observed plume  
89 behavior, in terms of travel times and spread (Ursino & Gimmi, 2004), scale and flow  
90 rate dependency of transport (Javaux et al., 2006b), and contaminant concentrations (Botros  
91 et al., 2012). While it is a common knowledge that applying the ADE or any of its ex-  
92 tension (e.g., Mobile-Immobile theory (Van Genuchten & Wierenga, 1974)) can success-  
93 fully describe experimental data under different spatial scales, the predicting capabil-  
94 ities of those theories remain indeed limited, which highlight the complexity to fully rep-  
95 resent the variety of processes engaged in the subsurface.

96 In this context, it is worth mentioning that, although molecular diffusion is a pro-  
97 cess that is sometimes accounted for in numerical experiments (C. J. Cremer et al., 2016),  
98 its effect on transport is often disregarded. Nevertheless, some theoretical studies have  
99 highlighted diffusive transport as a potentially important process controlling factor of  
100 solute behavior under both unsaturated and saturated conditions (Weissmann et al., 2002;  
101 Nissan & Berkowitz, 2019; Cirpka & Kitanidis, 2002).

102 The importance of diffusion is in most cases studied relatively to advection. The  
103 Peclet number ( $Pe$ ), comparing advective and diffusive characteristic times, is then the  
104 reference metric to characterize dominance of either process to the overall transport. Im-  
105 portantly, it has been shown that the Peclet number controls the effect of heterogene-  
106 ity on solute transport. This observation has been made at different spatial scales and  
107 in both saturated and unsaturated conditions. For instance, studies by Nissan & Berkowitz  
108 (2019) at the (saturated) pore scale, Cirpka & Kitanidis (2002) at the (unsaturated) site

109 scale and (Weissmann et al., 2002) in a regional aquifer show that high  $Pe$  values (i.e.,  
110 a predominance of advection over diffusion) leads to more anomalous behavior compared  
111 to low  $Pe$  values. Inversely, transport at low  $Pe$  (i.e., diffusion-dominant) is character-  
112 ized by shorter residence times in stagnant zones, which reduces the anomalous behav-  
113 ior of transport. In simple terms, a strong diffusion reduces the “delay” in very low ve-  
114 locity zones of the porous medium by favoring the transfer of solute mass from these quasi-  
115 stagnant areas to more mobile ones. It has been also shown at the pore scale and un-  
116 der saturated conditions that this sensitivity of transport to  $Pe$  is accentuated by increas-  
117 ing the degree of heterogeneity in the porous media (Nissan & Berkowitz, 2019). Such  
118 transport dynamic remains to be confirmed at larger scale and under unsaturated con-  
119 ditions.

120 From the previous, it is obvious that the effect of molecular diffusion on transport  
121 is well documented, but the process is in most cases represented as being uniform (i.e.,  
122 described by a constant diffusion coefficient). Yet, it is also well documented that in any  
123 porous system, the presence of solid-air-liquid interfaces influences the diffusion paths  
124 of solute species (Boudreau, 1996). The effect of water content/porosity on the effective  
125 diffusive process is often represented as a dependence of the diffusion coefficient to tor-  
126 tuosity (Shen & Chen, 2007; Ghanbarian et al., 2013; Van Cappellen & Gaillard, 2018).  
127 In unsaturated soils, spatial and temporal variability in the water content can then make  
128 the diffusion process highly heterogeneous. Yet, rare are the studies that have explic-  
129 itly analyzed the effect of a tortuosity-dependency of the diffusion coefficient, especially  
130 under heterogeneous conditions. For instance, C. J. Cremer et al. (2016) uses the Milling-  
131 ton & Quirk (1961) method to account for tortuosity but the authors do not assess the  
132 relevance or the importance of such approach on diffusive transport.

133 This study aims on the understanding of conservative transport in unsaturated soils,  
134 and more specifically on the complex interplay between spatial heterogeneity of SHPs,  
135 advection and diffusion. As mentioned above, real soils are structured at many differ-  
136 ent scales (horizons, macropores, anisotropy, etc) and these components are expected to  
137 add additional complexity to water flow. In this study, we focused solely on the effect  
138 of small scale heterogeneity and its impact on transport, similar to the studies of Roth  
139 & Hammel (1996) and Hammel & Roth (1998). After analyzing the complex synergis-  
140 tic control of soil heterogeneity and infiltration flux, we will focus more specifically on

141 the superposed impact of diffusion and of its spatial variability on heterogeneous trans-  
 142 port.

## 143 2 Method

144 In the following, we briefly present the theory for i) simulating water flow and con-  
 145 servative transport in unsaturated soils, ii) representing heterogeneity with MMT, and  
 146 finally, iii) we provide an overview of all the tested numerical experiments.

### 147 2.1 Flow and transport

148 *Flow.* For a rigid, non-swelling, isotropic porous medium, water flow under vari-  
 149 able saturated conditions is described by the Richards-Richardson equation (Richards,  
 150 1931; Richardson, 1922):

$$\frac{\partial \theta}{\partial t} = -\nabla \cdot \theta \mathbf{u} = \nabla \cdot [K \nabla h] + \frac{\partial K}{\partial z} \quad (1)$$

151 where  $z$  is the vertical coordinate [L],  $h$  is the pressure head [L],  $\theta$  is the volumetric wa-  
 152 ter content [ $\text{L}^3 \text{L}^{-3}$ ],  $\mathbf{u}$  is the pore water velocity [ $\text{L T}^{-1}$ ] and  $K$  [ $\text{L T}^{-1}$ ] is the saturated/unsaturated  
 153 conductivity as a function of  $\theta$  or  $h$ . A prerequisite of Equation 1 is that the air pres-  
 154 sure in the soil at any system state is equal to the atmospheric pressure (single flow).

155 Eq. 1 assumes that, at the continuum scale (Cushman, 1984), a local equilibrium  
 156 between water content and pressure head is always valid (Diamantopoulos & Durner, 2012).  
 157 This relationship is described by the water retention curve:

$$h(S_e) = \frac{1}{\alpha} [S_e^{-n/(n-1)} - 1]^{(1/n)}, \quad (2)$$

158 where  $S_e$  [-] is the effective saturation given by:

$$S_e(\theta) = \frac{\theta - \theta_r}{\theta_s - \theta_r}, \quad (3)$$

and  $\alpha$  [ $\text{L}^{-1}$ ] and  $n$  [-] are shape parameters.  $\theta_s$  [ $\text{L}^3 \text{L}^{-3}$ ] and  $\theta_r$  [ $\text{L}^3 \text{L}^{-3}$ ] are saturated  
 and residual water contents. Finally, the conductivity as a function of effective satura-  
 tion is given by:

$$K(S_e) = K_s S_e^\tau [1 - (1 - S_e^{n/(n-1)})^{1-1/n}]^2 \quad (4)$$

159 For all the simulations presented in this work, we assumed a simulation domain of  
 160 80 cm in the horizontal direction ( $L_x$ ) and 240 cm in the vertical direction ( $L_z$ ). The  
 161 domain was discretized in cells of size  $d_x = 1$  cm and  $d_z = 2$  cm, respectively, resulting  
 162 in  $n_x = 80$  numerical nodes in the x-direction and  $n_z = 120$  in the z-direction. The length  
 163 of the domain was chosen to ensure 10 correlation lengths in each direction in order to  
 164 capture the full (i.e., ergodic) effect of heterogeneity (presented below in paragraph 2.2).  
 165 At the top nodes ( $z=0$  cm), a constant flux boundary condition was chosen, whereas at  
 166 the bottom ( $z=240$  cm) a unit-hydraulic head gradient was assumed. For the numer-  
 167 ical solution of Eq. 1, the finite-volume method as implemented in the Daisy model (Hansen  
 168 et al., 2012; Holbak et al., 2021) has been used.

*Transport.* Transport in the unsaturated zone for a conservative solute is described  
 by the advection-dispersion equation:

$$\frac{\partial(\theta c)}{\partial t} = -\nabla \cdot (\theta \mathbf{u} c) + \nabla \cdot (\theta \mathbf{D} \cdot \nabla c), \quad (5)$$

169 where  $c$  [ $\text{M L}^{-3}$ ] is the solute concentration,  $\theta$  [ $\text{L}^3 \text{L}^{-3}$ ] is the water content and  $\mathbf{D}^w$  [ $\text{L}^2$   
 170  $\text{T}^{-1}$ ] is the hydrodynamic dispersion tensor in the water phase given by (Bear, 1972):

$$\mathbf{D} = (\alpha_T |\mathbf{u}| + D_m) \delta + (\alpha_L - \alpha_T) \frac{\mathbf{u} \mathbf{u}^T}{|\mathbf{u}|}, \quad (6)$$

171 where  $\alpha_L$  [L] and  $\alpha_T$  [L] is the longitudinal and transverse dispersivities, respectively,  
 172  $D_m$  [ $\text{L}^2 \text{T}^{-1}$ ] is the molecular diffusion and  $\delta$  is the Kronecker delta function.

The ADE was solved using the Random Walk Particle Tracking (RWPT) method,  
 expressed as:

$$\mathbf{x}_p(t + \Delta t) = \mathbf{x}_p(t) + \mathbf{A}(\mathbf{x}_p, t) \Delta t + \mathbf{B}(\mathbf{x}_p, t) \cdot \xi(t) \sqrt{\Delta t}, \quad (7)$$

173 where  $\mathbf{x}_p$  is the particle location,  $\Delta t$  is the time step of the particles jump and  $\xi$  is a vec-  
 174 tor of independent, normally distributed random variables with zero mean and unit vari-  
 175 ance.

$$\mathbf{A} = \mathbf{u}(\mathbf{x}_p) + \nabla \cdot \mathbf{D}(\mathbf{x}_p) + \frac{1}{\theta(\mathbf{x}_p)} \mathbf{D}(\mathbf{x}_p) \cdot \nabla \theta(\mathbf{x}_p). \quad (8)$$

The displacement matrix relates to the dispersion tensor as:

$$2\mathbf{D} = \mathbf{B} \cdot \mathbf{B}^T. \quad (9)$$

176 The RWPT approach, implemented in the code RW3D (Fernández-García et al.,  
 177 2005; Henri & Fernández-García, 2014, 2015), is further described for application in un-  
 178 saturated conditions by Henri & Diamantopoulos (2022), who also shows how the La-  
 179 grangian method avoids numerical issues typically produced by Eulerian schemes.

*Diffusion.* The effective diffusion coefficient ( $D_m$ ) was considered to be dependent on the local water content value (Shen & Chen, 2007):

$$D_m(\theta) = D_w \times \tau_w(\theta), \quad (10)$$

where  $D_w$  [ $L^2 T^{-1}$ ] is the diffusion coefficient in free water, and  $\tau_w(\theta)$  is the water content dependent tortuosity.  $\tau_w(\theta)$  is typically described empirically. Different models are frequently used, and in this study the relationship described by Millington & Quirk (1961) was used:

$$\tau_w(\theta) = \frac{\theta^{7/3}}{\theta_s^2}. \quad (11)$$

For comparison, we also consider the relationship proposed by Møldrup et al. (1997):

$$\tau_w(\theta) = 0.66 \times \left( \frac{\theta}{\theta_s} \right)^{8/3}. \quad (12)$$

180 The Millington & Quirk (1961) tortuosity model is expected to perform better for  
 181 sands, since it was derived assuming randomly distributed particles of equal size. On the  
 182 other hand, the tortuosity model proposed by Møldrup et al. (1997) is expected to per-  
 183 form better across soil types (Šimunek et al., 2013).

184 For each simulation,  $10^5$  particles were injected randomly over a transect of 40 cm  
 185 located at the center of the top of the domain. To avoid potential subsampling due to  
 186 particles leaving the sides of the domain, a semi-infinite width was considered by trans-  
 187 ferring particles leaving the domain at  $x=0$  and  $x=L_x$  to the other side of the domain,  
 188 at  $x=L_x$  and  $x=0$ , respectively. The impact of such approximation, previously used by,  
 189 e.g., Cirpka & Kitanidis (2002), appears to be minor on both apparent velocity and dis-  
 190 persion, and does not therefore affect our conclusions (see Supplementary Information,  
 191 Figure S1).

The time step between particle jumps was defined to preserve the advective displacement, which was done using a grid Courant number ( $gCu$ ) as:

$$\Delta t = gCu \times \Delta s / \min\{u_x, u_y, u_z\}, \quad (13)$$

**Table 1.** Hydraulic properties of the reference material used for all simulations: saturated ( $\theta_s$ ) and residual ( $\theta_r$ ) water contents, shape parameters ( $\alpha$ ,  $n$ ), saturated hydraulic conductivity ( $K_s$ ).

Material	$\theta_r$ [ $\text{cm}^3 \text{cm}^{-3}$ ]	$\theta_s$ [ $\text{cm}^3 \text{cm}^{-3}$ ]	$\alpha$ [ $\text{cm}^{-1}$ ]	$n$ [-]	$K_s$ [ $\text{cm h}^{-1}$ ]
Loam	0.00	0.49	0.0066	1.68	1.8

192 where  $\Delta s$  is the characteristic size of the grid cell.

## 193 2.2 Representation of soil heterogeneity

194 Small scale soil heterogeneity was modeled using the MMT method (Miller & Miller,  
195 1956; Sadeghi et al., 2016). Briefly, the theory assumes that similarities at the pore scale  
196 geometry yields characteristic length or scaling factors ( $\zeta$ ), which scale the physical prop-  
197 erties of porous media, in this case the water retention and hydraulic conductivity curve  
198 (Roth & Hammel, 1996; Schelle et al., 2013; Sadeghi et al., 2016). For each location  $\mathbf{x}$ ,  
199 we can then calculate location-dependent soil hydraulic properties by:

$$h(\mathbf{x}, \theta) = h^*(\theta) \frac{1}{\zeta(\mathbf{x})}, \quad (14)$$

$$K(\mathbf{x}, \theta) = K^*(\theta) \zeta(\mathbf{x})^2, \quad (15)$$

200 where  $h^*(\theta)$  and  $K^*(\theta)$  are reference material properties, described in Eq. 2 and  
201 Eq. 4. Detailed theoretical considerations for MMT along with an overview of theory  
202 applications is provided in Sadeghi et al. (2016). For all simulations, we assumed a sin-  
203 gular loam material and the parameters of Eq. 2-4 are provided in Table 1. The spatial  
204 distribution of the log-scaling factor  $\chi \equiv \log_{10}(\zeta)$  (presented above) was geostatistically  
205 described as a multi-Gaussian model characterized by an isotropic Gaussian covariance  
206 function with zero mean and a standard deviation  $\sigma_\chi$ . Different  $\sigma_\chi$  values have been tested  
207 in this study. Finally, the correlation length in  $x$  ( $\lambda_x$ ) and  $z$  ( $\lambda_z$ ) was fixed to 8 cm and  
208 24 cm, respectively, following the work of Schlüter et al. (2012).

209 The Miller-Miller theory assumes that porosity, and thus water content at satu-  
210 ration ( $\theta_s$ ), is constant (through out this work equal to  $0.49 \text{ cm}^3 \text{cm}^{-3}$ , Table 1). To test

211 the implications of spatial distributed  $\theta_s$ , we also ran a set of simulations scaling  $\theta_s$  lin-  
 212 early as a function of the local  $K_s$  value, with a minimum and maximum value of 0.3 and  
 213 0.6, respectively. In that way, the test simulations assumed that high values of  $\theta_s$  coin-  
 214 cide with high values of  $K_s$ . This was only done for a high heterogeneity and a low mean  
 215 velocity ( $\sigma_\chi = 0.5$  and  $q = 0.01$  mm/h, diffusion dominated process), which represent  
 216 the scenario most likely to be affected by an assumed constant  $\theta_s$ .

### 217 **2.3 Tested scenarios**

218 Water flow was simulated for a series of steady-state simulations, assuming three  
 219 different degrees of heterogeneity ( $\sigma_\chi = 0.1, 0.3, 0.5$ ) and two different imposed verti-  
 220 cal water fluxes ( $q_{z,in} = 0.01, 1$  mm/h), and thus, different hydraulic structures (Ta-  
 221 ble 2). The low flux represents a scenario strongly dominated by diffusion (low mean ve-  
 222 locity), whereas the high flux represents a scenario with a stronger advective component,  
 223 as observed during an infiltration period. For each combination of  $\sigma_\chi$  and  $q_{z,in}$ , 20 re-  
 224 alizations have been created. While this limited number of realization is not likely to be  
 225 sufficient for a stochastic analysis, observing results from a series of equiprobable flow  
 226 fields will allow to determine if our observation are realization specific or systematic.

227 For all the water flow simulations, solute transport was also simulated. The non-  
 228 represented effect of heterogeneity within a grid cell was accounted for by setting a grid-  
 229 scale dispersivity values of 0.1 cm in the longitudinal direction (i.e.,  $z$ ), and 0.01 cm in  
 230 in the transverse direction (i.e.,  $x$ ). Moreover,  $D_w$  was fixed to  $1.6 \text{ cm}^2/\text{d}$  ( order of mag-  
 231 nitude similar to, e.g., C. J. Cremer et al. (2016)). To better understand the implica-  
 232 tions of a spatially variable diffusion process, we tested 2 different methods on simulat-  
 233 ing the diffusion coefficient (Table 2):

- 234 • A spatially variable, tortuosity (i.e., water content) dependent diffusion coefficient  
 235 ( $D_m(\mathbf{x})$ ), with a tortuosity model described by (Millington & Quirk, 1961), as de-  
 236 scribed in Eq. 11;
- 237 • A spatially averaged diffusion coefficient ( $\bar{D}_m$ ).

238 The diffusion coefficient was considered to be the same values in the  $x$  and  $z$  direction.

239 Finally, we evaluated the effect of transient conditions on solute transport in a highly  
 240 heterogeneous soil ( $\sigma_\chi = 0.5$ , Table 2). Transient conditions are caused by an infiltra-

**Table 2.** Tested scenarios.

Description	Heterogeneity	Water flow	Diffusion
Steady state simulations (20 realizations)	$\sigma_\chi = 0.1$	$q_{z,in} = 0.01$ mm/h	Constant, averaged ( $\bar{D}_m$ )
	$\sigma_\chi = 0.3$	$q_{z,in} = 1$ mm/h	Tortuosity dependent ( $D_m(x)$ )
	$\sigma_\chi = 0.5$		
Transient simulations (1 realization)	$\sigma_\chi = 0.5$	1 day of strong infiltration	Constant, averaged ( $\bar{D}_m$ )
		15 days of strong infiltration	Tortuosity dependent ( $D_m(x)$ )

241 tion period followed by a long redistribution period. Two different infiltration periods  
 242 ( $t_{inf}$ ) are considered: 1 and 15 days. The two models of diffusion tested for the steady  
 243 state simulations are here also considered.

### 244 3 Results

#### 245 3.1 Small scale soil heterogeneity and advective flux

246 In this section, we analyze simulation results of a single realization. Nevertheless,  
 247 we also present outputs from the ensemble of 20 realizations in term of arrival time statis-  
 248 tics to ensure that observations made on a single realization are consistent across real-  
 249 ization.

250 *Flow fields.* Throughout our analysis, the intensity of the advective flux is char-  
 251 acterized by the Peclet number ( $Pe$ ), which is estimated as:

$$Pe = \frac{\bar{u}_z \lambda_z}{D_m}. \quad (16)$$

252 where  $\bar{u}_z$  [ $L T^{-1}$ ] is the average pore water velocity in the  $z$  direction.

253 The resulting Peclet numbers, for each degree of heterogeneity, was equal to  $3.3 \times 10^{-1}$ ,  
 254  $3.3 \times 10^{-1}$ ,  $3.4 \times 10^{-1}$ , respectively, for the high flux; and equal to  $4.0 \times 10^{-2}$ ,  $2.9 \times 10^{-2}$ ,  
 255  $1.9 \times 10^{-2}$ , respectively, for the low flux. According to the calculated Peclet numbers, all  
 256 scenarios are diffusion dominated ( $Pe < 1$ ). However, the low  $q_{z,in}$  simulations can be  
 257 characterised as strongly dominated by diffusion, due to the one order of magnitude lower  
 258 Peclet number.

259 The spatial variability of SHPs appears to significantly control both saturation and  
 260 local water fluxes. Clear patterns of quasi-dry ( $\theta < 0.1$ ) and near-saturated ( $\theta \approx \theta_s$ )  
 261 zones emerges when the degree of heterogeneity is increased (Figure 1, left frames; re-  
 262 sults from the lower degree of heterogeneity are shown in Supplementary Information,  
 263 Figure S2 and Figure S3).

264 The spatial variability in saturation is also highly sensitive to the intensity of the  
 265 infiltration flux (Figure 1, compare upper and lower left frames). Globally, saturation  
 266 is logically increased in case of higher  $Pe$ . Moreover, the degree of heterogeneity in com-  
 267 puted  $\theta$  in case of high  $\sigma_\chi$  appears to decrease when infiltration is stronger. We indeed  
 268 observe an increased predominance of fully saturated areas ( $\theta \approx \theta_s$ ), which is a direct  
 269 effect of MMT and the inherent assumption of equal saturated water content.

270 Similar observation can be made while analyzing the combined effect of soil het-  
 271 erogeneity and input flux on the spatial variability of computed water (Darcian) fluxes  
 272 (Figure 1, middle frame) and pore velocities (Figure 1, right frame): (1) Increasing  $\sigma_\chi$   
 273 generates clear zones of low velocity and fast paths, and (2) increasing the infiltration  
 274 flux globally increases fluxes and increase the portion of the soil column occupied by high  
 275 velocity zones. These results are globally consistent with past work such that of Roth  
 276 (1995), who also observed the clear formation of islands of low and high fluxes due to  
 277 a similar Miller-Miller heterogeneous media and the sensitivity of this hydraulic struc-  
 278 ture to the input flux.

279 *Spatial moments.* The effect of heterogeneity and infiltration flux on the dynamic  
 280 hydraulic structure is reflected on the transport behavior of the applied particles. We  
 281 first analyze the lower spatial moments of the plume: the first moment,  $z_g$ , represents  
 282 the location of the center of mass, and the second spatial moment,  $S_{zz}$ , quantifies the  
 283 spread around the centroid of the plume.

284 Spatial moments are evaluated until particles start to leave the downstream edge  
 285 of the domain to reflect the dynamics of the entire plume. Only results from simulations  
 286 using the ‘‘Millington and Quirk’’ model of tortuosity is shown throughout our analy-  
 287 sis. The analysis using the ‘‘Moldrup et al.’’ model leads to similar results as shown in  
 288 Supplementary Information, Figure S4.

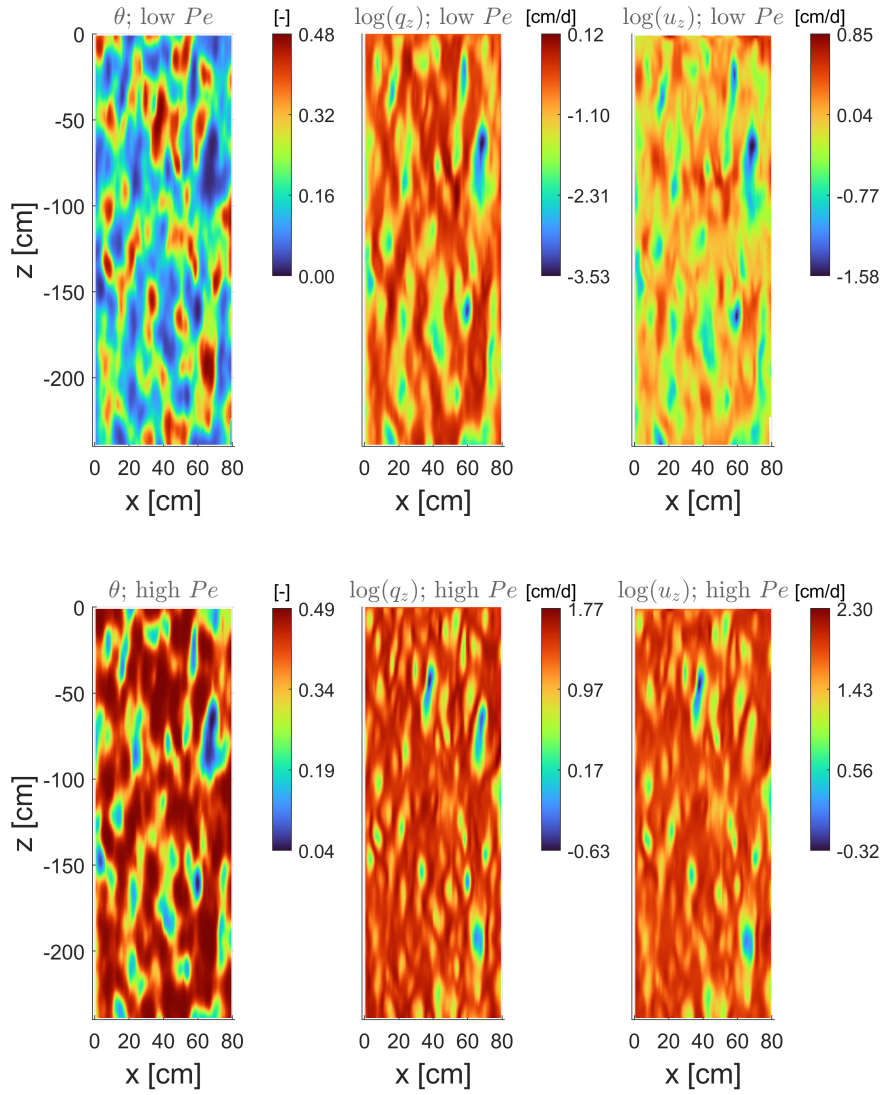


**Figure 1.** Resulting spatial distribution of the water content ( $\theta$ ) for the highest degree of soil heterogeneity ( $\sigma_\chi = 0.5$ ) and for a high recharge flux (i.e., high Peclet number; bottom frames) and a low recharge flux (i.e., low Peclet number; top frames).

289 The center of mass of the plume is highly sensitive to the degree of heterogeneity  
 290 in SHPs for the case of low  $Pe$  number (Figure 2). For the same infiltration flux, the plume  
 291 moves downward faster in case of low  $\sigma_\chi$  (Figure 2, top left frame). The effective veloc-  
 292 ities in the downward direction associated to each  $\sigma_\chi$  values,  $v_z^*$ , can be quantified as the  
 293 slope of the linear regression of  $z_g(t)$ , giving: 0.12, 0.08 and 0.05 cm/d for the low in-  
 294 put flux scenario, respectively, and 6.1, 6.0, 5.2 cm/d for the high input flux scenario.  
 295 Characteristic advection times can then be estimated as:  $t_{adv} = L_z/v_z^*$ .

296 Interestingly, the temporal evolution of the first spatial moment observed for the  
 297 low  $Pe$  case presents a non-linearity that increases with  $\sigma_\chi$ . This results to periods of  
 298 acceleration and of slowing down of the center of mass of the plume and not to a con-  
 299 stant effective velocity as observed in case of  $\sigma_\chi=0.1$ . The sensitivity of the effective ve-  
 300 locity to the degree of heterogeneity is lower in case of high  $Pe$  (Figure 2, top right frame).  
 301 This non-linearity appears to be more or less pronounced depending on the realizations  
 302 (Supplementary Information, Figure S5).

303 The spread of the plume appears to be less sensitive to  $\sigma_\chi$  in case of a low  $Pe$  than  
 304 in case of a high  $Pe$  (Figure 2, compare bottom frames). For a high  $Pe$ , the spread is  
 305 significantly increased for the highest degree of heterogeneity. For the low  $Pe$ , a low in-  
 306 put flux applied on a highly heterogeneous media leads to different regimes of spread of  
 307 the plume, with an intensification of the spread at early and intermediate times (Fig-  
 308 ure 2, bottom left frame). These fluctuations are observed for most realizations (Sup-  
 309 plementary Information, Figure S6). Yet, the average magnitude of the spread remains  
 310 globally similar for all  $\sigma_\chi$ , unlike for a high  $Pe$ .

311 *Breakthrough curves.* Such observations have clear implications in term of mass  
 312 transfer from the soil to deeper layers and into the aquifer. When heterogeneity is in-  
 313 creased in a low velocity system, the breakthrough curve recorded at the bottom of the  
 314 simulated domain presents a later mass arrival and an increased spread, i.e., lower peak  
 315 of mass and mass arrival for a longer period (Figure 3, top left frame). Distinctively, early  
 316 mass arrival appears insensitive to the degree of heterogeneity in case of high input flux,  
 317 unlike macrodispersion, which sensitively increases with  $\sigma_\chi$  (Figure 3, bottom left frame).

318 Globally, those results are consistent with the direct observation of non-Fickian trans-  
 319 port in macroscopically homogeneous unsaturated media with similar high velocity (Bromly  
 320 & Hinz, 2004).

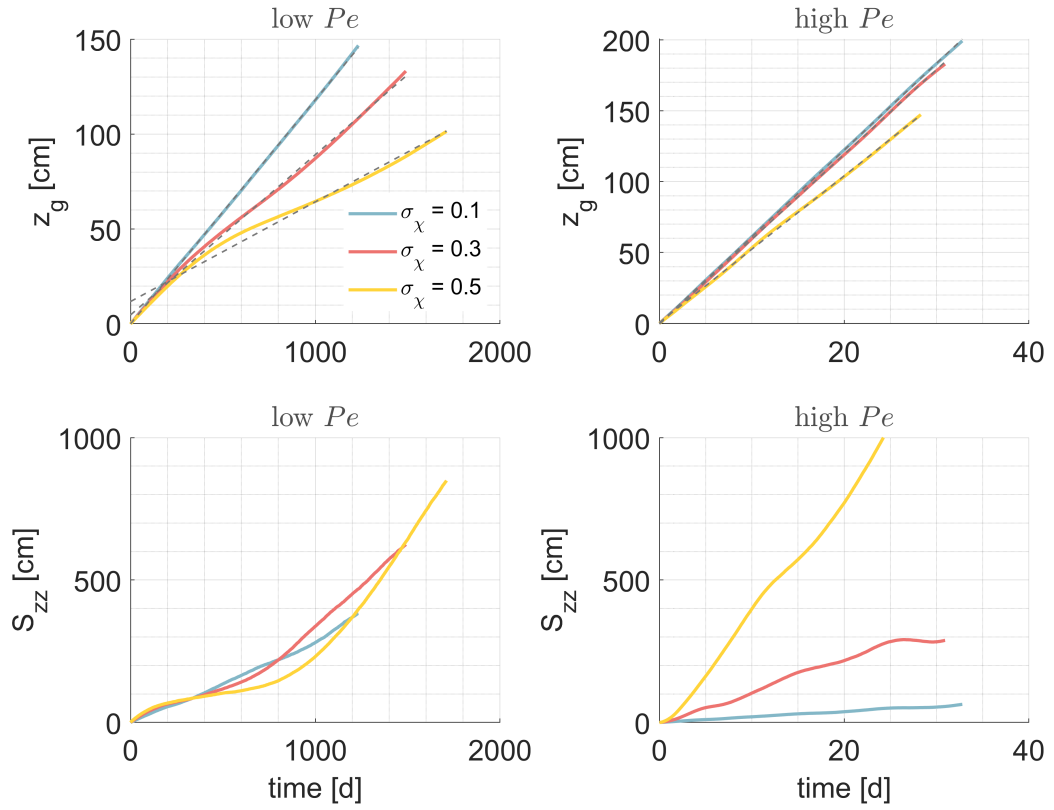


**Figure 2.** First (center of mass location,  $z_g$ ; top frames) and second (spread about the centroid,  $S_{zz}$ ; bottom frames) normalized spatial moments for each degree of heterogeneity of the soil structure and for the 2 input fluxes. The dashed grey lines on the top frames are linear regressions for the temporal evolution of  $z_g$ . The slopes of the regression represent effective velocities.

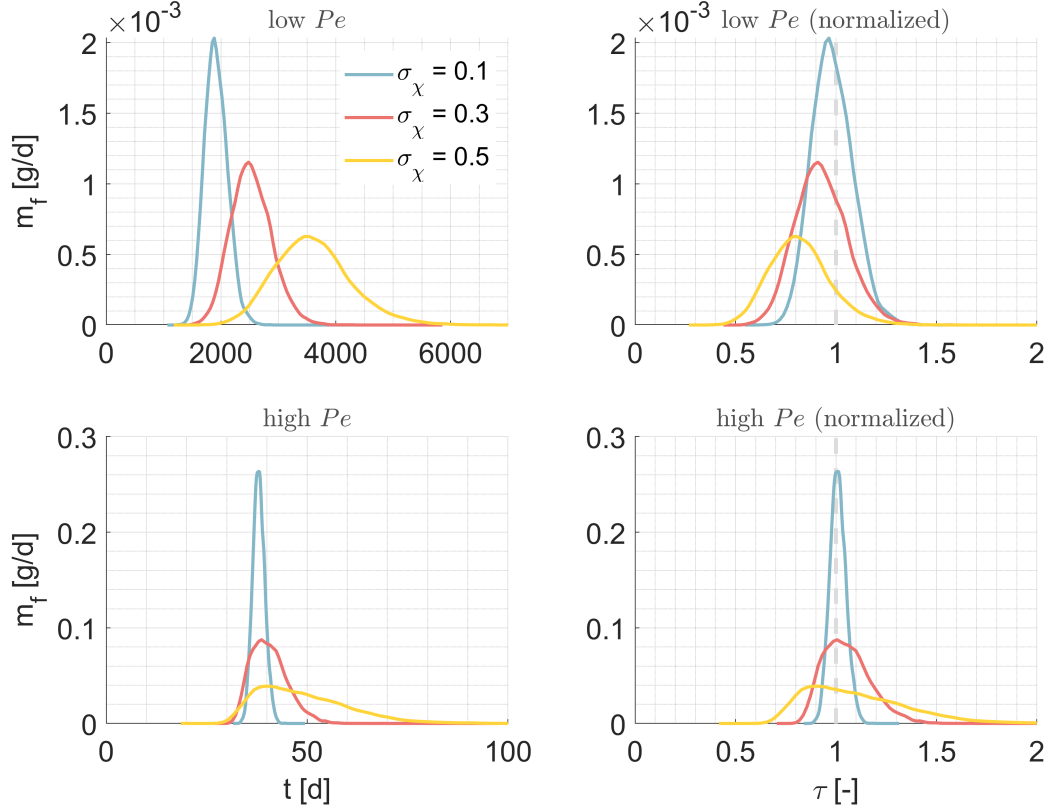


**Figure 3.** Breakthrough curves (BTCs) resulting from simulations in soil of different degree of heterogeneity, for a high recharge flux (i.e., high Peclet number; bottom frames) and a low recharge flux (i.e., low Peclet number; top frames). Right frames show the BTCs considering a time normalized by the advective time. The diffusion coefficient is considered spatially variable (tortuosity dependent).

321 Observing the plume behavior in a series of 20 realization of the heterogeneity in  
 322 the SHPs is consistent with the analysis made on single BTCs. For the high  $Pe$  system,  
 323 early arrival times ( $t_5$ ) are less sensitive to  $\sigma_\chi$  than late arrival times ( $t_{95}$ ; Supplemen-  
 324 tary Information, Figure S7, left frames), while all arrival times are increased with het-  
 325 erogeneity when  $Pe$  is lower (Figure S7, right frames). Also, travel times *pdfs* allow to  
 326 observe that the variability among realizations in late arrival times is significantly in-  
 327 creased with the degree of heterogeneity.

328 The first spatial moment is often used to subsequently estimate the effective ve-  
 329 locity ( $v_z^*$ ) and the time of arrival of the center of mass of the plume at *any* distance from  
 330 the source. Applying this approach is valid in case of high input flux (Figure 3, bottom

331 right frame). The BTCs are centered around a unit values of time normalized by  $t_{adv}$ ,  
 332 regardless of the degree of heterogeneity. However, we observe that  $v_z^*$  does not prop-  
 333 erly predict the motion of the plume in case of low flux and high  $\sigma_\chi$  (Figure 3, top right  
 334 frame). Normalizing the BTCs' time by the characteristic advective time ( $t_{adv}$ ) leads to  
 335 faster first arrival of mass for low  $Pe$  and high  $\sigma_\chi$  systems, reflecting an overall overes-  
 336 timation of the effective velocity.

337 This results from the non-linear behavior of the first spatial moment observed in  
 338 soils characterized by a low  $Pe$  and a high  $\sigma_\chi$  (Figure 2). Indeed, the predictive capac-  
 339 ities of the first spatial moment implies a linear evolution of the center of mass location,  
 340 reflecting a constant effective velocity, which is often observed in saturated conditions.  
 341  $t = t_{adv}$  would then be associated to the arrival of the center of the plume at the char-  
 342 acteristic distance used to estimated  $t_{adv}$  ( $L_z$  in our case). Yet, in case of low flux, the  
 343 center of mass of the plume is affected by critical moments of fast and slow motion, which  
 344 render more complex the estimation of an effective behavior.

### 345 **3.2 Importance of diffusion**

346 In this section, our analysis focuses on the effect of diffusion on transport. We first  
 347 analyze the relevance of considering a realistically heterogeneous diffusion coefficient ( $D_m(x)$ ,  
 348 blue curves in Figures 4 and 5) by comparing corresponding BTCs from simulations dis-  
 349 regarding the diffusive process (yellow lines). The implications of considering a spatially  
 350 homogeneous diffusion coefficient ( $\bar{D}_m$ ) will be analyzed in the following section.

351 *High Peclet number.* For a high  $Pe$ , considering diffusion has a moderate effect  
 352 on macrodispersion. In case of low heterogeneity, disregarding diffusion all together de-  
 353 creases macrodispersion (Figure 4), which is the expected expression of the process. In-  
 354 creasing  $\sigma_\chi$  renders more complex the impact of diffusion on transport: Early arrival times  
 355 are mostly unchanged but macrodispersion is decreased by adding diffusion, decreasing  
 356 the very pronounced tailing (i.e., elongated late arrivals) generated by the heterogene-  
 357 ity in the advective flux. This phenomena has been previously observed by few studies  
 358 under various conditions (Nissan & Berkowitz, 2019; Cirpka & Kitanidis, 2002; Weiss-  
 359 mann et al., 2002) and is explained by the capacity of diffusive motion to move mass away  
 360 from quasi-stagnant zones, reducing this way the potential for very late arrivals (i.e., tail-

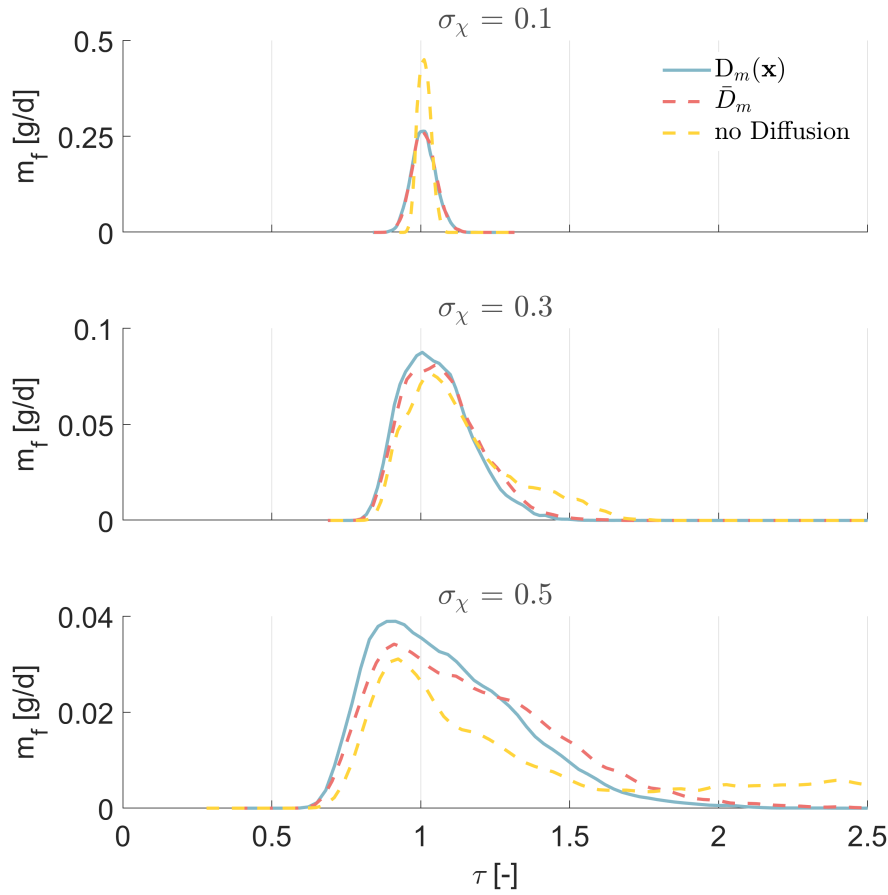


**Figure 4.** Breakthrough curves (BTCs) resulting from simulations using a spatially variable, tortuosity-dependent diffusion coefficient ( $D_m(x)$ ) and a spatially averaged diffusion coefficient ( $\bar{D}_m$ ) and no diffusion, for soils of different degree of heterogeneity. Results are shown for the higher Peclet number. Times are normalized by the characteristic advective time of the  $D_m(x)$  scenario.

361 ing). Here again, these observations are valid across realizations (Supplementary Infor-  
 362 mation, Figure S8).

363 *Low Peclet number.* The effect of diffusion on the overall transport dynamics for  
 364 the low  $Pe$  case is significant, both in term of arrival time and plume spread. For low  
 365 degree of heterogeneity ( $\sigma_\chi=0.1$ ), macrodispersion is increased by including diffusion in  
 366 the simulations (Figure 5, top frame), which is expected and similar to the effect observed  
 367 in case of a high  $Pe$ . However, when  $\sigma_\chi$  increases, not including diffusion does not sig-  
 368 nificantly change the early arrivals but prevents late arrival of mass, leading to a non-

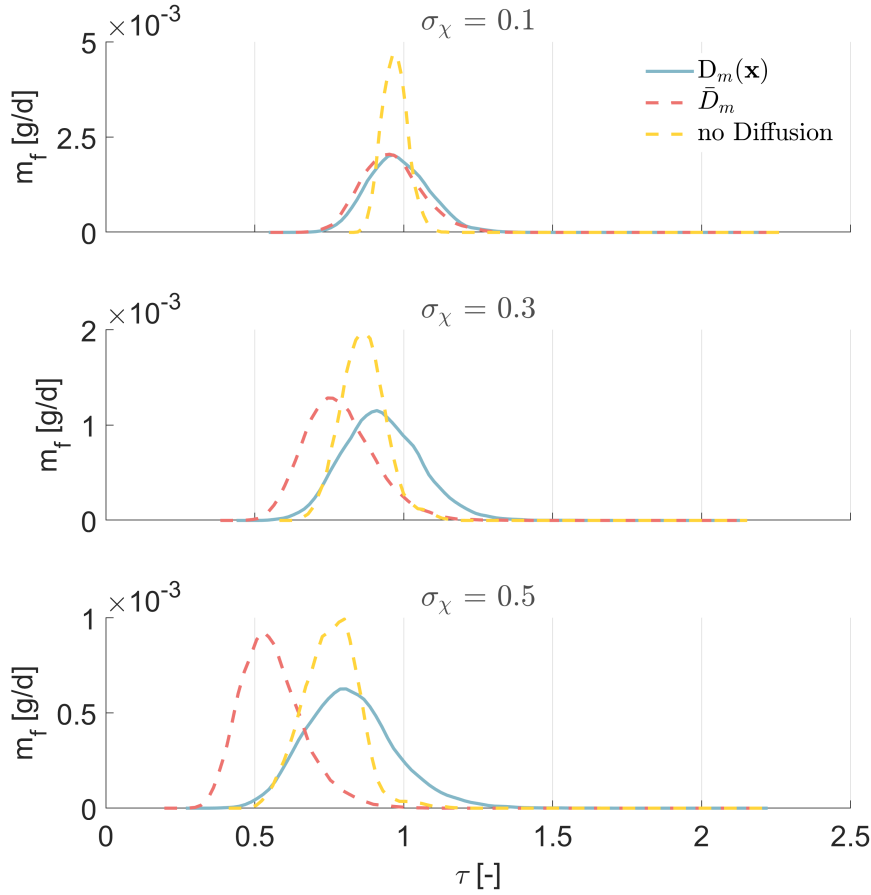


**Figure 5.** Breakthrough curves (BTCs) resulting from simulations using a spatially variable, tortuosity-dependent diffusion coefficient ( $D_m(x)$ ), a spatially averaged diffusion coefficient ( $\bar{D}_m$ ) and no diffusion, for soils of different degree of heterogeneity. Results are shown for the lower Peclet number. Times are normalized by the characteristic advective time of the  $D_m(x)$  scenario.

369 Gaussian, negatively skewed BTC (Figure 5, lower frame). BTCs appears then to be more  
 370 sensitive to  $Pe$  as the degree of heterogeneity increases.

371 At the same time, BTCs sensitivity to  $\sigma_\chi$  is specific to the  $Pe$  number. When  $\sigma_\chi$   
 372 increases, the counter-intuitive macrodispersion-reducing effect of diffusion observed for  
 373 high  $Pe$  is not observed for a lower  $Pe$ , which disagrees with the previous works of Nis-  
 374 san & Berkowitz (2019); Cirpka & Kitanidis (2002); Weissmann et al. (2002). This re-  
 375 lates with our consideration of spatial variable diffusion process. In case of high  $q_{z,in}$ ,  
 376 low velocity zones are characterized by high diffusion coefficients ( $> 10^0$  cm<sup>2</sup>/d; Fig-  
 377 ure 6 lower frame). This is because these zones are characterized by close to saturation

378 water content but low hydraulic conductivity. This favors the mobilizing of mass that  
 379 would be otherwise trapped in a system without diffusion, due to the low local veloc-  
 380 ities. Late arrivals are then prevented. Due to the tortuosity model, the opposite is ob-  
 381 served in case of low flux: diffusion values in quasi-stagnant zones are the lowest ( $< 10^{-3}$   
 382  $\text{cm}^2/\text{d}$ ; Figure 6 upper frame), due to the low local water content. Residence times in  
 383 low velocity zones can then remain relatively high, which allows late arrivals. Interest-  
 384 ingly, in a low velocity system without diffusion, mass reaching a fast channel is likely  
 385 to remain in high velocity zones for the remaining of its transport toward the bottom  
 386 of the domain. Transport occurs then predominantly in fast channels, reducing the im-  
 387 portance of late arrivals. Adding diffusion would favor the transfer of mass from these  
 388 high velocity zones to more stagnant ones, increasing this way the contribution of late  
 389 arrivals. Such behavior is consistent across realizations (Supplementary Information, Fig-  
 390 ure S9). Moreover, accounting for a spatially variable saturated water content leads to  
 391 similar conclusions (Supplementary Information, Figure S10).

### 392 **3.3 Effect of Spatially Variable Diffusion**

393 To further understand the implications of spatial variability in the diffusion coef-  
 394 ficient, we compare BTCs resulting from simulations with a water content dependent dif-  
 395 fusion ( $D_m(x)$ ) coefficient (assuming tortuosity model of Millington and Quirk) and with  
 396 a homogeneous, averaged diffusion ( $\bar{D}_m$ ).

397 In our modeling setting, the range of diffusion coefficient for a single realization is  
 398 highly dependent on the degree of heterogeneity of the SHPs and on the infiltration rate.  
 399 In case of lower  $q_{z,in}$ , we obtain exponentially decreasing histograms of  $D_m$  values in case  
 400 of a high degree of heterogeneity, with a range of diffusion coefficient from 0 to  $1.2 \text{ cm}^2/\text{d}$   
 401 (Figure 7, top frame). The histogram turns more and more Gaussian-like when  $\sigma_\chi$  de-  
 402 creases, with a narrowing range of values (from 0 to 0.3 for  $\sigma_\chi = 0.1$ ).

403 In case of a larger infiltration rate, ranges of  $D_m(x)$  values are globally more spread  
 404 (Figure 7, bottom frame). Histograms are slightly increasing in case of high degree of  
 405 heterogeneity, and still Gaussian-like for  $\sigma_\chi = 0.1$ .

406 *Advection dominated scenario* For the high  $Pe$  scenario, the spatial variability  
 407 in the diffusion coefficient appears to have no real impact on transport in a mildly het-  
 408 erogeneous soil (Figure 4, top frame, compare blue and red lines). When the spatial vari-

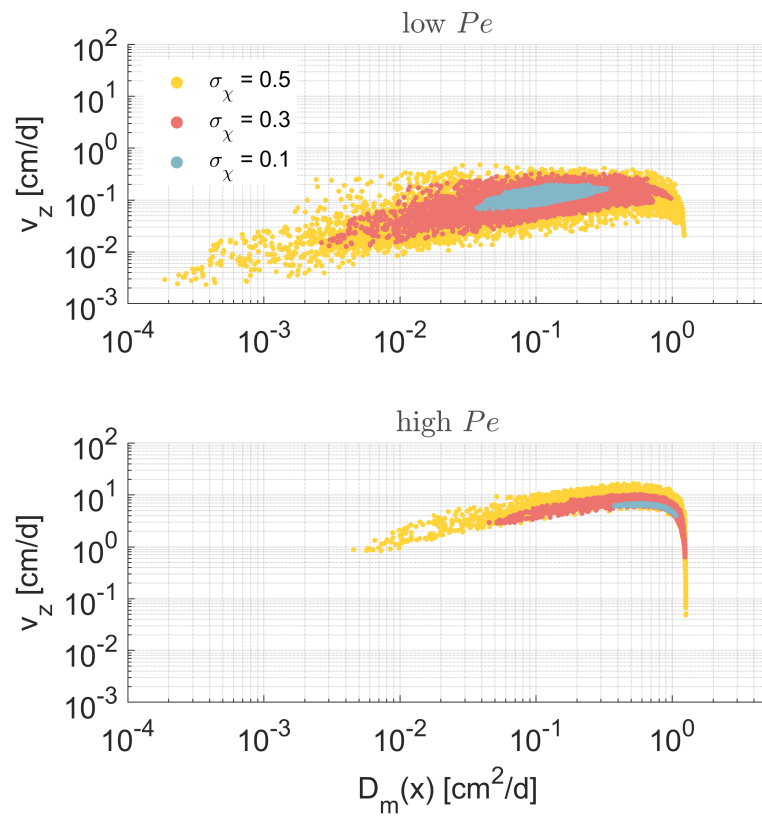


**Figure 6.** Relationship between the vertical velocity and the water content dependent diffusion coefficient for each degree of the heterogeneity in the soil structure and for the 2 Peclet numbers.

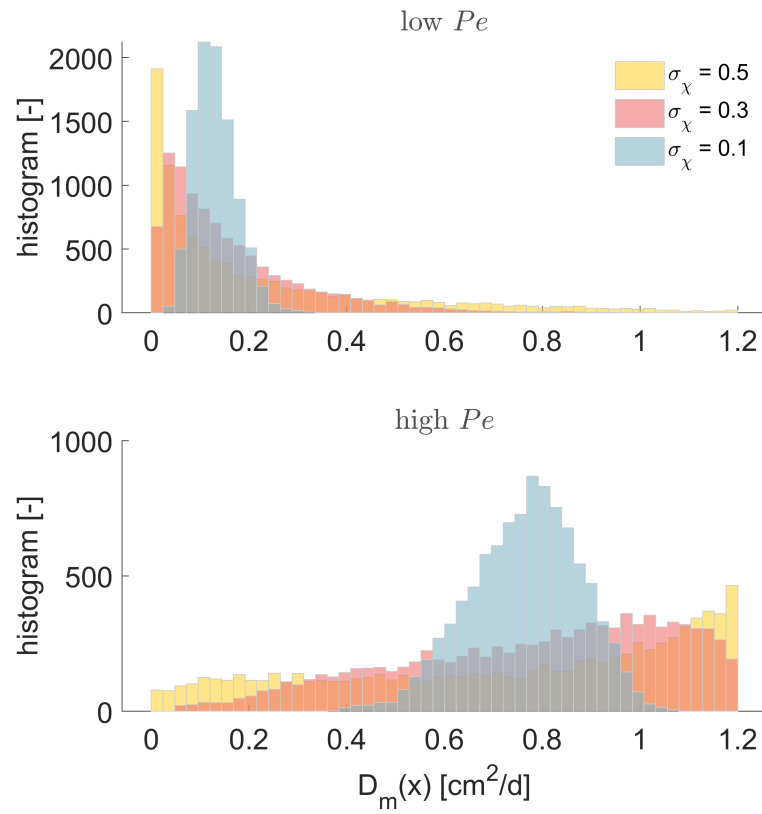


**Figure 7.** Histograms of the spatially variable, tortuosity-dependent diffusion coefficient for each degree of soil heterogeneity and for a high recharge flux (i.e., high Peclet number; bottom frame) and a low recharge flux (i.e., low Peclet number; top frame).

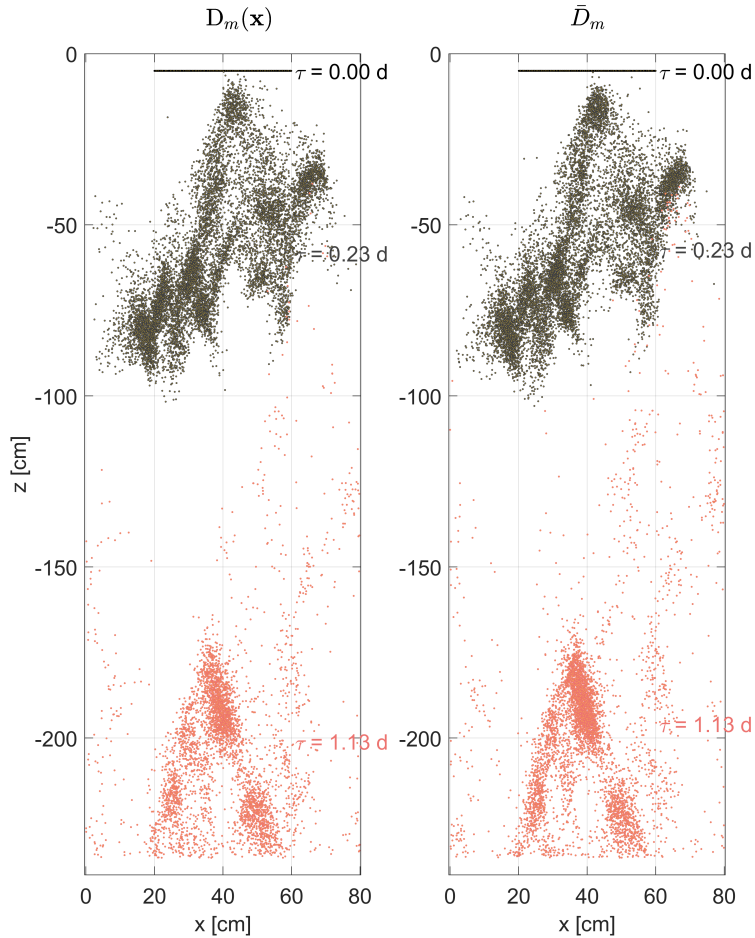


**Figure 8.** Plume snapshots from simulations using a spatially variable, tortuosity-dependent diffusion coefficient ( $D(x)$ ) and a spatially averaged diffusion coefficient ( $\bar{D}_m$ ), for soils of a high degree of heterogeneity ( $\sigma_\chi = 0.5$ ). Results are shown for the higher Peclet number.

409 ability in SHPs is more pronounced, correlating the local diffusion coefficient to the tor-  
 410 tuosity (and therefore the water content) slightly decreases the macrodispersion and the  
 411 tailing of the BTC (Figure 4, bottom frame).

412 Observing the plume of particles in a highly heterogeneous soil allows to identify  
 413 zones of accumulation of mass, which is slightly accentuated in case of spatially averaged  
 414 diffusion coefficient (Figure 8). Globally, the implications in considering the spatial vari-  
 415 ability in diffusion coefficient for a strongly advective system are moderate. Diffusion co-  
 416 efficients in low velocity zones are higher than the mean values, which, following the pre-  
 417 viously discussed phenomena, leads to a reduction of late arrivals.

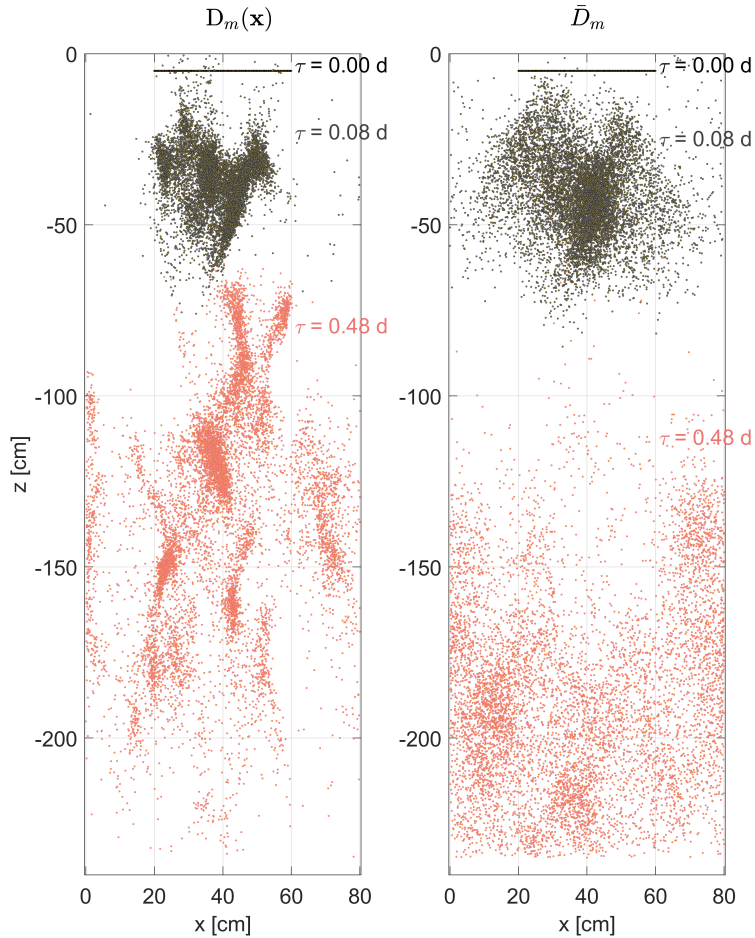


**Figure 9.** Plume snapshots from simulations using a spatially variable, tortuosity-dependent diffusion coefficient ( $D(x)$ ) and a spatially averaged diffusion coefficient ( $\bar{D}_m$ ), for soils of a high degree of heterogeneity ( $\sigma_\chi = 0.5$ ). Results are shown for the low Peclet number.

418 *Diffusion dominated scenario.* When diffusive process is more dominant, account-  
 419 ing for the spatial variability of the diffusion coefficient has a much greater impact on  
 420 plume behavior. For a high  $\sigma_\chi$ , applying a spatially averaged diffusion coefficient leads  
 421 to significantly earlier arrival of mass and to a lesser spread of the plume (Figure 5, lower  
 422 frames).

423 Snapshots of the particle plume in a highly heterogeneous soil display a significantly  
 424 pronounced accumulation of mass in specific zones of the soil if diffusion is considered  
 425 tortuosity-dependent (Figure 9).

426 Low diffusion coefficient values in low velocity zones result in an increased residence  
 427 time in those areas, forming pockets of mass, which can only leave the domain at rel-  
 428 atively late time. On the other hand, applying an average (but still larger) diffusion co-  
 429 efficient in those low velocity zones allows an earlier mobilization of mass, generating an-  
 430 ticipated arrivals. Note that this remains true even compared to a purely advective sys-  
 431 tem, which, despite maintaining mass in fast channels, can still be affected by the rel-  
 432 atively long presence of mass in low velocity areas at early times (partly due to the in-  
 433 jection of mass in low velocity zones).

### 434 3.4 Transient conditions.

435 Natural systems are characterized by periods of infiltration (i.e., strongly advec-  
 436 tive flux) and others of mostly slow mass redistribution (i.e., mostly diffusive transport).  
 437 Figure 10 shows BTCs resulting from simulations with homogeneous and heterogeneous  
 438 diffusion coefficients, for different distances of the control plane ( $x_{cp}$ ) and for 2 differ-  
 439 ent durations of the infiltration period ( $t_{inf}=1$  day and 15 days). The temporal discretiza-  
 440 tion of fluxes, water contents and diffusion coefficients was set to 1 hour, which produces  
 441 similar results than for a finer time step (Supplementary Information, Figure S11). The  
 442 effect of transience in the diffusion process is displayed by comparing BTCs resulting from  
 443 temporally variable diffusion coefficients (plain lines) and from temporally averaged co-  
 444 efficients (dashed lines). For these 2 cases, the water flux and the water content are still  
 445 considered transient.

446 For any infiltration period, results display an insensitivity of the BTCs to the spa-  
 447 tial variability in diffusion at the control plane near the source ( $x_{cp} = 2 \times \lambda_z$ ; Figure  
 448 10, top frames).

449 For BTCs recorded near the center of the domain ( $x_{cp} = 4 \times \lambda_z$ ), the spatial vari-  
 450 ability in the diffusion coefficient generates slightly more diffuse mass arrival, with a later  
 451 peak and later late arrivals, only if the infiltration period is short (1 day; Figure 10, mid-  
 452 dle frames). In case of a longer infiltration period (characterized by a strongly advec-  
 453 tive transport), BTCs at mid-distance are mostly identical for a homogeneous or a het-  
 454 erogeneous diffusion coefficient.

455 Further downstream ( $x_{cp} = 9\lambda_z$ ), applying a tortuosity-dependent diffusion co-  
 456 efficient produces significantly more diffuse BTCs, with similar early mass arrival than

457 with a homogeneous  $D_m$ , but with a lower peak of mass and later late arrivals (Figure  
 458 10, bottom frames). This mass dynamic is observed for both a short (1 day) and a long  
 459 (15 days) initial period of strongly advective transport. For all tested BTCs, we observed  
 460 no significant effect of transience in the diffusion coefficient itself.

461 The two very distinct regimes of diffusive transport associated to a high and a low  
 462 advective flux explains the main dynamic of the simulated transient transport. At short  
 463 travel distance, the insensitivity of the solution to the diffusion model can be explained  
 464 by both the limited sampling of soil heterogeneity occurring over only 2 correlation lengths  
 465 and by the low impact of spatial variability in diffusion on strongly advective systems.  
 466 For longer infiltration period, the limited impact of heterogeneity in the diffusion is ob-  
 467 served further downstream ( $x_{cp} = 2\lambda_z$ ). Yet, with increased travel distances, the ef-  
 468 fect of spatially variable diffusion coefficient on strongly diffusive systems takes over, re-  
 469 gardless of the infiltration duration.

### 470 **3.5 Homogenization of diffusion**

471 To evaluate the relevancy in determining effective, homogenized diffusion coefficient  
 472 other than a spatially averaged values, we tested the performance of the minimum and  
 473 the maximum values of  $D(x)$ .

474 Homogenizing the diffusion coefficient leads to poor performances in case of low  
 475  $Pe$  systems, regardless of the diffusion coefficient values used (Figure 11, upper frame).  
 476 Applying the maximum values of diffusion overestimates macrodispersion and leads to  
 477 early travel times, while the minimum values underestimates the plume spread, despite  
 478 reproducing relatively well the time of first arrivals.

479 Thus, no effective, homogenized values of diffusion can be determined in a low  $Pe$   
 480 system. When velocity is relatively low, zones of low and of high diffusion coefficient have  
 481 a complex combined effect on transport that evolves as the plume moves through the het-  
 482 erogeneous domain. Therefore, even when the spatial variability in the SPHs, control-  
 483 ling advective fluxes is explicitly described, not accounting for the spatial variability of  
 484 the diffusion would require to artificially adjust effective advection. Such curve-fitting  
 485 approach would compromise the physical understanding of the system, which may have  
 486 detrimental consequences on the applicability of the model.

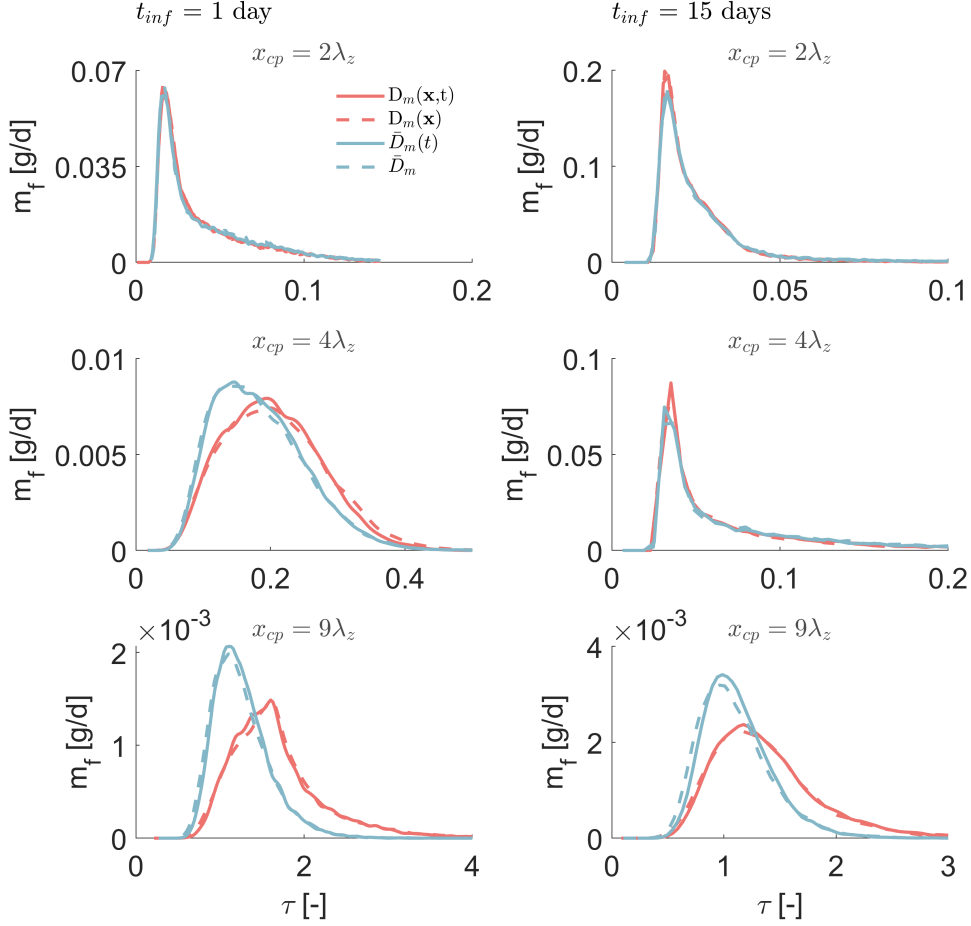


**Figure 10.** Breakthrough curves (BTCs) at three control planes (CP) resulting from simulations using a spatially variable, tortuosity-dependent diffusion coefficient ( $D_m(x)$ ) and a spatially averaged diffusion coefficient ( $\bar{D}_m$ ) for 1 day of infiltration (left hand) and 15 days of infiltration (right hand). Diffusion coefficients are considered transient ( $D_m(x,t)$  and  $\bar{D}_m(t)$ ) or steady state (temporally averaged). For all simulations, a high degree of heterogeneity in the SHPs ( $\sigma_\chi = 0.5$ ) is considered. Times are normalized by the characteristic advective time estimated for each duration of the infiltration period ( $t_{inf}$ ).

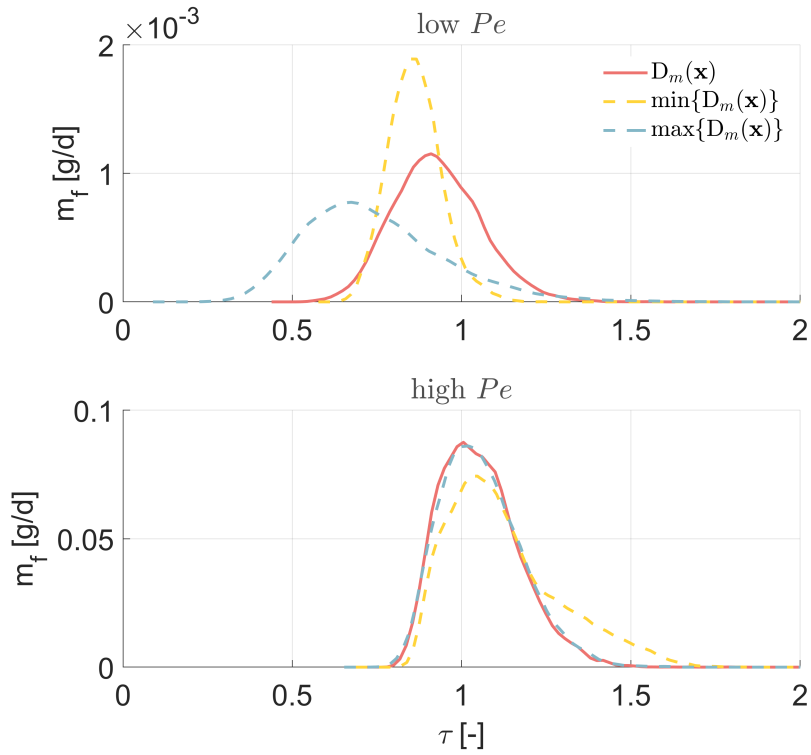


**Figure 11.** Breakthrough curves (BTCs) resulting from simulations using a spatially variable diffusion coefficient (red plain lines), the minimum (yellow dashed lines) and the maximum (blue dashed lines) values of  $D(x)$ , for a high recharge flux (bottom frames) and a low recharge flux (top frames). The degree of heterogeneity is described by  $\sigma_\chi=0.3$ . Times are normalized by the characteristic advective time of the  $D_m(x)$  scenario.

487 In case of high  $Pe$  number, a maximum values of  $D(x)$  produces satisfactory re-  
488 sults, while a minimum values tends to overestimate BTC tailing ((Figure 11, lower frame)).  
489 As advection remains the main controlling process, only the zones of high values of dif-  
490 fusion coefficients impact the transport. Maximizing the homogenized diffusion coeffi-  
491 cient reproduces then properly the release of mass from low velocity zones that prevent  
492 tailing to occur.

#### 493 **4 Concluding remarks**

494 Through a series of numerical simulations, this study analyzed the complex, syn-  
495 ergistic effect of (small scale) soil heterogeneity, advection and diffusion on conservative  
496 transport in unsaturated soils. Key findings are:

- 497 • The control of heterogeneity on transport is Peclet number dependent. For a low  
498 Peclet number, the mean advective time increases with the degree of soil hetero-  
499 geneity, while macrodispersion remains globally unchanged. The opposite is ob-  
500 served for the high Peclet case, which is characterized by a significant increase of  
501 (non-Fickian) macrodispersion and no real change in the mean advective flux when  
502 soil heterogeneity increases. The sensitivity of high Peclet systems to the degree  
503 of soil heterogeneity observed at the pore scale under saturated conditions by Nis-  
504 san & Berkowitz (2019) remains then valid at larger scale and for unsaturated con-  
505 ditions.
- 506 • Diffusion appears to be a key process controlling residence time of solutes in soils  
507 since it distributes contaminant mass in or out of low velocity zones. Thus, the  
508 impact of diffusion on transport is also highly dependent to the Peclet number,  
509 but only for a relatively high degree of heterogeneity. In this case, for a high Peclet  
510 number, diffusion decreases macrodispersion by allowing the remobilization of mass  
511 trapped in quasi-stagnant zones. This phenomena have been previously described  
512 by e.g., Weissmann et al. (2002) for a saturated aquifer and are now also observed  
513 for unsaturated conditions. Yet, in a low Peclet system, diffusion increases late  
514 arrival of mass. This appears to be linked to the tortuosity dependence of the dif-  
515 fusion coefficient assumed in this study. Unlike for high Peclet systems, our sim-  
516 ulated low Peclet soils are characterized by low values of the diffusion coefficient

517 in low velocity zones (due to the low water saturation value), which prevents the  
518 counter-intuitive reduction of macrodispersion when diffusion is considered.

- 519 • Thus, the spatial variability in the diffusion process is also a potential significant  
520 factor to understand transport behavior of solutes in soils. The impact of tortuosity-  
521 dependent diffusion process was found highly dependent on both the degree of het-  
522 erogeneity and the Peclet number due to (1) the importance that the diffusive pro-  
523 cess has in regard to the advective flux, and (2) the saturation dependence of the  
524 distribution of diffusion coefficients over the soil profile. Homogenizing the diffu-  
525 sion coefficient will disregard the dynamic feedback between mass accumulation  
526 in zones of low advective flux and the potential release of this mass, which is func-  
527 tion of the magnitude of the local diffusive process. The empirical relationship be-  
528 tween local tortuosity and the diffusion coefficient has then important implications  
529 in the dynamic of transport.

530 The practical implications of our theoretical study are potentially important. In-  
531 deed, different parametrization of the heterogeneity, velocity and diffusion can lead to  
532 significantly different first arrival of mass to the groundwater, more or less long term late  
533 arrivals and different peak concentrations reaching soil-connected water bodies. More-  
534 over, natural and cultivated soils are ubiquitously transient systems characterized by im-  
535 portant temporal variation in the advection flux. Periods of low and high Peclet num-  
536 bers due to infiltration or irrigation will result in periods of Fickian and non-Fickian trans-  
537 port characterized with significantly different mean advective velocity and effective dis-  
538 persion. The flow condition at the moment of field or laboratory observations is there-  
539 fore a key element to be considered to understand in depth the dynamic of the solute  
540 plume. This possible complex control of soil heterogeneity, Peclet number and diffusion  
541 on transport is expected to critically affect reaction and reactive transport, which remains  
542 to be investigated.

543 Globally, our outputs clearly highlight that small scale heterogeneity in soils and  
544 its overall impact on the spatial variability in diffusion must be considered to properly  
545 predict transport. Yet, a detailed characterization of this spatial variability is in most  
546 cases technically and economically infeasible. Upscaling approaches reproducing this com-  
547 plex impact of heterogeneity on advection, diffusion and therefore hydraulic structure  
548 are then required. Upscaling the effect of heterogeneity on *advective* fluxes has been the

549 focus on an important effort, mostly in saturated aquifers. Techniques such as the Multi-  
550 Rate Mass Transfer model (Haggerty & Gorelick, 1995), Continuous Time Random Walk  
551 (Berkowitz et al., 2006), and the fractional Advection-Dispersion Equation (Benson et  
552 al., 2000) have indeed been developed to reproduce late arrival times, which is typically  
553 the main BTC feature characterizing non-Fickian transport in saturated media. Yet, our  
554 work shows that both the heterogeneous advective flux and diffusive flux should be si-  
555 multaneously upscaled in soils. Indeed, as our results display, (1) a simple homogeniza-  
556 tion of the diffusion coefficient is not sufficient due to the complex and dynamic mass  
557 transfer from and into zones of low velocities, and (2) temporal variations in fluxes con-  
558 ditions the effective impact of diffusion on transport. Guo et al. (2019) exposed the dif-  
559 ficulties of upscaling techniques to perform well under transient conditions, which the  
560 authors attempted to solve later on by explicitly accounting for the advective flux de-  
561 pendence of mass transfer coefficients (Guo et al., 2020). In a future study, one could  
562 attempt to develop a similar approach for unsaturated soils, accounting for both tran-  
563 sient advective fluxes and transient diffusive fluxes.

564 To finish, it is important to emphasize on the theoretical and incomplete nature  
565 of this work. For instance, real soils are in more cases more heterogeneous than what has  
566 been assumed in this study (biopores, cracks, hydrophobicity, etc). Moreover, our con-  
567 clusions rely on the application of a series of (well established) equations but also on an  
568 empirical relationship between diffusion and tortuosity. While this relation is based on  
569 observations, its impact on transport under heterogeneous conditions remains to also be  
570 validated by in-situ or laboratory observations.

## 571 **Open Research Section**

572 This study is theoretical by nature and does not utilize any known database. In-  
573 stead, model parameters are listed throughout the manuscript. Flow simulations can be  
574 reproduced using the Daisy model (Hansen et al., 2012; Holbak et al., 2022) available  
575 at: <https://daisy.ku.dk/download/>. Transport simulations can be reproduced using  
576 the code RW3D (Henri & Diamantopoulos, 2022). Its source files and an executable are  
577 available at: <https://doi.org/10.5281/zenodo.6607599>.

578 **Acknowledgments**

579 The authors gratefully acknowledge the financial support through the Research Exec-  
580 utive Agency of the European Commission, Grant Agreement number: 896470.

581 **References**

- 582 Bear, J. (1972). *Dynamics of Fluids in Porous Media*. New York: American Elsevier  
583 Publishing Company. (764 p.)
- 584 Benson, D. A., Wheatcraft, S. W., & Meerschaert, M. M. (2000). The fractional-  
585 order governing equation of lévy motion. *Water Resources Research*, *36*(6), 1413-  
586 1423. Retrieved from [https://agupubs.onlinelibrary.wiley.com/doi/abs/10](https://agupubs.onlinelibrary.wiley.com/doi/abs/10.1029/2000WR900032)  
587 [.1029/2000WR900032](https://agupubs.onlinelibrary.wiley.com/doi/abs/10.1029/2000WR900032) doi: <https://doi.org/10.1029/2000WR900032>
- 588 Berkowitz, B., Cortis, A., Dentz, M., & Scher, H. (2006). Modeling non-fickian  
589 transport in geological formations as a continuous time random walk. *Re-*  
590 *views of Geophysics*, *44*(2). Retrieved from [https://agupubs.onlinelibrary](https://agupubs.onlinelibrary.wiley.com/doi/abs/10.1029/2005RG000178)  
591 [.wiley.com/doi/abs/10.1029/2005RG000178](https://agupubs.onlinelibrary.wiley.com/doi/abs/10.1029/2005RG000178) doi: [https://doi.org/10.1029/](https://doi.org/10.1029/2005RG000178)  
592 [2005RG000178](https://doi.org/10.1029/2005RG000178)
- 593 Botros, F. E., Onsoy, Y. S., Ginn, T. R., & Harter, T. (2012, nov). Richards  
594 Equation-Based Modeling to Estimate Flow and Nitrate Transport in a Deep  
595 Alluvial Vadose Zone. *Vadose Zone Journal*, *11*(4), vzj2011.0145. Retrieved from  
596 <http://doi.wiley.com/10.2136/vzj2011.0145> doi: [10.2136/vzj2011.0145](https://doi.org/10.2136/vzj2011.0145)
- 597 Boudreau, B. P. (1996). The diffusive tortuosity of fine-grained unlithified sedi-  
598 ments. *Geochimica et Cosmochimica Acta*, *60*(16), 3139-3142. Retrieved from  
599 <https://www.sciencedirect.com/science/article/pii/0016703796001585>  
600 doi: [https://doi.org/10.1016/0016-7037\(96\)00158-5](https://doi.org/10.1016/0016-7037(96)00158-5)
- 601 Bromly, M., & Hinz, C. (2004). Non-fickian transport in homogeneous unsat-  
602 urated repacked sand. *Water Resources Research*, *40*(7). Retrieved from  
603 <https://agupubs.onlinelibrary.wiley.com/doi/abs/10.1029/2003WR002579>  
604 doi: <https://doi.org/10.1029/2003WR002579>
- 605 Cirpka, O. A., & Kitanidis, P. K. (2002). Numerical evaluation of solute disper-  
606 sion and dilution in unsaturated heterogeneous media. *Water Resources Research*,  
607 *38*(11), 2-1-2-15. doi: [10.1029/2001wr001262](https://doi.org/10.1029/2001wr001262)
- 608 Cremer, C. J., Neuweiler, I., Bechtold, M., & Vanderborght, J. (2016, jun). So-  
609 lute Transport in Heterogeneous Soil with Time-Dependent Boundary Condi-

- 610 tions. *Vadose Zone Journal*, 15(6), vzj2015.11.0144. Retrieved from <http://doi.wiley.com/10.2136/vzj2015.11.0144> doi: 10.2136/vzj2015.11.0144
- 611
- 612 Cremer, C. J. M., & Neuweiler, I. (2019, dec). How Dynamic Boundary Conditions  
613 Induce Solute Trapping and Quasi-stagnant Zones in Laboratory Experiments  
614 Comprising Unsaturated Heterogeneous Porous Media. *Water Resources Research*,  
615 55(12), 10765–10780. Retrieved from <https://onlinelibrary.wiley.com/doi/10.1029/2018WR024470> doi: 10.1029/2018WR024470
- 616
- 617 Cushman, J. H. (1984). On unifying the concepts of scale, instrumentation, and  
618 stochastics in the development of multiphase transport theory. *Water Resources  
619 Research*, 20(11), 1668-1676. Retrieved from [https://agupubs.onlinelibrary  
620 .wiley.com/doi/abs/10.1029/WR020i011p01668](https://agupubs.onlinelibrary.wiley.com/doi/abs/10.1029/WR020i011p01668) doi: [https://doi.org/10.1029/  
621 WR020i011p01668](https://doi.org/10.1029/WR020i011p01668)
- 622 Diamantopoulos, E., & Durner, W. (2012). Dynamic nonequilibrium of water flow in  
623 porous media: A review. *Vadose Zone J.*, 11(0).
- 624 Fernández-García, D., Illangasekare, T. H., & Rajaram, H. (2005). Differences in the  
625 scale-dependence of dispersivity estimated from temporal and spatial moments in  
626 chemically and physically heterogeneous porous media. *Adv. Water Res.*, 28(7),  
627 745-759.
- 628 Forrer, I., Kasteel, R., Flury, M., & Flühler, H. (1999, oct). Longitudinal and lateral  
629 dispersion in an unsaturated field soil. *Water Resources Research*, 35(10), 3049–  
630 3060. Retrieved from <http://doi.wiley.com/10.1029/1999WR900185> doi: 10  
631 .1029/1999WR900185
- 632 Ghanbarian, B., Hunt, A. G., Ewing, R. P., & Sahimi, M. (2013). Tortuosity in  
633 Porous Media: A Critical Review. *Soil Science Society of America Journal*, 77(5),  
634 1461–1477. doi: 10.2136/sssaj2012.0435
- 635 Guo, Z., Fogg, G. E., Brusseau, M. L., LaBolle, E. M., & Lopez, J. (2019). Mod-  
636 eling groundwater contaminant transport in the presence of large heterogeneity:  
637 a case study comparing mt3d and rwhet. *Hydrogeology Journal*, 27(4), 1363–  
638 1371. Retrieved from <https://doi.org/10.1007/s10040-019-01938-9> doi:  
639 10.1007/s10040-019-01938-9
- 640 Guo, Z., Henri, C. V., Fogg, G. E., Zhang, Y., & Zheng, C. (2020). Adaptive mul-  
641 tivariate mass transfer (ammt) model: A new approach to upscale regional-scale  
642 transport under transient flow conditions. *Water Resources Research*, 56(2),

- 643 e2019WR026000. Retrieved from <https://agupubs.onlinelibrary.wiley.com/doi/abs/10.1029/2019WR026000> doi: <https://doi.org/10.1029/2019WR026000>
- 644
- 645 Haggerty, R., & Gorelick, S. M. (1995). Multiple-rate mass transfer for modeling diffusion and surface reactions in media with pore-scale heterogeneity. *Water Resources Research*, *31*(10), 2383–2400. Retrieved from <https://agupubs.onlinelibrary.wiley.com/doi/abs/10.1029/95WR10583> doi: <https://doi.org/10.1029/95WR10583>
- 646
- 647
- 648
- 649
- 650 Hammel, K., & Roth, K. (1998, apr). Approximation of asymptotic dispersivity of conservative solute in unsaturated heterogeneous media with steady state flow. *Water Resources Research*, *34*(4), 709–715. Retrieved from <http://doi.wiley.com/10.1029/98WR00004> doi: 10.1029/98WR00004
- 651
- 652
- 653
- 654 Hansen, B., Dalgaard, T., Thorling, L., Sørensen, B., & Erlandsen, M. (2012). Regional analysis of groundwater nitrate concentrations and trends in denmark in regard to agricultural influence. *Biogeosciences*, *9*, 3277–3286.
- 655
- 656
- 657 Henri, C. V., & Diamantopoulos, E. (2022). Unsaturated transport modeling: Random-walk particle-tracking as a numerical-dispersion free and efficient alternative to eulerian methods. *Journal of Advances in Modeling Earth Systems*, *14*(9), e2021MS002812. Retrieved from <https://agupubs.onlinelibrary.wiley.com/doi/abs/10.1029/2021MS002812> (e2021MS002812 2021MS002812) doi: <https://doi.org/10.1029/2021MS002812>
- 658
- 659
- 660
- 661
- 662
- 663 Henri, C. V., & Fernández-García, D. (2014). Toward efficiency in heterogeneous multispecies reactive transport modeling: A particle-tracking solution for first-order network reactions. *Water Resour. Res.*, *50*(9), 7206–7230.
- 664
- 665
- 666 Henri, C. V., & Fernández-García, D. (2015). A random walk solution for modeling solute transport with network reactions and multi-rate mass transfer in heterogeneous systems: Impact of biofilms. *Adv.in Water Resour.*, *86*, 119.
- 667
- 668
- 669 Holbak, M., Abrahamsen, P., & Diamantopoulos, E. (2022). Modeling preferential water flow and pesticide leaching to drainpipes: The effect of drain-connecting and matrix-terminating biopores. *Water Resources Research*, *58*(7), e2021WR031608.
- 670
- 671
- 672 Holbak, M., Abrahamsen, P., Hansen, S., & Diamantopoulos, E. (2021). A physically based model for preferential water flow and solute transport in drained agricultural fields. *Water Resources Research*, *57*(3), e2020WR027954.
- 673
- 674
- 675 Jarvis, N., Koestel, J., & Larsbo, M. (2016). Understanding preferential flow in the

- 676 vadose zone: Recent advances and future prospects. *Vadose Zone Journal*, 15(12),  
677 1–11.
- 678 Javaux, M., Vanderborght, J., Kasteel, R., & Vanclooster, M. (2006a). Three-  
679 dimensional modeling of the scale-and flow rate-dependency of dispersion in a  
680 heterogeneous unsaturated sandy monolith. *Vadose Zone Journal*, 5(2), 515–528.
- 681 Javaux, M., Vanderborght, J., Kasteel, R., & Vanclooster, M. (2006b, may). Three-  
682 Dimensional Modeling of the Scale- and Flow Rate-Dependency of Dispersion  
683 in a Heterogeneous Unsaturated Sandy Monolith. *Vadose Zone Journal*, 5(2),  
684 515–528. Retrieved from <http://doi.wiley.com/10.2136/vzj2005.0056> doi:  
685 10.2136/vzj2005.0056
- 686 Khan, A. U.-H., & Jury, W. A. (1990). A laboratory study of the dispersion scale  
687 effect in column outflow experiments. *Journal of Contaminant Hydrology*, 5(2),  
688 119–131.
- 689 Miller, E., & Miller, R. (1956). Physical theory for capillary flow phenomena. *Jour-  
690 nal of Applied Physics*, 27(4), 324–332.
- 691 Millington, R. J., & Quirk, J. P. (1961). Permeability of porous solids. *Transactions  
692 of the Faraday Society*, 57, 1200. Retrieved from [http://xlink.rsc.org/?DOI=  
693 tf9615701200](http://xlink.rsc.org/?DOI=tf9615701200) doi: 10.1039/tf9615701200
- 694 Møldrup, P., Olesen, T., Rolston, D., & Yamaguchi, T. (1997). Modeling diffusion  
695 and reaction in soils: Vii. predicting gas and ion diffusivity in undisturbed and  
696 sieved soils. *Soil Science*, 162(9), 632–640.
- 697 Nissan, A., & Berkowitz, B. (2019, mar). Anomalous transport dependence on  
698 Péclet number, porous medium heterogeneity, and a temporally varying velocity  
699 field. *Physical Review E*, 99(3), 033108. Retrieved from [https://link.aps.org/  
700 doi/10.1103/PhysRevE.99.033108](https://link.aps.org/doi/10.1103/PhysRevE.99.033108) doi: 10.1103/PhysRevE.99.033108
- 701 Richards, L. A. (1931). Capillary conduction of liquids through porous mediums.  
702 *Journal of Applied Physics*, 1(5), 318–333.
- 703 Richardson, L. F. (1922). *Weather prediction by numerical process*. New York: Cam-  
704 bridge University Press. (Cambridge: Cambridge mathematical library)
- 705 Roth, K. (1995, sep). Steady State Flow in an Unsaturated, Two-Dimensional,  
706 Macroscopically Homogeneous, Miller-Similar Medium. *Water Resources Research*,  
707 31(9), 2127–2140. Retrieved from <http://doi.wiley.com/10.1029/95WR00946>  
708 doi: 10.1029/95WR00946

- 709 Roth, K., & Hammel, K. (1996, jun). Transport of conservative chemical through an  
710 unsaturated two-dimensional Miller-similar medium with steady state flow. *Water*  
711 *Resources Research*, *32*(6), 1653–1663. Retrieved from [http://doi.wiley.com/10](http://doi.wiley.com/10.1029/96WR00756)  
712 [.1029/96WR00756](http://doi.wiley.com/10.1029/96WR00756) doi: 10.1029/96WR00756
- 713 Russo, D. (1993). Stochastic modeling of macrodispersion for solute transport in  
714 a heterogeneous unsaturated porous formation. *Water Resources Research*, *29*(2),  
715 383–397. Retrieved from [https://agupubs.onlinelibrary.wiley.com/doi/abs/](https://agupubs.onlinelibrary.wiley.com/doi/abs/10.1029/92WR01957)  
716 [10.1029/92WR01957](https://doi.org/10.1029/92WR01957) doi: <https://doi.org/10.1029/92WR01957>
- 717 Russo, D. (2015, may). On the effect of connectivity on solute transport in spatially  
718 heterogeneous combined unsaturated-saturated flow systems. *Water Resources*  
719 *Research*, *51*(5), 3525–3542. Retrieved from [http://doi.wiley.com/10.1002/](http://doi.wiley.com/10.1002/2014WR016434)  
720 [2014WR016434](http://doi.wiley.com/10.1002/2014WR016434) doi: 10.1002/2014WR016434
- 721 Russo, D., & Fiori, A. (2009, mar). Stochastic analysis of transport in a combined  
722 heterogeneous vadose zone-groundwater flow system. *Water Resources Research*,  
723 *45*(3), 1–16. Retrieved from <http://doi.wiley.com/10.1029/2008WR007157>  
724 doi: 10.1029/2008WR007157
- 725 Russo, D., Zaidel, J., & Laufer, A. (2000). Numerical analysis of flow and transport  
726 in a combined heterogeneous vadose zone-groundwater system. *Advances in Water*  
727 *Resources*, *24*(1), 49–62. doi: 10.1016/S0309-1708(00)00026-9
- 728 Russo, D., Zaidel, J., & Laufer, A. (2001, aug). Numerical analysis of flow and  
729 transport in variably saturated bimodal heterogeneous porous media. *Water Re-*  
730 *sources Research*, *37*(8), 2127–2141. Retrieved from [http://doi.wiley.com/10](http://doi.wiley.com/10.1029/2001WR000393)  
731 [.1029/2001WR000393](http://doi.wiley.com/10.1029/2001WR000393) doi: 10.1029/2001WR000393
- 732 Sadeghi, M., Ghahraman, B., Warrick, A. W., Tuller, M., & Jones, S. B. (2016). A  
733 critical evaluation of the miller and miller similar media theory for application to  
734 natural soils. *Water Resources Research*, *52*(5), 3829–3846.
- 735 Schelle, H., Durner, W., Schlüter, S., Vogel, H.-J., & Vanderborght, J. (2013). Vir-  
736 tual soils: Moisture measurements and their interpretation by inverse modeling.  
737 *Vadose Zone Journal*, *12*(3), 1–12.
- 738 Schlüter, S., Vanderborght, J., & Vogel, H. J. (2012). Hydraulic non-equilibrium  
739 during infiltration induced by structural connectivity. *Advances in Water Re-*  
740 *sources*, *44*, 101–112. doi: 10.1016/j.advwatres.2012.05.002
- 741 Shen, L., & Chen, Z. (2007). Critical review of the impact of tortuosity on diffusion.

- 742 *Chemical Engineering Science*, 62(14), 3748-3755. Retrieved from <https://www>  
743 [.sciencedirect.com/science/article/pii/S0009250907003144](https://www.sciencedirect.com/science/article/pii/S0009250907003144) doi: <https://>  
744 [doi.org/10.1016/j.ces.2007.03.041](https://doi.org/10.1016/j.ces.2007.03.041)
- 745 Ursino, N., & Gimmi, T. (2004). Combined effect of heterogeneity, anisotropy  
746 and saturation on steady state flow and transport: Structure recognition  
747 and numerical simulation. *Water Resources Research*, 40(1), 1–12. doi:  
748 10.1029/2003WR002180
- 749 Van Cappellen, P., & Gaillard, J.-F. (2018). Biogeochemical dynamics in aquatic  
750 sediments. In *Reactive transport in porous media* (pp. 335–376). De Gruyter.
- 751 Vanderborght, J., Mallants, D., & Feyen, J. (1998, dec). Solute transport in a  
752 heterogeneous soil for boundary and initial conditions: Evaluation of first-order  
753 approximations. *Water Resources Research*, 34(12), 3255–3270. Retrieved from  
754 <http://doi.wiley.com/10.1029/98WR02685> doi: 10.1029/98WR02685
- 755 Van Genuchten, M., & Wierenga, P. (1974). *Simulation of one-dimensional solute*  
756 *transfer in porous media*. New Mexico State University, Agricultural Experiment  
757 Station. Retrieved from <https://books.google.dk/books?id=kxInAQAAAJ>
- 758 Vogel, T., Gerke, H. H., Zhang, R., & Van Genuchten, M. T. (2000). Model-  
759 ing flow and transport in a two-dimensional dual-permeability system with spa-  
760 tially variable hydraulic properties. *Journal of Hydrology*, 238(1-2), 78–89. doi:  
761 10.1016/S0022-1694(00)00327-9
- 762 Šimunek, J., Šejna, M., Saito, H., Sakai, M., & Van Genuchten, M. (2013). The  
763 hydrus-1d software package for simulating the movement of water, heat, and mul-  
764 tiple solutes in variably saturated media, version 4.17, hydrus software series 3,  
765 department of environmental sciences, university of california riverside, riverside,  
766 california. USA.
- 767 Weissmann, G. S., Zhang, Y., LaBolle, E. M., & Fogg, G. E. (2002). Dispersion of  
768 groundwater age in an alluvial aquifer system. *Water Resour. Res.*, 38(10), 1198.
- 769 Woods, S. A., Dyck, M. F., & Kachanoski, R. G. (2013, may). Spatial and tem-  
770 poral variability of soil horizons and long-term solute transport under semi-  
771 arid conditions. *Canadian Journal of Soil Science*, 93(2), 173–191. Retrieved  
772 from <http://www.nrcresearchpress.com/doi/10.4141/cjss2012-082> doi:  
773 10.4141/cjss2012-082

# Supporting Information for ”The effect of Small Scale Soil Heterogeneity on conservative Transport: the Key Role of (Spatially Variable) Diffusion”

Christopher V. Henri<sup>1</sup>, Efstathios Diamantopoulos<sup>2</sup>

<sup>1</sup>Geological Survey of Denmark and Greenland, Copenhagen, Denmark

<sup>2</sup>Department of Plant and Environmental Sciences, University of Copenhagen, Copenhagen, Denmark

## Contents of this file

1. Figures S1 to S11

---

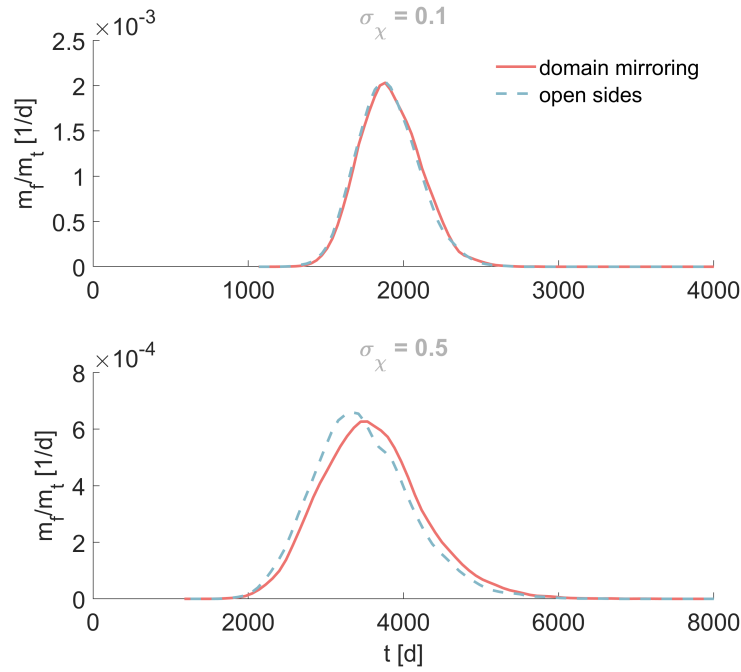


**Figure S1.** Mass fluxes (normalized by the total mass reaching the bottom of the domain) temporal evolution for a low (top) and high (bottom) degree of heterogeneity if particles are allowed to leave the sides of the domain (dashed blue line) and if particles are transferred to the opposite side of domain (plain red line). BTCs are shown for a low flux (diffusion dominated scenario).

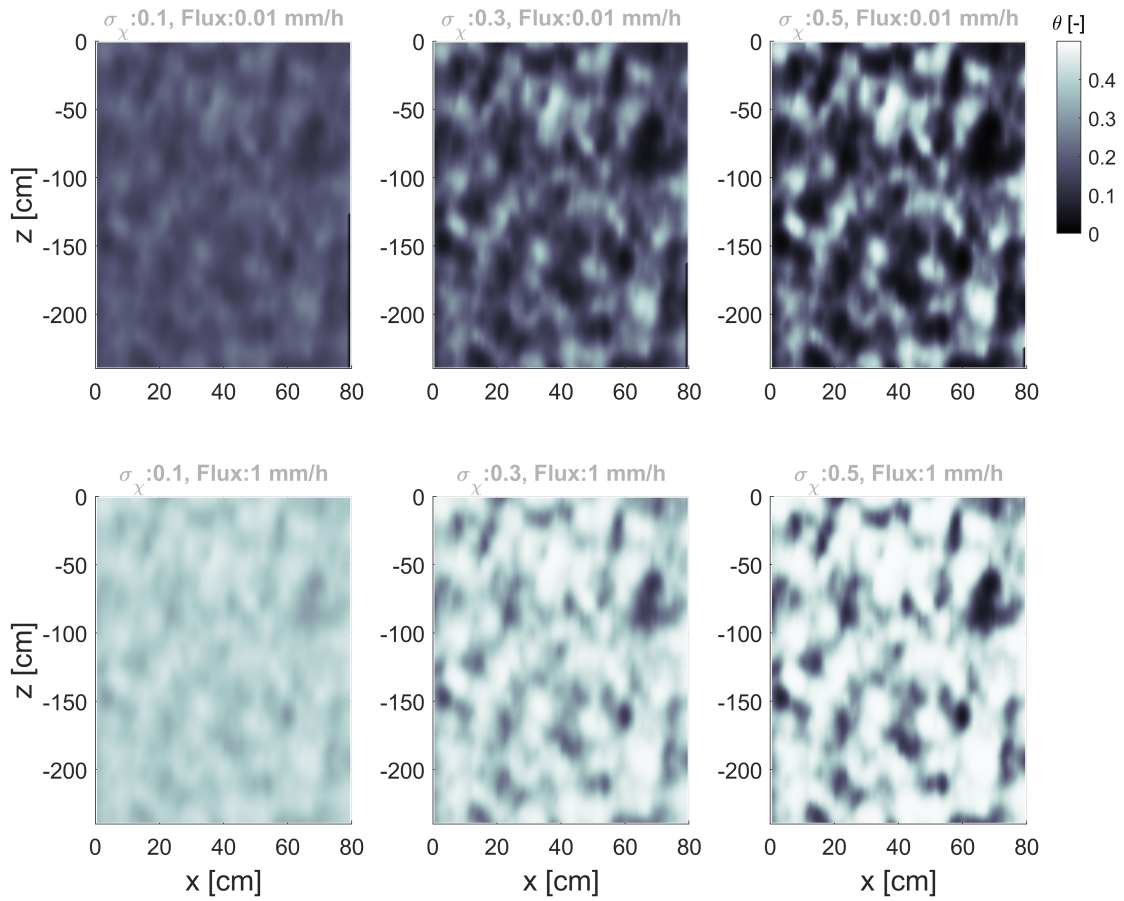


**Figure S2.** Resulting spatial distribution of the water content ( $\theta$ ) for each degree of soil heterogeneity and for a high recharge flux (top frames) and a low recharge flux (bottom frames).

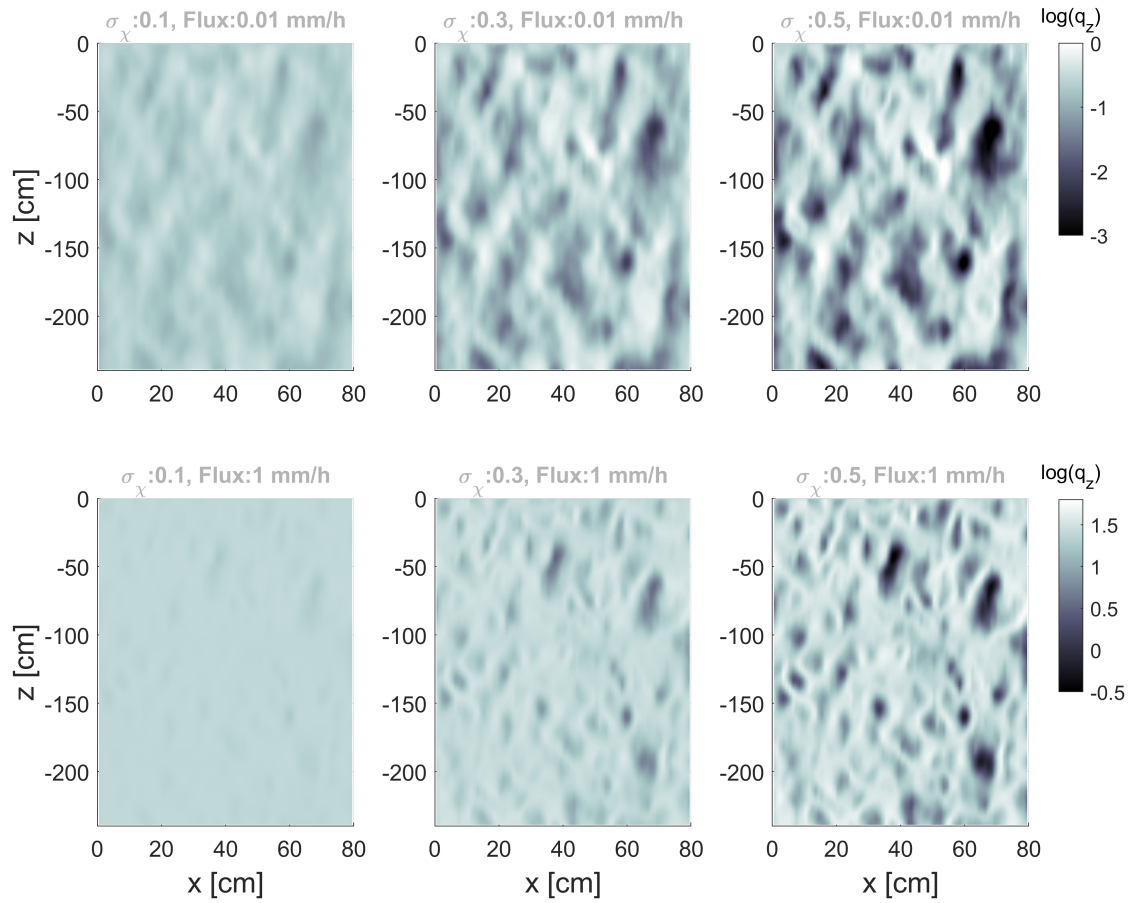


**Figure S3.** Resulting spatial distribution of the (logarithm of the) vertical Darcy flux ( $q_z$ ) for each degree of soil heterogeneity and for a high recharge flux (top frames) and a low recharge flux (bottom frames).

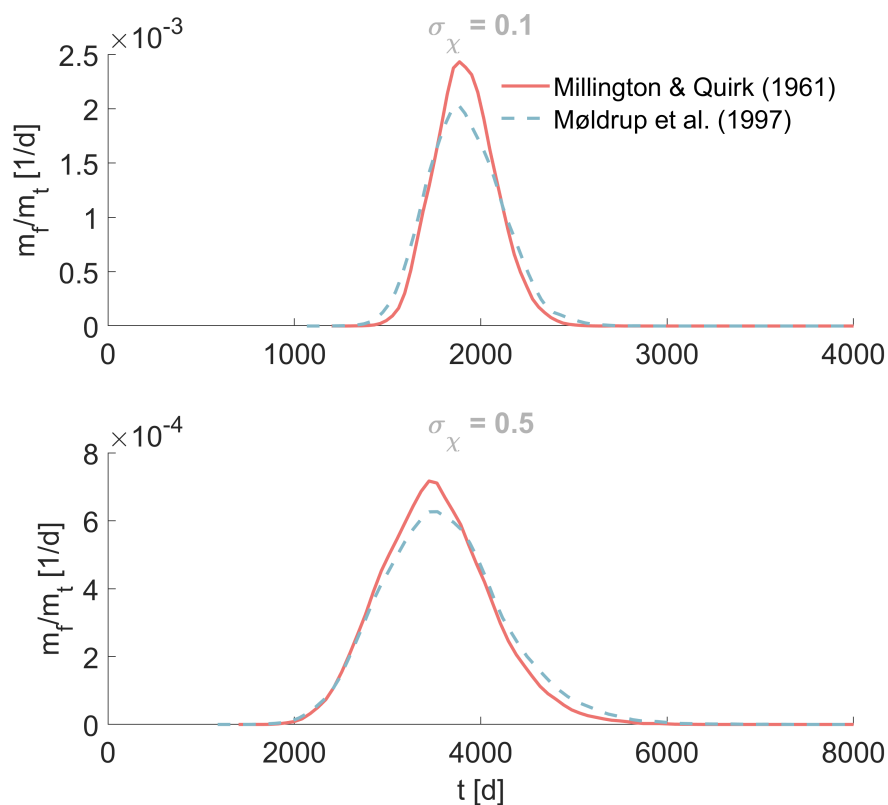


**Figure S4.** Mass fluxes temporal evolution for a low (top) and high (bottom) degree of heterogeneity if the Millington's model of tortuosity is used (plain red line) and if the Møldrup's model of tortuosity is used (dashed blue line). BTCs are shown for a low flux (diffusion dominated scenario) and the highest degree of heterogeneity.

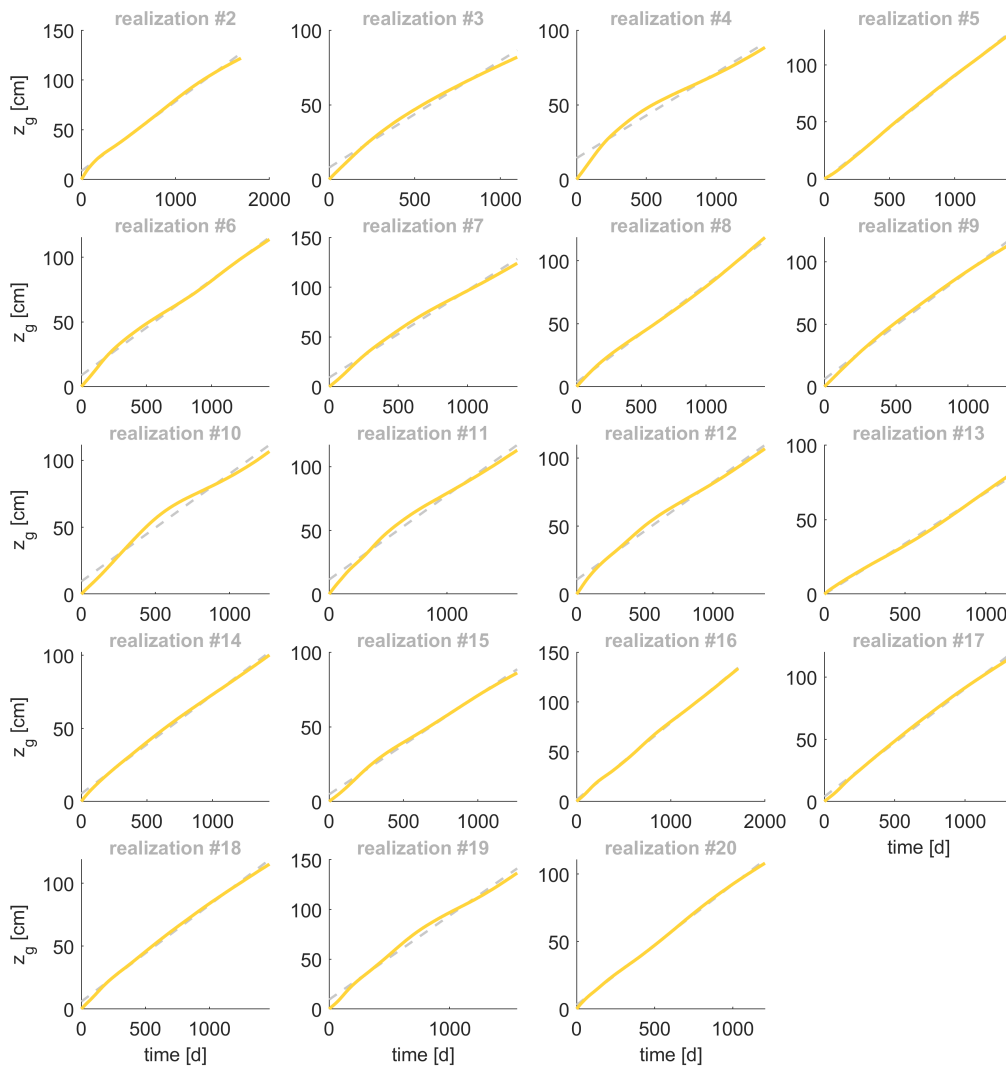


**Figure S5.** First spatial moment ( $Y_g$ ) temporal evolution for all realizations. Results are shown for a low flux and the highest degree of heterogeneity.

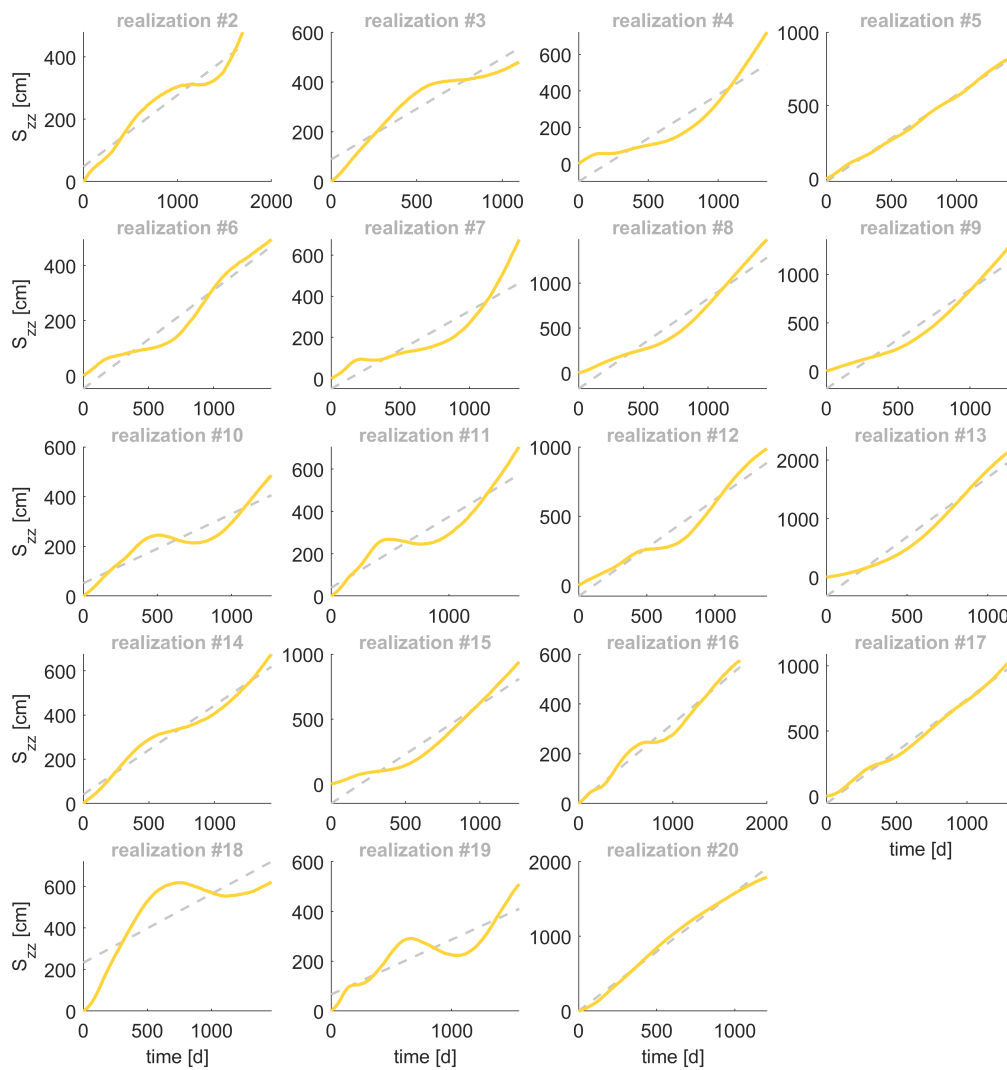


**Figure S6.** Second spatial moment ( $S_{zz}$ ) temporal evolution for all realizations.

Results are shown for a low flux and the highest degree of heterogeneity.

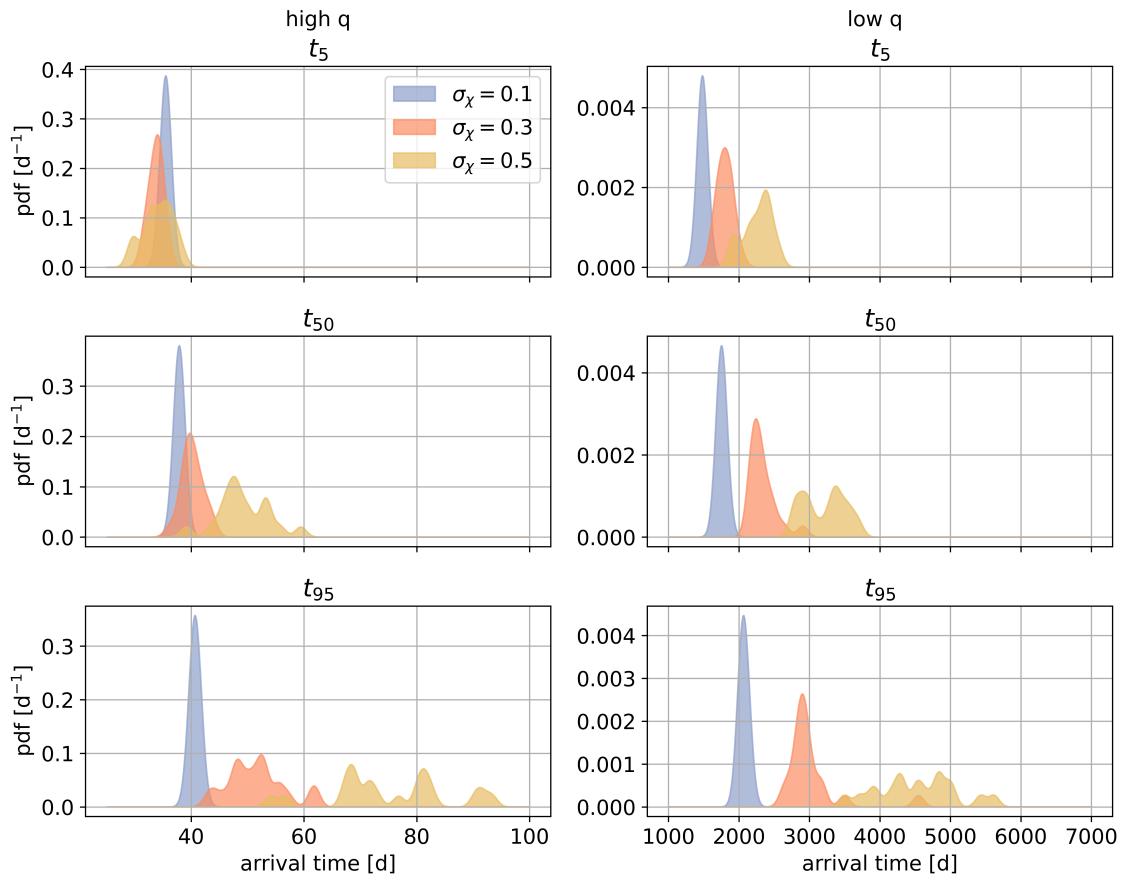


**Figure S7.** Probability density functions of the arrival time of 5 (top frames), 50 (middle frames) and 95% (bottom frames) of the total injected mass for each flow and heterogeneity scenario. The diffusion coefficient is considered spatially variable (tortuosity dependent).

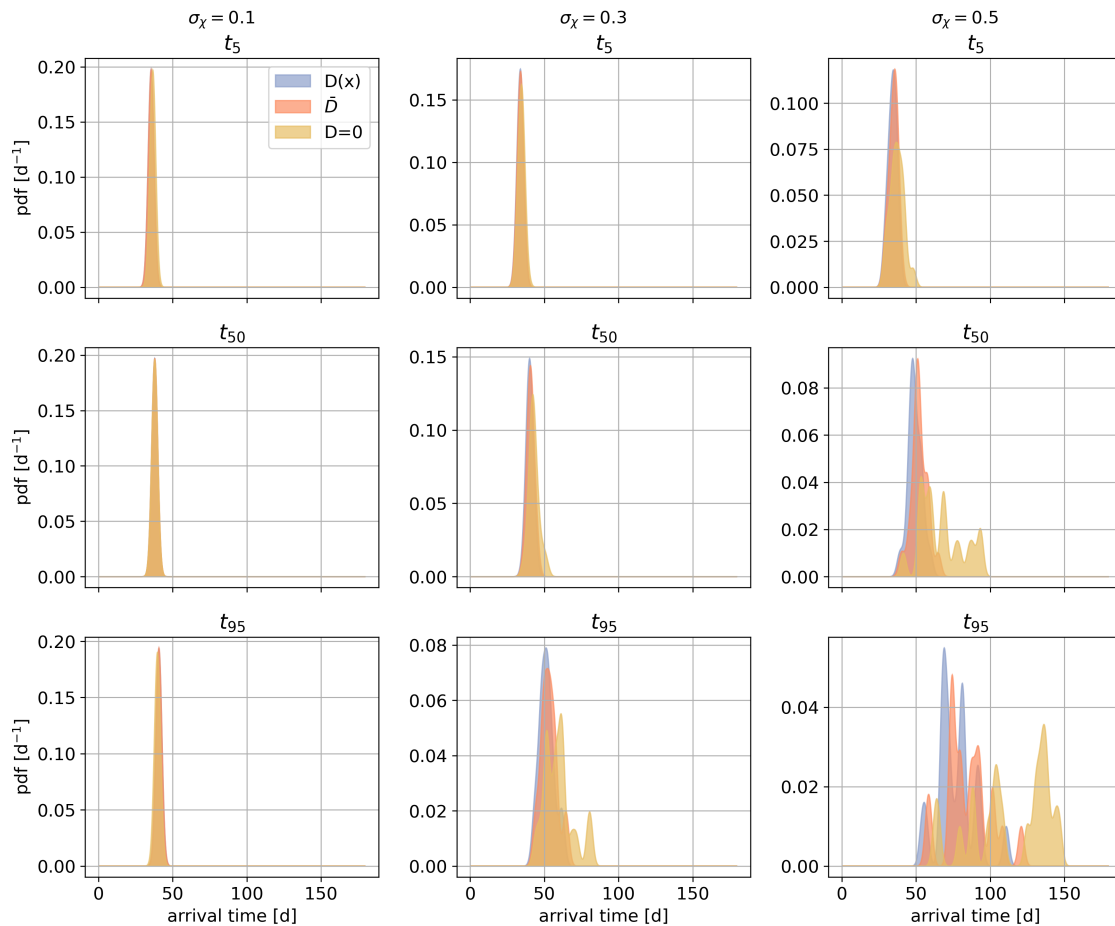


**Figure S8.** Probability density functions of the arrival time of 5 (top frames), 50 (middle frames) and 95% (bottom frames) of the total injected mass for each heterogeneity scenario and diffusion model. Results are shown for the higher Peclet number.

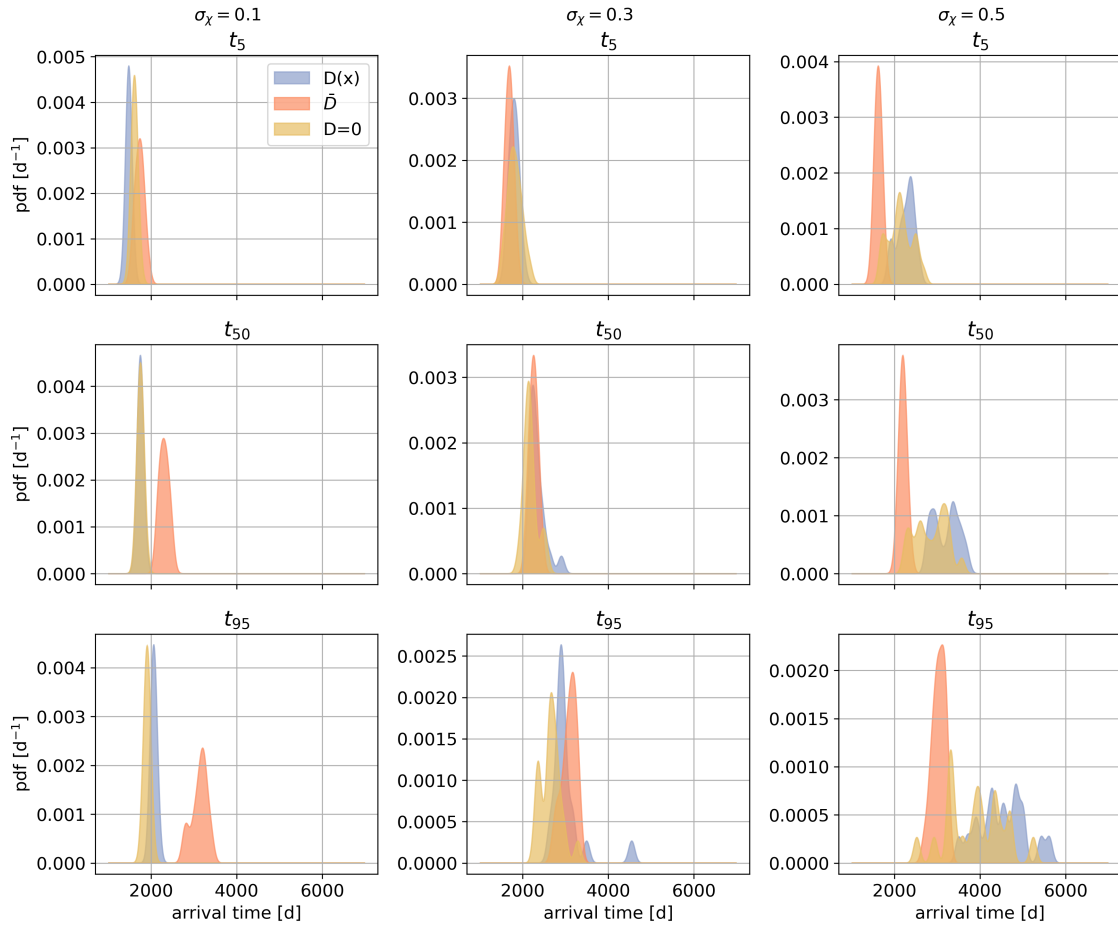


**Figure S9.** Probability density functions of the arrival time of 5 (top frames), 50 (middle frames) and 95% (bottom frames) of the total injected mass for each heterogeneity scenario and diffusion model. Results are shown for the lower Peclet number.

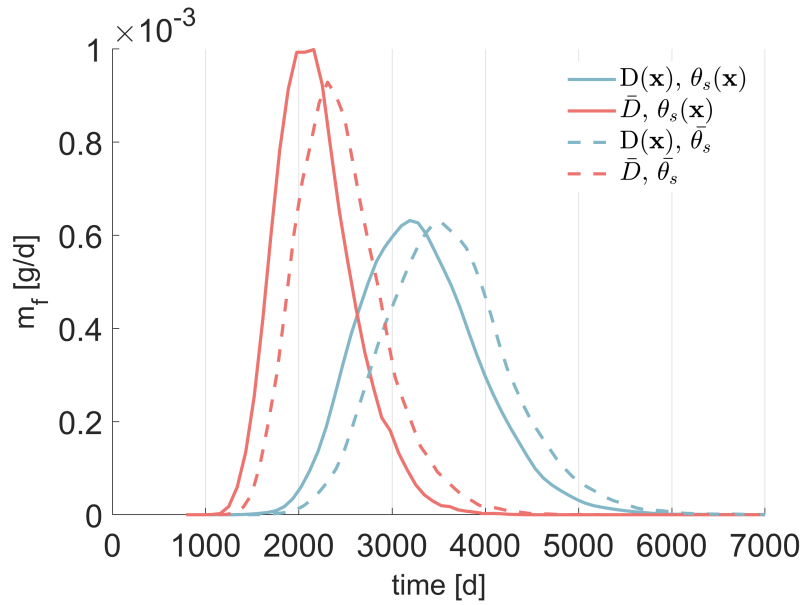


**Figure S10.** Mass fluxes temporal evolution for a spatially variable diffusion coefficient ( $D(x)$ , blue lines) or a homogeneous, averaged diffusion coefficient ( $\bar{D}$ , red lines) and for a spatially variable saturated water content ( $\theta_s(x)$ ) or a homogeneous, averaged saturated water content ( $\bar{\theta}_s$ ). BTCs are shown for a high degree of heterogeneity ( $\sigma_\chi = 0.5$ ) and a low flux (diffusion dominated scenario).

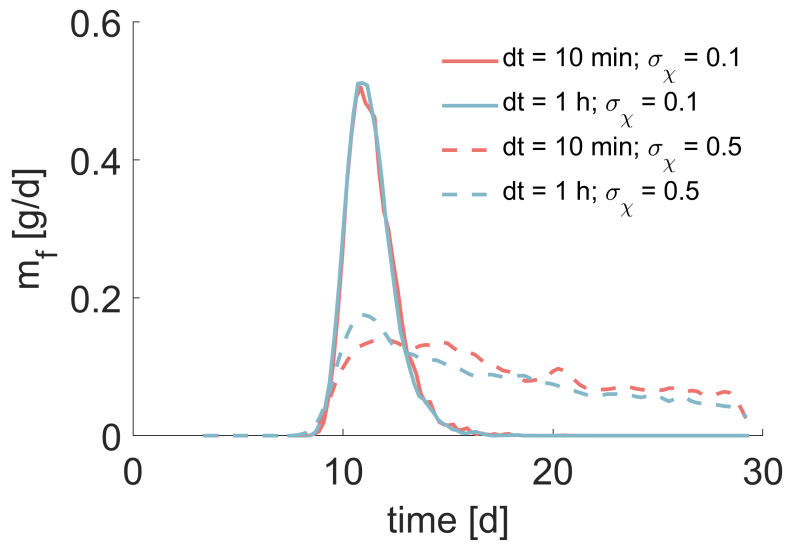


**Figure S11.** Mass fluxes temporal evolution for a low (plain lines) and high (dashed lines) degree of heterogeneity for 2 temporal discretization of the Darcy fluxes and the water content used in to solve the transport problem. *CP 80 cm; 10 days of infiltration*